THE SAGA OF YIG: SPECTRA, THERMODYNAMICS, INTERACTION AND RELAXATION OF MAGNONS IN A COMPLEX MAGNET

Vladimir CHEREPANOV

Department of Physics, University of Manitoba, Winnipeg, Manitoba, Canada R3T 2N2

Igor KOLOKOLOV

Institute of Nuclear Physics, Academy of Sciences, Novosibirsk 630080, Russian Federation

and

Victor L'VOV

Physics Department, The Weizmann Institute of Science, Rehovot 76100, Israel

NORTH-HOLLAND

PHYSICS REPORTS (Review Section of Physics Letters) 229, No. 3 (1993) 81–144.
North-Holland

PHYSICS REPORTS

The saga of YIG: spectra, thermodynamics, interaction and relaxation of magnons in a complex magnet

Vladimir Cherepanov[a, 1], Igor Kolokolov[b] and Victor L'vov[c, 1]

[a] *Department of Physics, University of Manitoba, Winnipeg, Manitoba, Canada R3T 2N2*
[b] *Institute of Nuclear Physics, Academy of Sciences, Novosibirsk 630080, Russian Federation*
[c] *Physics Department, The Weizmann Institute of Science, Rehovot 76100, Israel*

Received September 1992; editor I. Procaccia

Contents:

Introduction 83
1. Magnon spectra in YIG 88
1.1. Magnetic structure of YIG 88
1.2. Review of experimental results 90
1.3. Quadratic Hamiltonian 93
1.4. Magnon spectra and normal variables – the results of computer calculations 97
1.5. Quadratic Hamiltonian for spin waves in quasinormal varaibles 99
1.6. Perturbation theory for nondegenerate modes 103
1.7. Approximate calculation of the spectra 105
1.8. Determination of the exchange integrals in YIG 110
1.9. Temperature dependence of the magnetization and the exchange integrals 111
2. Magnon interaction and relaxation in YIG 113
2.1. Magnon interaction and relaxation theory 113
2.2. Experimental results 120
2.3. Exchange interactions of magnons 125
2.4. Magnetic dipole interaction and relaxation of ferromagnons 131
2.5. Ferromagnon relaxation at $k \to 0$ 137
2.6. Comparison of theoretical and experimental results 140
3. Conclusion 142
References 143

Abstract:

A review of magnon properties of yttrium–iron garnet (YIG), a classical object for experimental studies in magnetism, is presented. Both experimental and theoretical results concerned with thermodynamics and kinetics of YIG are described. The main purposes of the review are to introduce a new method of approximate calculation of the magnon spectra in magnets with large unit cell and to obtain by means of this method some basic properties of YIG. In particular, it is shown that the problem of calculating the frequencies of all the 20 magnon branches over the entire Brillouin zone contains two small parameters. First, because of the large number of magnetic atoms in the unit cell the distance between the nearest interacting magnetic atoms is small in comparison with the lattice constant and, accordingly, with the wavelength of a spin wave. An effective long-wavelength character thus arises in the problem. Second, there are a large number of wave-vector directions along which many elements of the Hamiltonian matrix vanish by symmetry in the basis which diagonalizes this matrix for $k = 0$. These matrix elements thus have an additional, angular smallness for arbitrary directions of $\boldsymbol{k}$. These matrix elements can be taken into account using perturbation theory. As a result, the large elements of the Hamiltonian matrix are few in number, and they can be eliminated by several two-dimensional rotations. Approximate expressions, differing from the computer calculations by $\lesssim 10\%$, are thus obtained for the frequencies.

Neutron scattering data are used to find the values of the exchange integrals in YIG and to obtain the magnon spectra. It is shown that in the energy range $T \lesssim 260$ K only magnons of the lower branch are excited; the spectrum of these "ferromagnons" is quadratic in the wave vector only up to 40 K and becomes linear in the region $\omega_k \gtrsim 40$ K. For temperatures up to 400 K the temperature dependence of the magnetization is calculated in the spin-wave approximation and good agreement with experimental data is found.

A brief review of experimental data on magnon relaxation in YIG is presented. The magnon–magnon interactions which cause the magnon relaxation are described. The amplitude of the four-magnon exchange interaction is determined, and the temperature correction to the frequency is evaluated. This temperature correction is positive, in contrast to the case of simple cubic ferromagnet with nearest-neighbour interaction. The exchange relaxation rate is calculated for normal and umklapp processes. It is shown that the magnetic dipole interaction is important only for the ferromagnons; the amplitude of this interaction and the corresponding relaxation rate are determined. Three-magnon scattering processes are allowed only for wave vectors larger than a certain k_l; at $k = k_l$ there is a discontinuity in the wave-vector dependence of the damping. A calculation is given for the nonvanishing contribution to the relaxation at $\boldsymbol{k} = 0$ on account of scattering processes involving optical magnons; this contribution is due to the local uniaxial anisotropy. The relative role of each of the investigated relaxation mechanisms is discussed, and the correspondence of the present results with the experimental data is examined.

Introduction

Yttrium–iron garnet ($Y_3Fe_5O_{12}$–YIG) is a marvel of nature. Its role in the physics of magnets is analogous to that of germanium in semiconductor physics, water in hydrodynamics, and quartz in crystal acoustics. There are several reasons for this. Firstly, it has the narrowest known ferromagnetic resonance line and the lowest spin-wave damping. Secondly, with 80 atoms in the unit cell, each of which must find its proper location, the YIG crystal growth was so well perfected that its acoustic damping is lower than that of quartz. Thirdly, it has a high Curie temperature $T_C = 560$ K, so that experiments can be done at room temperature. For all these reasons, YIG has become indispensable both in microwave technology and in experimental physics for studying new effects and phenomena in magnets.

Detailed studies have been made in YIG of the temperature dependence of the magnetization, specific heat, paramagnetic susceptibility, frequency and damping of long-wavelength spin waves, and much more. To analyze all these experimental data it is necessary first to know the spectrum of the elementary excitations of the magnet – the magnons.

Many important properties of the magnet were not understood for a long time. This is primarily because of the complex crystal structure of YIG: its unit cell contains four formula units of $Y_3Fe_2^{3+}Fe_3^{3+}O_{12}^{2-}$, with the magnetic ions Fe^{3+} occupying two inequivalent positions with regard to the character of its immediate O^{2-} environment–octahedral (a) and tetrahedral (d). There are twenty magnetic ions in all ($8a + 12d$) and, accordingly, twenty magnon branches in the energy range for 0 to 1000 K. The fundamental characteristics of a ferrite are the magnon frequency $\omega_j(\boldsymbol{k})$ (or the magnon energy $\hbar\omega_j(\boldsymbol{k})$) and relaxation time $\gamma_j^{-1}(\boldsymbol{k})$ (j is the number of the branch and $\boldsymbol{k}$ is the wave vector).

The purpose of the review is to present a theory of magnetic properties of YIG in the magnon approximation. This theory describes magnon spectra and relaxation as well as the thermodynamic properties of this ferrite in a wide temperature range from 0 to the room temperature.

The exchange interaction, which governs the magnetic order in YIG, is the strongest among magnetic interactions of various nature. The energy of this interaction decreases rapidly with the increase of the distance between magnetic ions. The strongest exchange interaction is that between nearest neighbours: ions Fe in (a) and (d) sites. This interaction is antiferromagnetic with the exchange constant $J_{ad} \approx -40$ K in the temperature scale. There are 8 Fe ions in (a) sites and 12 ones in the (d) sites in a unit cell. The spin of an ion Fe is $\frac{5}{2}$, therefore the magnetic moment of a unit cell is 10 μ (μ is Bohr magneton) at zero temperature. The next nearest neighbours are ions in (d) positions, with the exchange constant $J_{ad} \approx -13.4$ K, and the next after this d–d exchange interaction is a–a interaction, with the exchange constant $J_{aa} \approx -3.8$ K. The exchange interactions between further neighbours are negligible.

YIG can be considered as a ferromagnet with the magnet moment 10 μ per unit cell only in low-energy limit. Only ferromagnetic magnon, or ferromagnon, branch is essential in this limit. Its energy is easily calculated because all the twenty magnetic moments in the primitive cell oscillate almost in phase and can be treated as one common magnetic moment.

The ferromagnon spectrum in the exchange interaction approximation in the low frequency limit is quadratic in the wave number k [1]:

$$\omega(k) = \omega_{ex}(ak)^2 , \quad \omega_{ex} = \tfrac{5}{16}(8J_{aa} + 3J_{ad} - 5J_{ad}) , \tag{1}$$

where a is the lattice constant and ω_{ex} is the "exchange" frequency. $a \simeq 12.5$ Å and $\omega_{ex} \simeq 40$ K in YIG.

It has long been known [2] that formula (1) is valid in a rather small region of k space ($ak \lesssim 1$), with a volume less than 1% of the volume $2(2\pi/a)^3$ of the whole Brillouin zone. The magnon energy in this region does not exceed 40 K. To describe the thermodynamic and kinetic properties of YIG at higher temperatures, one cannot treat the crystal as a one-sublattice ferromagnet, even if only the lower spin-wave branch is excited. The point is that even for $ak \leq 1$ one cannot assume that the magnetic moment of all twenty ions in a unit cell oscillate in phase. Therefore, to find the spin-wave frequencies (including those of the lower branch) one must, generally speaking, solve the complete problem of the oscillations of the twenty magnetic sublattices, which amounts to the diagonalization of a 40×40 matrix. It is simple enough to calculate the frequencies of all the twenty magnetic branches at $k = 0$ using group theory and making use of the high degree of symmetry of the problem: the invariance of the exchange interaction with respect to rotations and the symmetry (group O_h^{10}) of the garnet lattice [3]. Harris [2] has constructed a perturbation theory for $ak \ll 1$ and found a correction $\sim k^4$ to the frequency of the lower branch (1). However, in his computer calculation he evaluated the magnon frequencies $\omega_j(\boldsymbol{k}), j = 1, \ldots, 20$ for the most symmetric direction $\boldsymbol{k} \parallel [111]$ and for several rather arbitrarily chosen values of the exchange integrals. It turned out that the frequencies of the 19 "optical" branches densely fill the interval from 200 to 600 K, and so, generally speaking, there is no temperature interval in which magnons are excited on only two branches. The widespread opinion that YIG can be treated approximately as a two-sublattice ferrimagnet is therefore lacking foundation. Later experimental investigation of inelastic neutron scattering in YIG carried out by Plant [4] confirmed this picture.

The simplest way to study magnetic properties of YIG would be to calculate all the magnon frequencies in the entire Brillouin zone numerically. Nevertheless, this way proved unacceptable because there were some contradictory data about the values of the exchange constants in YIG. In addition, our aim was not only to calculate some numbers concerning YIG properties but to estimate the most important physical processes in complex magnetic systems. The first step of such a research was to find the spectra of magnons, the elementary excitations in the system. The first chapter of the review is aimed at studies of the magnon spectra in YIG. The magnetic structure of the magnet and the exchange interaction Hamiltonian are described in the section 1.1. In section 1.2 a brief review of experimental results concerning thermodynamical properties of YIG and the inelastic neutron scattering is presented. The rest of the chapter is concentrated on the theory of magnon spectra in YIG. A progress in the theory of the magnon spectra in such a complicated magnet is due to two hidden small parameters. The first of these parameters is related to the large number of magnetic atoms in the unit cell ($Z = 20$). The distance between nearest neighbours is therefore smaller than the lattice constant. As a result, a suitably constructed long-wavelength approximation is valid over the entire Brillouin zone. The second small parameter is due to high degree of YIG crystal symmetry. There are a large number of matrix elements of the Hamiltonian matrix vanishing in the symmetric directions of the wave vector (e.g. [100] or [111]). Since there are many such symmetric directions, these matrix elements assume an "angular" smallness in arbitrary directions as well. The magnon approximation for the spin Heisenberg Hamiltonian is studied in section 1.3.

The quadratic part of the Hamiltonian function in the magnon Bose operators determines the magnon frequencies $\omega_j(\boldsymbol{k}), j = 1, 2, \ldots, 20$. To evaluate these frequencies it is generally necessary to diagonalize a 40×40 matrix. However, in the exchange approximation for a collinear structure, the problem reduces to the diagonalization of a 20×20 matrix [2].

Before proceeding with the analytical solution, we made detailed computer studies of the problem: using an iterative procedure we evaluated the functions $\omega_j(\boldsymbol{k})$ and the eigenvectors for all

$j = 1, \ldots, 20$ and different sets of exchange integrals and for the directions $\boldsymbol{k} \parallel [111]$, [100], [110] and [113]. The results of these calculations are presented in section 1.4. Analysis of these results shows that the eigenvectors of magnons of ferromagnetic and antiferromagnetic types have a very simple structure, and their frequencies can be found easily in the entire Brillouin zone. In particular for the lowest, ferromagnon branch, the spectrum is quadratic: $\omega_1(\boldsymbol{k}) = \omega_{ex}(ak)^2$ only up to energies of 40 K; after this, as we have shown [5], the spectrum $\omega_1(\boldsymbol{k})$ becomes almost linear: $\omega_1(\boldsymbol{k}) \approx -\Delta + \omega_\ell(ak)$ ($\Delta \approx \omega_\ell/2 \approx \omega_{ex} \approx 40$ K).

In sections 1.5–1.7 we construct an approximate analytical theory of the magnon spectra of YIG. In section 1.5.1 we transform the Hamiltonian matrix to the "irreducible" basis of the point group O_h. It is well known [6] that the representation generated by the permutation of the eight iron ions in a positions in the unit cell YIG decomposes into two one-dimensional representations τ_1 (identical) and τ_3 and two three-dimensional representations τ_7 and τ_9. The permutation representation of the 12 ions in d positions decomposes into two one-dimensional representations τ_1 and τ_4, two-dimensional representations τ_5 and τ_6, and two three-dimensional representations τ_8 and τ_9. Because the representations τ_1 and τ_9 occur twice, the Hamiltonian matrix contains four pairs of off-diagonal elements even for $\boldsymbol{k} = 0$. In section 1.5 we eliminate these for arbitrary $\boldsymbol{k}$ with the aid of four separate canonical u–v transformations, each of which involves only one pair of the basis functions. In such a representation, which we call "quasi-normal", the Hamiltonian matrix is diagonal for $\boldsymbol{k} = 0$. Its diagonal elements serve as an approximation for the spin-wave frequencies and, in the nondegenerate case, describe these frequencies well over the entire Brillouin zone. Before we give these frequencies, let us introduce the following notation for the combinations of trigonometric functions which occur in them,

$$\begin{aligned} &\alpha_{ijl} = \cos 2q_i \cos q_j \cos q_l\,, \quad \gamma_{ijl} = \cos 2q_i, \sin q_j \sin q_l\,, \quad \eta_{ijl} = \cos 2q_i \cos q_j\,, \\ &\chi_{ijl} = \sin 2q_i \sin q_j\,, \quad \nu_{ijl} = \cos 2q_i \cos 2q_j \cos 2q_l\,, \quad \rho_{ijl} = \cos 2q_i \sin 2q_j \sin 2q_l\,. \end{aligned} \tag{2}$$

Here the indices k, j and l take on the values $x, y, z, i \neq j \neq l \neq i$, and $\boldsymbol{q} = a\boldsymbol{k}/8$, where $\boldsymbol{k}$ is the wave vector of the spin waves. The functions α_{ijl}, γ_{ijl}, etc. are combined into symmetrical groups $\alpha_\pm$, $\gamma_\pm$, etc., which are sums over even and odd permutations of the indices x, y, z. For example,

$$\begin{aligned} &\alpha_+ = (\alpha_{xyz} + \alpha_{zxy} + \alpha_{yzx})/3\,, \quad \alpha_- = (\alpha_{zyx} + \alpha_{yxz} + \alpha_{xzy})/3\,, \\ &\alpha = (\alpha_+ + \alpha_-)/2\,. \end{aligned} \tag{3}$$

The twenty branches of the magnon spectrum of YIG can be broken down into three groups according to the nature of the oscillations for $k = 0$.

(1) *a branches.* On these branches only the spins in the a positions oscillate at $k = 0$. There are four such branches: $\omega_3(\boldsymbol{k})$, $\omega_{7j}(\boldsymbol{k}), j = 1, 2, 3$. Here the first frequency index corresponds to the number of the irreducible representation, and the second one corresponds to the number of the basis function in the irreducible representation, if the latter is not one-dimensional. The frequencies of the a branches in the quasinormal approximation are

$$\begin{aligned} &\omega_3^0(\boldsymbol{k}) = \omega_a + 40J_{aa}\nu(\boldsymbol{k})\,, \quad \omega_a = -30J_{ad} + 40J_{aa}\,, \\ &\omega_{71}^0(\boldsymbol{k}) = \omega_{73}^0(\boldsymbol{k}) = \omega_a - 20J_{aa}\rho(\boldsymbol{k})\,. \end{aligned} \tag{4}$$

(2) *d branches.* On these branches only the d spins oscillate at $\boldsymbol{k} = 0$:

$$\omega_4^0(\boldsymbol{k}) = \omega_d + 20J_{dd}\alpha(\boldsymbol{k}), \quad \omega_d = -20(J_{ad} - J_{dd}), \quad \omega_{51}^0(\boldsymbol{k}) = \omega_d + 10J_{dd}\alpha(\boldsymbol{k}),$$

$$\omega_{62}^0(\boldsymbol{k}) = \omega_d - 10J_{dd}\alpha(\boldsymbol{k}), \quad \omega_{81}^0(\boldsymbol{k}) = \omega_d + 20J_{dd}\gamma(\boldsymbol{k}), \tag{5}$$

$$\omega_{82}^0(\boldsymbol{k}) = \omega_{83}^0(\boldsymbol{k}) = \omega_d - 10J_{dd}\gamma(\boldsymbol{k}).$$

The notation here follows the same principles as for the a branches.

(3) *a–d branches.* Here the spins at both the a and d positions oscillate. These branches arise because the same irreducible representations (τ_1 and τ_9) occur in the decomposition of the a and d permutation representations. Since the identity representation τ_1 is one-dimensional, while the representation τ_9 is three-dimensional, there are eight a–d branches. Their frequencies in the quasinormal approximation can be written in the form

$$\left.\begin{matrix}\omega_{ap}(\boldsymbol{k}) \\ \omega_{dp}(\boldsymbol{k})\end{matrix}\right\} = \tfrac{1}{2}\left[\sqrt{(A_p + D_p)^2 - 4|B_p^2|} \pm (A_p - D_p)\right];$$

$$p = 1, 91, 92, 93, \quad A_1(\boldsymbol{k}) = \omega_a - 40J_{aa}\nu(\boldsymbol{k}), \quad A_{91} = \omega_a - 40J_{aa}\rho(\boldsymbol{k}), \tag{6}$$

$$A_{92} = A_{93} = \omega_a + 20J_{aa}\rho(\boldsymbol{k}), \quad D_1(\boldsymbol{k}) = \omega_d - 20J_{dd}\alpha(\boldsymbol{k}), \quad D_{91}(\boldsymbol{k}) = \omega_d - 20J_{dd}\gamma(\boldsymbol{k}),$$

$$D_{92}(\boldsymbol{k}) = D_{93}(\boldsymbol{k}) = \omega_d + 10J_{dd}\gamma(\boldsymbol{k}), \quad B_1(\boldsymbol{k}) = 10\sqrt{6}J_{ad}\eta(\boldsymbol{k}),$$

$$|B_{91}(\boldsymbol{k})| = 10\sqrt{2}|J_{ad}|[\eta(\boldsymbol{k}) - \chi(\boldsymbol{k})], \tag{7}$$

$$|B_{92}(\boldsymbol{k})| = |B_{93}(\boldsymbol{k})| = 10\sqrt{2}|J_{ad}|[\eta(\boldsymbol{k}) - \chi(\boldsymbol{k})/2].$$

The letter index d is assigned to four modes [including the ferromagnetic (FM) mode τ_{d1}]. The excitation of a magnon of this type decreases the magnetization of YIG by one Bohr magneton, just as the excitation of any d-branch magnon does. On the other hand, the excitation of a magnon of the four branches with index a (including the antiferromagnetic (AFM) mode τ_{a1}) increases the magnetization by one Bohr magneton. This property is shared by any a mode.

In section 1.6 we obtain corrections to expressions (4), (5), and (6) for the frequencies $\omega_{d1}^0(\boldsymbol{k})$, $\omega_{a1}^0(\boldsymbol{k})$, $\omega_4^0(\boldsymbol{k})$ and $\omega_3^0(\boldsymbol{k})$ of the spin waves which are nondegenerate at $\boldsymbol{k} = 0$, using second-order perturbation theory in the off-diagonal elements of the Hamiltonian matrix in the quasinormal representation. The expressions obtained for the frequencies are entirely satisfactory and differ from the results of the numerical calculation by no more than a few percent.

In section 1.7 we construct a perturbation theory for the frequencies of the spin waves which are doubly and triply degenerate at $\boldsymbol{k} = 0$. The problem here is complicated by two factors. Firstly, because of the degeneracy it is necessary to exactly diagonalize matrices of dimensionality 2×2 or 3×3. Secondly the series expansion in $\boldsymbol{k}$ of several matrix elements which "mix" nearby modes of different representations begins with the first power of $\boldsymbol{k}$. Therefore, in a significant part of the Brillouin zone these matrix elements cannot be taken into account by perturbation theory and one is obliged to make exact canonical transformations to eliminate them. Only in this representation can one use the standard perturbation theory. We have carried out this program and found the

frequencies of the twenty spin-wave branches for the symmetric directions $\boldsymbol{k} \parallel [100]$ and $\boldsymbol{k} \parallel [111]$. Then for arbitrary directions of $\boldsymbol{k}$ we study qualitatively the frequencies of the degenerate spin wave branches, which have activation energies of no more than 300–400 K.

In the last subsection of section 1.8, we calculate the temperature dependence of the magnetization and specific heat of YIG in the approximation of noninteracting spin waves. The results are in good agreement with experimental data [7, 8].

The second chapter of the review deals with magnon interactions and relaxation in YIG. Those are the fundamental characteristics describing the response of any system to an external ac field. Almost all experiments aimed at magnon excitation have been carried out in the microwave frequency range where only magnons with energies 0.1–5 K can be excited. Nevertheless, all magnons with energy lower or of order of the temperature are involved in the processes of low energy magnon relaxation. Magnon interactions can be described by higher order terms of the Hamiltonian expansion in the series of magnon amplitudes. The theory of magnon interaction and relaxation based on the random phase approximation is presented in the section 2.1. The kinetic equation for magnons and the equation for their energy dependence on the occupation numbers is obtained. In section 2.2 we consider some experimental results concerned with magnon relaxation in the microwave range. Originally these data were interpreted using the theory for magnon relaxation in ferromagnets having a quadratic dispersion relation. It has been pointed out that the wave-vector dependent part of the ferromagnon damping $\Gamma(\boldsymbol{k}) = \gamma_1(\boldsymbol{k}) - \gamma_1(0)$ is due mainly to the three-magnon dipole–dipole and four-magnon exchange interactions with other ferromagnons [9]. It should be noted that the ferromagnon spectrum is quadratic only up to energies of 40 K after this the spectrum $\omega_1(k)$ becomes almost linear. Consequently, for $T > 40$ K the theory of the ferromagnon relaxation in YIG should differ substantially from the corresponding theory for ferromagnets. Furthermore, at $T \gtrsim 260$ K other types of magnons are excited, and the scattering by these magnons must also be taken into account.

The present study deals with the interactions of magnons in YIG in thermodynamic equilibrium at temperatures up to 300 K. We consider the exchange and magnetic-dipole terms in the YIG Hamiltonian and also a term due to the local uniaxial crystallographic anisotropy, find the corresponding amplitudes of the three- and four-magnon processes, and calculate the relaxation rate and the correction to the magnon energy due to these interactions.

In section 2.3 we study the magnon exchange interaction. We evaluate the temperature correction to the ferromagnon frequency to the first order in the interaction. This correction is positive, in contrast to the case of ferromagnets, and it is proportional to $(T/T_C)^{5/2}$ at temperatures up to 150 K, in agreement with experiment. The exchange-relaxation rate of the magnons is found as a function of the wave vector and temperature. In the region $T \lesssim 250$ K this rate agrees with the familiar expression for ferromagnets [10]. At higher temperatures, at which the main contribution to the exchange damping is from the magnons of the linear part of the spectrum, the temperature dependence of the damping becomes stronger.

In section 2.4 we study the magnetic dipole interaction of magnons. It is shown that this interaction is substantial only for the ferromagnons, since the variable magnetization component, which is due to optical modes, is practically absent. The amplitude of the three-magnon magnetic dipole interaction is well approximated over the entire Brillouin zone by the familiar long-wavelength asymptotic expression for the amplitude of this process in a ferromagnet. However, the magnetic dipole relaxation of the long-wavelength ferromagnons in YIG differs substantially from the corresponding relaxation in ferromagnets, since it is due to processes of coalescence with ferromagnons near the boundary of the Brillouin zone. The conservation laws admit these processes for k larger than a certain k_ℓ (see (2.90) below); at $k = k_\ell$ the processes of coalescence with

the ferromagnons are turned on over the entire linear region of the spectrum, leading to a jump in the wave-vector dependence of the relaxation rate at $k = k_f$. In the region $k < 3k_f$ the relaxation rate is nearly constant, and it is only for $k > 3k_f$ that the damping is linear in k, as it is in a ferromagnet. In spite of the fact that the amplitude of the magnetic dipole interaction is independent of the direction of the wave vectors with respect to the crystallographic axes, the damping of the long-wavelength ferromagnons is anisotropic because of the nonspherical shape of the Brillouin zone.

As we know, the contributions to the ferromagnon relaxation from the dipole–dipole and exchange interactions go to zero as $\boldsymbol{k} \to 0$, but experiment reveals the presence of a nonzero damping $\gamma_1(0)$ even in very pure samples [11]. This damping depends linearly on temperature in the range 150–350 K, and so it is natural to assume that it is due to three-wave processes. Kasuya and LeCraw, who first detected the damping $\gamma_1(0)$ in 1961, assumed that the relaxation of the long-wavelength ferromagnons is due to their scattering by a phonon and a ferromagnon with $k \approx 4 \times 10^6\ \mathrm{cm}^{-1}$, and the interaction is caused by modulation of the local uniaxial anisotropy constant in the field of the phonon[11, 12]. From that time on the relaxation of ferromagnons with $\boldsymbol{k} \to 0$ and other poorly understood properties of the damping of ferromagnons with $\boldsymbol{k} \neq 0$ (e.g., its anisotropy) were commonly attributed to "Kasuya–LeCraw processes". However an accurate analysis of this mechanism shows that the estimate of the damping $\gamma_1(0)$ in ref. [10] is at least an order of magnitude too large.

In section 2.5 we show that the main relaxation mechanism for long-wavelength ferromagnons is their coalescence with "optical" magnons having a gap in their spectrum. The gaps of the nineteen optical magnons in YIG exceed 200 K, whereas the frequency of the ferromagnons at $\boldsymbol{k} \to 0$ is of the order of 1 K. Therefore, the three-magnon processes involving low-wavelength ferromagnons are allowed near points of intersection or tangency of the optical branches of the spectrum. We show that these processes are due to the uniaxial crystallographic anisotropy of the Fe^{3+} ions and calculate the corresponding contribution to the relaxation of ferromagnons with $\boldsymbol{k} \to 0$.

In section 2.6 we compare the contributions to the ferromagnon relaxation in the various wave-vector and temperature regions and discuss the relationship of our results with experiment.

Section 3 presents the conclusion of our review.

1. Magnon spectra in YIG

1.1. Magnetic structure of YIG

1.1.1. Crystal structure of YIG

In contrast to natural garnet ($Ca_3Al_2Si_3O_{12}$), yttrium iron garnet cannot be found in the earth, it can be grown in vitro only [13, 14]. The structure of YIG coincides with that of natural garnet. The difference is that Ca is substituted by Y, and both Al and Si are substituted by Fe. The crystal structure of garnet is shown in fig. 1. The lattice has bcc structure, therefore a unit cell takes up a half of a cube with the lattice constant $a = 12.4$ Å in YIG. The space group of garnet is O_h^{10}. Only Fe ions have magnetic moment in YIG. There are eight octahedral sites (a) occupied by Al and twelve tetrahedral sites (d) occupied by Si in natural garnet. Fe ions occupy both a and d sites in YIG. The difference between these sites consists in different configurations of neighbouring O ions which are responsible for formation of the superexchange interaction between magnetic ions. The coordinates of the octahedral sites in units of the lattice constant are: $(0,0,0)$, $(0,\frac{1}{2},\frac{1}{2})$, $(\frac{1}{2},0,\frac{1}{2})$, $(\frac{1}{2},\frac{1}{2},0)$, $(\frac{1}{2},\frac{1}{2},\frac{1}{2})$, and $(\frac{1}{4},\frac{1}{4},\frac{1}{4})$ in the first octant. The coordinates of the tetrahedral sites in this

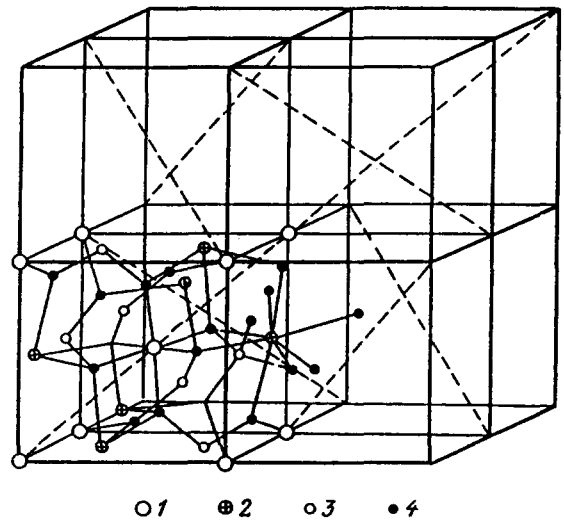

Fig. 1. Elementary cell of garnet. (1): (*a*) positions, (2): (*c*) positions, (3): (*d*) positions, (4): O ions.

octant are $(\frac{3}{8}, 0, \frac{1}{4})$, $(\frac{1}{4}, \frac{3}{8}, 0)$, and $(0, \frac{1}{4}, \frac{3}{8})$. One can find some more detailed information about YIG and related magnetic garnets in ref. [15].

1.1.2. Exchange interaction and spin Hamiltonian

In YIG the nearest magnetic neighbours are Fe ions in *a* and *d* sites. Each ion in *a* site has six nearest neighbours in *d* sites and each ion in *d* site has four nearest neighbours in *a* sites. The distance between nearest *a* and *d* sites is 3.46 Å [15]. Next nearest neighbours are Fe ions in tetrahedral sites, the distance between them is 3.79 Å [15]. There are four next nearest neighbours. The distance between two nearest sites *a* is 5.37 Å, there are eight neighbouring sites *a* for each *a* site. The superexchange interaction decreases rapidly with the increase of the distance between magnetic ions because electron configurations at Fe and O ions are well localized. An analysis of various experimental data: inelastic neutron scattering, temperature dependence of magnetization, and magnon spectrum in the microwave range, carried out in the review showed that the *a–d* exchange interaction is the strongest. The constant of *d–d* interaction is four times smaller, and the constant of *a–a* interaction is one order smaller than that of *a–d* interaction. Interaction between more distant magnetic moments is negligible.

As a result, the Heisenberg Hamiltonian H_{ex} is written in the form

$$H_{ex} = -2\sum_{n}\left(J_{aa}\sum_{i,j=1,j>i}^{8}\boldsymbol{S}_i(\boldsymbol{R}_{in})\sum_{d_{ij}}\boldsymbol{S}_j(\boldsymbol{R}_{in}+\boldsymbol{d}_{ij}) + J_{ad}\sum_{i=1}^{8}\sum_{j=9}^{20}\boldsymbol{S}_i(\boldsymbol{R}_{in})\sum_{d_{if}}\boldsymbol{S}_j(\boldsymbol{R}_{in}+\boldsymbol{d}_{ij})\right.$$
$$\left. + J_{dd}\sum_{i,j=9,j>i}^{20}\boldsymbol{S}_i(\boldsymbol{R}_{in})\sum_{d_{ij}}\boldsymbol{S}_j(\boldsymbol{R}_{in}+\boldsymbol{d}_{ij})\right). \tag{1.1}$$

Here n numbers the primitive cell, i and j number the sublattices ($i = 1, \ldots, 8$ number the *a* ions, $i = 9, \ldots, 20$ number the *d* ions), $\boldsymbol{S}_i(\boldsymbol{R}_{in})$ are the spin and coordinate of an ion of the ith sublattice in the nth cell and $\boldsymbol{d}_{ij}$ is the distance to the nearest neighbour in the jth sublattice. For the exchange

integrals we take the values

$$J_{ad} = -40.0 \pm 0.2\,\mathrm{K}\,, \quad J_{ad} = -13.4 \pm 0.2\,\mathrm{K}\,, \quad J_{aa} = -3.8 \pm 0.4\,\mathrm{K} \tag{1.2}$$

We shall discuss the question of refining the values of the exchange integrals for YIG later on in this review.

The constants of exchange interaction are negative, therefore the magnetic moments of ions in a and d positions are opposite in the low-temperature phase. The magnetization of YIG is due to unequal numbers of ions in these positions.

1.2. Review of experimental results

1.2.1. Thermodynamical properties of YIG

Thermodynamical properties of YIG spin system were actively investigated from the moment of YIG discovery until the mid sixties. The temperature dependences of the magnetization [16–19, 7], specific heat [20–23] and average magnetic moments of Fe ion in a and d sites [24–27, 17, 18] were measured. The problem was to find the values of exchange integrals J_{ad}, J_{dd} and J_{aa} from these data and to develop a consistent theory of YIG thermodynamical properties.

The temperature dependence of magnetization which is the most important thermodynamical characteristic is shown in fig. 2 [7]. This dependence differs from that for a ferromagnet with the same Curie temperature and spin per unit cell significantly. The first attempt to explain the dependence for YIG was to take in account two sublattices, of spins in a and d sites, in the mean field approximation [16, 7, 28]. The constants J_{ad}, J_{dd} and J_{aa} were found to fit the experimental data [7].

Unfortunately, the values of the exchange integrals $J_{ad} = -25.36$ K, $J_{dd} = -11.86$ K, $J_{aa} = -8.45$ K obtained that way proved not quite reasonable. In particular, they showed that the

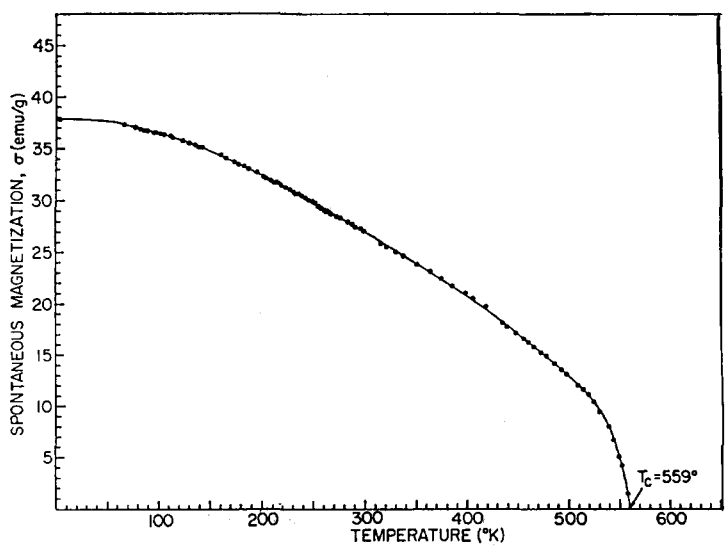

Fig. 2. Spontaneous magnetization of YIG [7]

energy of exchange interaction decreases with the distance very gradually: the constants of d–d and a–a interactions came 40% and 30% of the greatest a–d interaction constant. In addition, these values of the exchange constants provided an unacceptably small value for the magnon stiffness,

$$\omega_{ex} = -\tfrac{5}{16}(5J_{ad} - 3J_{dd} - 8J_{aa}) , \tag{1.3}$$

which was measured independently by microwave techniques [29, 30] and was obtained from the specific heat investigations [20, 23, 21]. The reason for such discrepancies is that the mean field theory is too rough to describe properties of real magnets in detail: it does not predict correct values of the Curie temperature and the critical exponents and it provides an incorrect low-temperature dependence of the magnetization because of neglecting magnons.

The studies of the specific heat of YIG at low temperature resulted in a reasonable agreement with the data from microwave studies (table 1). The problem was in the separation of contributions of diverse nature into the specific heat. It is relatively simple to separate magnon and phonon specific heats at low temperature, because the former is proportional to $T^{3/2}$ and the latter is proportional to T^3. However, at higher temperature the influence of optical magnons and phonons is significant, and it is impossible to separate these contributions without knowing the spectra of optical magnons and phonons. In particular, the temperature dependence of the specific heat deviates from $\sim T^3$ for temperature higher 10 K.

Another attempt to develop a suitable theory describing the thermodynamical properties of YIG was made by Harris [32, 2]. He studied magnon spectra of YIG in order to calculate the low-temperature magnetization and specific heat. This way is absolutely consistent but the exchange constants were not known at that time. Harris found that the quadratic approximation for the ferromagnon spectrum,

$$\omega_k = \omega_{ex}(ak)^2 , \tag{1.4}$$

is satisfactory in a small part of the Brillouin zone $(ak) \lesssim 1$ and obtained corrections to the terms $\sim T^3$ in the magnetization and specific heat dependences at low temperature. He also calculated the magnon spectra numerically for several arbitrarily chosen sets of exchange integrals.

Table 1
Summary of magnon stiffness data for YIG [7].

		D[a] (erg cm)^2
Magnetization	Anderson, 1964 [7]	29.9×10^{-30}
	Pauthenet, 1958 [16]	43
	Aléonard, 1960 [19]	44
	Wojtowicz, 1962 [31]	115
Specific heat	Endmonds and Petersen, 1959 [20]	51
	Harris and Meyer, 1961 [23]	63
	Kunzler et al. 1960 [21]	83
	Shinozaki, 1961 [22]	83
Microwave	Turner, 1960 [29]	99
	LeCraw and Walker, 1961 [30]	96

[a] $D = \omega_{ex} a^2$.

Unfortunately, the magnon spectra are fairly sensitive to the values of exchange integrals and therefore the calculated spectra would not help to explain the properties of YIG.

Since the mid sixties there was no significant progress in the studies of thermodynamical properties of YIG because of the absence of a suitable theory which could provide a correct interpretation of the variety of experimental data.

1.2.2. Magnon spectra: neutron scattering

Magnon spectra can also be obtained from inelastic neutron scattering data. It is probably the most direct way to investigate the magnon spectra. The most detailed investigation of the inelastic neutron scattering in YIG was carried out by Plant [4]. Three magnon branches were found for various directions of the magnon quasimomentum. Some of these results are presented in fig. 3. Unfortunately, even neutron scattering could not give the full picture of all twenty magnon branches in YIG because the amplitude of inelastic neutron scattering by optical magnons in YIG is fairly small compared to that for ferromagnon ("acoustic" magnon) scattering. Nevertheless, the data presented in ref. [4] provide an opportunity to obtain the values of the exchange constants J_{ad}, J_{dd}, and J_{aa}.

Formally, there are many possible sets of the values to fit the experimental data depending on a hypothesis about types of the three magnon branches observed. But acceptance of some additional information about reasonable values of the exchange integrals, in particular, (i) the value of the magnon stiffness obtained from microwave and specific heat measurements agrees with formula (1), (ii) the supposition that the three exchange constants are sufficient to describe all the magnon spectra, and (iii) the condition of stability of the ground state, lead to a single set of the exchange integrals.

The set of exchange integrals which we obtained from Plant's data differs from that obtained by Plant himself. The reason for this disagreement is that the set reported by Plant yields an instability of the ground state and involves a significant exchange interaction between further neighbours. The problem of a search for the set of exchange constants is discussed in section 1.4 in more detail.

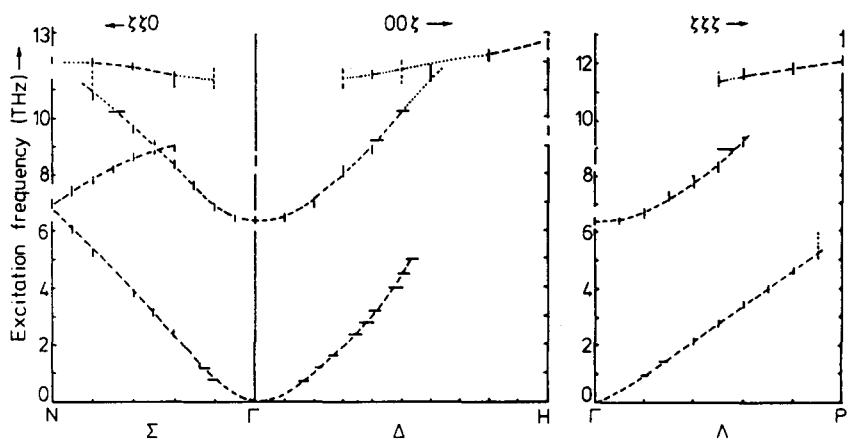

Fig. 3. Room-temperature results for magnon dispersion in YIG. $\Sigma: \boldsymbol{k} \parallel [110]$, $\Delta: \boldsymbol{k} \parallel [100]$, $\Lambda: \boldsymbol{k} \parallel [111]$ [4].

1.3. Quadratic Hamiltonian

1.3.1. Ground state and canonical variables

In order to find the magnon spectrum in a magnet one has to know the spin dynamics and the ground state. The dynamical properties of YIG spin system are described by the exchange Hamiltonian (1.1). However, the spin dynamics caused by the exchange interaction is very complicated in terms of the spin variables $\boldsymbol{S}_i$ because the dynamical equations

$$\mathrm{d}\boldsymbol{S}_i/\mathrm{d}t = \mathrm{i}[H, \boldsymbol{S}_i] \tag{1.5}$$

are fairly nonlinear. The usual way to avoid this problem is to express the spin operators $\boldsymbol{S}_i$ in terms of creation and annihilation Bose-like operators or in terms of canonical variables, in the classical limit. These operators can be introduced either by the Holstein–Primakoff ansatz [33],

$$\begin{aligned} &S_j^z = S_0 - a_j^\dagger a_j\,, \quad S_j^x - iS_j^y \equiv S_j^- = \sqrt{2S_0}\, a_j^\dagger \sqrt{1 - a_j^\dagger a_j/2S_0}\,, \\ &S_j^\dagger = (S_j^-)^\dagger = \sqrt{2S_0}\, a_j \sqrt{1 - a_j^\dagger a_j/2S_0}\, a_j \end{aligned} \tag{1.6}$$

or by the Dyson–Maleev ansatz [34, 35]

$$S_j^z = S_0 - a_j^\dagger a_j\,, \quad S_j^- = \sqrt{2S_0}\, a_j^\dagger\,, \quad S_j^\dagger = \sqrt{2S_0}\,[a_j - (1/2S_0)\, a_j^\dagger a_j^2] \tag{1.7}$$

being in agreement with the algebra of spin operators. In both the cases the operators $a, a^\dagger$ cannot be treated as Bose-operators in the strict sense because of finite dimensionality of the spin states space. In the low-temperature limit the occupation numbers $\langle a_j^\dagger a_j \rangle$ are small. This allows one (i) to consider the Bose-like operators $a_j^\dagger$ and a_j in eqs. (1.6) and (1.7) as simple Bose operators with an infinite number of states, and (ii) to neglect the nonlinear in $a_j^\dagger, a_j$ terms in the dynamic equations (1.5). The influence of the nonlinear terms manifests itself in the magnon relaxation and the temperature dependence of the magnon spectra. These magnon properties owing to magnon interaction described by the nonlinear terms are discussed in chapter 2.

The criterion for the temperature allowing one to neglect the influence of magnon interaction on the magnetization, magnon spectra, etc. in YIG is $T \lesssim 350$ K. More precisely, there are some differences in low-temperature criteria for various quantities, which are discussed in chapter 2. The linear approximation in the dynamic equations (1.5) is equivalent to the quadratic approximation in the Hamiltonian expressed in terms of the operators $a_j^\dagger, a_j$. It should be noted that the operators $a_j^\dagger, a_j$ can be considered classical field amplitudes in the linear approximation. These classical amplitudes obeying the canonical conditions, i.e. the Poisson brackets, are as follows [36]:

$$\{a_i, a_j\} = 0\,, \quad \{a_i, a_j^*\} = \delta_{ij}\,. \tag{1.8}$$

These conditions substitute commutation conditions for the operators $a_j^\dagger, a_j$. The operator nature of the spin variables results in the ground state energy and zero temperature magnetization but not in the magnon spectrum in this approximation.

It is worth mentioning here the problem of the ground state of ferrimagnets with mutually opposite directed sublattices. In this case Néel-like vacuum $|0\rangle_{\mathrm{N}}$ being nullified by all the annihilation operators:

$$a_j|0\rangle_{\mathrm{N}} = 0 \tag{1.9}$$

is not an eigenstate of the Heisenberg Hamiltonian. Anderson had shown in his early work [37] devoted to the quantum Heisenberg antiferromagnet that the true ground state can be considered as a magnon gas against the Néel-state background. The vacuum magnons slightly renormalize the ground state energy, zero temperature magnetization, magnon spectra etc. These corrections can be found easily when the magnon spectra and the transformation from the spin variables to the magnon amplitudes are known. Here we estimate these corrections only. For a spin with antiferromagnetic exchange interaction with its nearest neighbours, the mean longitudinal projection of the spin differs from its maximum value S_0. The difference ΔS can be estimated as follows [38],

$$\Delta S/S_0 \lesssim 1/SZ \,. \tag{1.10}$$

Here Z is the number of nearest neighbours. For a spin in (a) site there are $Z_a = 6$ nearest neighbours, therefore

$$\Delta S_a/S_0 \lesssim 1/6S_0 = \tfrac{1}{15} \,. \tag{1.11}$$

For a spin in (d) site, $Z_d = 4$, so

$$\Delta S_d/S_0 \lesssim 1/4S_0 = \tfrac{1}{10} \,. \tag{1.12}$$

Thus the sublattice magnetizations at zero temperature deviate a little from their quassiclassical values (which are $8S_0$ for (a) sublattice and $12S_0$ for (d) sublattice). Nevertheless, the temperature dependent part of the magnetization is proportional to the number of thermal magnons. This part of magnetization is very insensitive to the vacuum magnons, because the vacuum magnons manifest themselves only in a week renormalization of the thermal magnon spectra owing to magnon–magnon interactions.

If the mean-field corrections are unimportant it is more convenient to use the Holstein–Primakoff variables (1.6) because of their "hermiticity". (This property is useful for derivation of the kinetic equation.) As for the first-order perturbation theory effects considered here, the expansion of eqs. (1.6) and (1.7) coincide in this order.

1.3.2. Quadratic Hamiltonian and diagonalization procedure

The Heisenberg Hamiltonian of the spin system in YIG is discussed in section 1.1. It can be written as

$$H = -2\sum_n \Bigg(J_{aa} \sum_{i=1,\, j>i}^{8} \boldsymbol{S}_i(\boldsymbol{R}_{in}) \sum_{d_{ij}} \boldsymbol{S}_j(\boldsymbol{R}_{in} + \boldsymbol{d}_{ij}) + J_{ad} \sum_{i=1}^{8} \sum_{j=9}^{20} \boldsymbol{S}_i(\boldsymbol{R}_{in}) \sum_{d_{ij}} \boldsymbol{S}_j(\boldsymbol{R}_{in} + \boldsymbol{d}_{ij})$$
$$+ J_{dd} \sum_{i=9,\, j>i}^{20} \boldsymbol{S}_i(\boldsymbol{R}_{in}) \sum_{d_{ij}} \boldsymbol{S}_j(\boldsymbol{R}_{in} + \boldsymbol{d}_{ij}) \Bigg) \,. \tag{1.13}$$

Here n is the number of the primitive cell, i and j are the numbers of the sublattices: $i = 1, \ldots, 8$ for a ions, $i = 9, \ldots, 20$ for d ions, $\boldsymbol{S}_i(\boldsymbol{R}_{in})$ are the spin and coordinate of the ith sublattice in the nth cell, and $\boldsymbol{d}_{ij}$ is the distance between nearest neighbours of the ith and jth sublattices.

In order to obtain the magnon properties we substitute the spin operator S_i by functions of creation and annihilation operators according to the Holstein–Primakoff transform (1.6). To

determine the spectrum and eigenvectors of the oscillations, we consider the quadratic part of the Hamiltonian $H^{(2)}$ and transform into $\boldsymbol{k}$ space by the formula

$$a_j(\boldsymbol{k}) = \frac{1}{\sqrt{N}} \sum_n a_{jn} \exp(-\mathrm{i}\boldsymbol{k}\cdot\boldsymbol{R}_{jn}) , \tag{1.14}$$

where N is the number of cells in the crystal. Then

$$H^{(2)} = \sum_{\boldsymbol{k}} H_{\boldsymbol{k}} ,$$

$$\begin{aligned} H_{\boldsymbol{k}} &= \sum_{i,j=1}^{20} \{F_{ij}(\boldsymbol{k}) a_i^*(\boldsymbol{k}) a_j(\boldsymbol{k}) + [G_{ij}(\boldsymbol{k}) a_i^*(\boldsymbol{k}) a_j^*(-\boldsymbol{k}) + \text{c.c.}]\} \\ &= \sum_{i,j=1}^{8} A_{ij}(\boldsymbol{k}) a_i^*(\boldsymbol{k}) a_j(\boldsymbol{k}) + \sum_{i,j=9}^{20} D_{ij}(\boldsymbol{k}) a_i^*(\boldsymbol{k}) a_j(\boldsymbol{k}) \\ &\quad + \sum_{i=1}^{8} \sum_{j=9}^{20} [B_{ij}(\boldsymbol{k}) a_i^*(\boldsymbol{k}) a_j^*(-\boldsymbol{k}) + \text{c.c.}] , \end{aligned} \tag{1.15}$$

$$A_{ij} = A\delta_{ij} + 2S_0 J_{aa}\gamma_{ij}(\boldsymbol{k}) , \quad A = 2S_0(6J_{ad} - 8J_{aa}) , \quad D_{ij} = D\delta_{ij} + 2S_0 J_{dd}\gamma_{ij}(\boldsymbol{k}) ,$$

$$D = 8S_0(J_{ad} - J_{dd}) , \quad B_{ij} = 2S_0 J_{ad}\gamma_{ij}(\boldsymbol{k}) , \quad \gamma_{ij}(\boldsymbol{k}) = \sum_{\boldsymbol{d}_{ij}} \exp(i\boldsymbol{k}\cdot\boldsymbol{d}_{ij}) , \tag{1.16}$$

$$A_{ij} = A_{ij} , \quad D_{ji} = D_{ij} .$$

A similar form of the matrices A, B, and C is given in the paper by Harris [32], from which we have adopted the notation in eq. (1.15). The appearance of blocks of zeros in the matrices F_{ij} and G_{ij} is a consequence of the collinearity of the sublattices and the high symmetry of the exchange interaction.

It is well known that a quadratic Hamiltonian in its general form,

$$H_{\boldsymbol{k}} = \sum_{i,j}^{N} \{P_{ij}(\boldsymbol{k}) a_i^\dagger(\boldsymbol{k}) a_j(\boldsymbol{k}) + \tfrac{1}{2}[Q_{ij}(\boldsymbol{k}) a_i^\dagger(\boldsymbol{k}) a_j^\dagger(\boldsymbol{k}) + \text{c.c.}]\} , \tag{1.17}$$

can be diagonalized by the linear transformation

$$b_i(\boldsymbol{k}) = \sum_{j=1}^{N} [u_{ij} a_j(\boldsymbol{k}) + v_{ij} a_j^\dagger(-\boldsymbol{k})] . \tag{1.18}$$

Here the matrices U and V obey the canonical conditions

$$UU^\dagger - VV^\dagger = I , \quad UV^\dagger - VU^\dagger = 0 . \tag{1.19}$$

These conditions are the conditions for new operators $b_i(\boldsymbol{k})$, $b_i^\dagger(\boldsymbol{k})$ to be Bose operators. Consequently, a $(2N \times 2N)$ matrix Λ,

$$\Lambda = \begin{pmatrix} P & \vdots & Q \\ \cdots & \cdots & \cdots \\ -Q^\dagger & \vdots & P^\dagger \end{pmatrix}, \tag{1.20}$$

can be transformed into a diagonal matrix by the linear transformation

$$Y\Lambda Y^{-1} = \begin{pmatrix} \Omega & \vdots & 0 \\ \cdots & \cdots & \cdots \\ 0 & \vdots & -\Omega \end{pmatrix}, \tag{1.21}$$

where

$$Y = \begin{pmatrix} U & \vdots & V \\ \cdots & \cdots & \cdots \\ V & \vdots & U \end{pmatrix}, \quad Y^{-1} = \begin{pmatrix} U^\dagger & \vdots & -V^\dagger \\ \cdots & \cdots & \cdots \\ -V^\dagger & \vdots & U^\dagger \end{pmatrix}, \tag{1.22}$$

and Ω is the diagonal matrix $\Omega_{ij} = \omega_i \delta_{ij}$. The eigenvalues $\omega_i(k)$ are the very magnon spectra sought. The matrices P and Q contain some zero blocks for YIG:

$$P = \begin{pmatrix} A & \vdots & 0 \\ \cdots & \cdots & \cdots \\ 0 & \vdots & D \end{pmatrix}, \quad Q = \begin{pmatrix} 0 & \vdots & B \\ \cdots & \cdots & \cdots \\ B^\dagger & \vdots & 0 \end{pmatrix}. \tag{1.23}$$

As a result, the problem of finding the eigenfunctions and eigenvectors of the spin-wave oscillations reduces to the diagonalization of a 20×20 matrix,

$$\Lambda = \begin{pmatrix} A & B \\ -B^\dagger & D \end{pmatrix} \tag{1.24}$$

where the matrices A, B, and D represent the quadratic Hamiltonian $H^{(2)}$ (1.15). The diagonalizing transformation matrix $\tilde{Y}$ can be expressed in terms of a (8×8) matrix U_1, a (12×12) matrix U_2, a (8×12) matrix V, and a (12×8) matrix V_2,

$$\tilde{Y} = \begin{pmatrix} U_1 & \vdots & V_1 \\ \cdots & \cdots & \cdots \\ V_2 & \vdots & U_2 \end{pmatrix}, \quad \tilde{Y}^{-1} = \begin{pmatrix} U_1^\dagger & \vdots & -V_2^\dagger \\ \cdots & \cdots & \cdots \\ -V_1^\dagger & \vdots & U_2^\dagger \end{pmatrix}. \tag{1.25}$$

The first eight eigenvalues Λ here coincide with the eigenfrequencies, while the remaining twelve differ in sign.

The old variables a_j are expressed in terms of the new variables b_j by the matrix $\tilde{Y}^{-1}$,

$$a_i(\boldsymbol{k}) = \sum_{j=1}^{8} u_{ji}^{(1)}(\boldsymbol{k}) b_j(\boldsymbol{k}) - \sum_{j=9}^{20} v_{ji}(\boldsymbol{k}) b_j^{\dagger}(-\boldsymbol{k}) , \quad i = 1, \ldots, 8 ,$$
$$a_i^{\dagger}(-\boldsymbol{k}) = -\sum_{j=1}^{8} v_{ji}(\boldsymbol{k}) b_j(\boldsymbol{k}) + \sum_{j=9}^{20} u_{ji}^{(2)}(\boldsymbol{k}) b_j^{\dagger}(-\boldsymbol{k}) , \quad i = 9, \ldots, 20 . \tag{1.26}$$

In the new variables the Hamiltonian takes the diagonal form

$$H_k = \sum_{j=1}^{20} \omega_j(\boldsymbol{k}) b_j^{\dagger}(\boldsymbol{k}) b_j(\boldsymbol{k}) . \tag{1.27}$$

1.4. *Magnon spectra and normal variables of the quadratic Hamiltonian – the results of computer calculations*

1.4.1. *Results of computer calculations and the values of the exchange integrals*

In order to make concrete computer calculations, one must assign numerical values to the exchange integrals J_{ad}, J_{dd} and J_{aa}. These values can be found from experimental data only. There are a number of contradictory results concerning the exchange constants in YIG discussed in section 1.2. Our point of view is that the most reliable values of the exchange integrals can be obtained from analysis of inelastic neutron scattering data presented by Plant [4]. We used the set of exchange integrals

$$J_{ad} = -39.8 \text{ K} , \quad J_{dd} = -13.4 \text{ K} , \quad J_{aa} = -3.8 \text{ K} . \tag{1.28}$$

A further analysis of the inelastic scattering data leading to this set of values is presented further in section 1.8.

The magnon spectra evaluated by computer for $\boldsymbol{k} \parallel [100]$ and [110] with the values of exchange integrals (1.28) are given in fig. 4. The behaviour of the ferromagnetic mode $\omega_{d1}(\boldsymbol{k})$ at small values of ak is, of course, described by formula (1) in the introduction.

An interesting question is, up to what values of ak does the dispersion relation remain quadratic to an accuracy of, say, 10%? The answer can be obtained by analyzing the next term of the expansion in (1). For the standard values of J (eq. (1.28)) the coefficient of the $(ak)^4$ term is 8.5 K, and so the sought value is $ak \simeq 0.7$. For such values of k, we find $\omega_{d1} = 25$ K. At larger values of the frequency $\omega_{d1}(\boldsymbol{k})$ the dispersion relation is not in any sense quadratic. It is of fundamental importance that as ak increases the dispersion relation approaches a straight line,

$$\omega_{d1}(\boldsymbol{k}) = -\Delta + \omega_{\prime}(ak) . \tag{1.29}$$

The results of the computer calculations showed that the constants Δ and $\omega_{\prime}$ do not depend on the direction of the wave vector $\boldsymbol{k}$ (i.e. the spectrum (1.29) is isotropic) and they depend mostly on the exchange stiffness ω_{ex} but not on all the values of the exchange integrals. It was found that

$$\Delta \simeq \omega_{ex} \simeq 40 \text{ K} , \quad \omega_e \simeq 2\omega_{ex} = 80 \text{ K} . \tag{1.30}$$

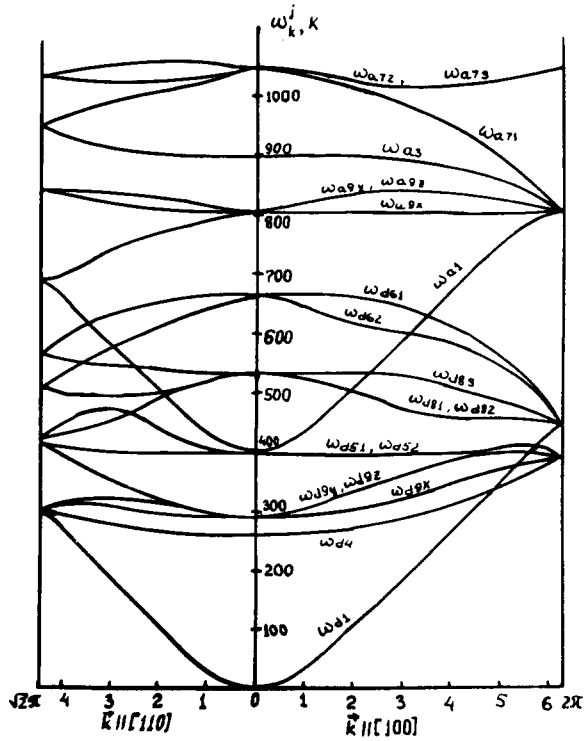

Fig. 4. Magnon spectra for the symmetric directions $\boldsymbol{k} \parallel [110]$, [100] and for the values of the exchange constants (1.28). $T = 0$ K [5].

The spectrum $\omega_{d1}(\boldsymbol{k})$ is not linear and anisotropic only in the vicinity of the edge of the Brillouin zone. This part of the spectrum is not universal, it depends on all the values of exchange integrals J_{ad}, J_{dd}, and J_{aa}. Nevertheless, the volume of that part of the Brillouin zone where the spectrum deviates from the linear behavior (1.30) is negligibly small for most quantities.

1.4.2. Ferromagnon and antiferromagnon modes

In an overview of the spectra it strikes one that the antiferromagnetic $\omega_{a1}(\boldsymbol{k})$ branch runs almost parallel to the ferromagnetic branch $\omega_{d1}(\boldsymbol{k})$ and they both are not noticeably perturbed in their multiple crossing of other branches. In the language of perturbation theory this means that the eigenvectors of the FM and AFM modes are practically unmixed with the other eigenvectors. Neglecting such an intermixing, we can obtain simple analytical expressions for the frequencies $\omega_{a1}(\boldsymbol{k})$ and $\omega_{d1}(\boldsymbol{k})$ of the FM and AFM branches over the entire Brillouin zone. To do this we assume that in (1.15) the oscillation amplitudes of all eight a and all twelve d spins are equal ($a_1 = \cdots = a_8, a_9 = \cdots = a_{20}$) and obtain

$$i\frac{da_i}{dt} = A_1 a_i + B_1 a_j^*\,, \quad -i\frac{da_j^*}{dt} = B_1 a_i + D_1 a_j^*\,, \quad i = 1, \ldots, 8, \quad j = 9, \ldots, 20\,. \tag{1.31}$$

Hence, we obtain for $\omega_{d1}(\boldsymbol{k})$ and $\omega_{a1}(\boldsymbol{k})$ the expressions (6) given in the introduction. The notation used for the coefficients is given in eq. (7).

Our assumptions about the equality of the amplitudes of the oscillations of the spins of the a and d ions is equivalent to the replacement of the 20-sublattice ferrite by a two-sublattice model. Here,

however, we have assumed that the phases of the oscillations of spins a and d are not the same over the unit cell, but rather $a(\boldsymbol{R}_{jn}) \sim \exp(\mathrm{i}\boldsymbol{k}\cdot\boldsymbol{R}_{jn})$, in accordance with eq. (1.14). The presence of a phase factor is a fundamental improvement over the naive two-sublattice model with identical phases of the oscillations within a unit cell. The two-sublattice approximation proposed here, as we shall show in section 1.8 gives quantitative description of the ferromagnetic and "antiferromagnetic" magnons over almost the entire Brillouin zone.

The success permitted us to suppose that the intermixing of all the remaining modes at values of ak that are not small is nevertheless in some sense small. To demonstrate this we determined in a numerical experiment the projections of the 20 eigenvectors for $\boldsymbol{k} \neq 0$ onto the eigenbasis for $\boldsymbol{k} = 0$ and found that the transition matrix between these bases is nearly block diagonal, with the eigenvectors of the same representations intermixed in the blocks.

1.5. Quadratic Hamiltonian for spin waves in quasinormal variables

Making use of the experience of previous investigators in regard to the application of group theory for analysis of the spectrum of homogeneous oscillations ($\boldsymbol{k} = 0$) of the magnetic systems of YIG [14, 39, 32], let us formulate an analytical theory for evaluating the frequencies $\omega_j(\boldsymbol{k})$ of all twenty types of spin waves.

1.5.1. Irreducible basis

Any transformation from the YIG symmetry group, O_h^{10}, produces a permutation of 8 sublattices of (a) type. This permutation can be described by an (8×8) permutation matrix which consists of elements equal either to 1 or to 0. The set of these matrices generates an eight-dimensional reducible representation of the point group O_h. This representation is constructed of two one-dimensional irreducible representations: τ_1 (identical) and τ_3, and of two three-dimensional irreducible representations: τ_7 and τ_9 [6]. The basis of the permutational representation can be given in lines of an unitary matrix as

$$U_a = \frac{1}{\sqrt{8}} \begin{pmatrix} 1 & 1 & 1 & 1 & 1 & 1 & 1 & 1 \\ 1 & 1 & 1 & 1 & -1 & -1 & -1 & -1 \\ \sqrt{3} & -1/\sqrt{3} & -1/\sqrt{3} & -1/\sqrt{3} & \sqrt{3} & -1/\sqrt{3} & -1/\sqrt{3} & -1/\sqrt{3} \\ 0 & 1 & \lambda^2 & \lambda & 0 & 1 & \lambda^2 & \lambda \\ 0 & 1 & \lambda & \lambda^2 & 0 & 1 & \lambda & \lambda^2 \\ \sqrt{3} & -1/\sqrt{3} & -1/\sqrt{3} & -1/\sqrt{3} & -\sqrt{3} & 1/\sqrt{3} & 1/\sqrt{3} & 1/\sqrt{3} \\ 0 & 1 & \lambda^2 & \lambda & 0 & -1 & -\lambda^2 & -\lambda \\ 0 & 1 & \lambda & \lambda^2 & 0 & -1 & -\lambda & -\lambda^2 \end{pmatrix},$$

$$\lambda = \exp(2\mathrm{i}\pi/3)\,. \tag{1.32}$$

Each of the irreducible representations is presented in eq. (1.32) only one time, therefore the matrix U_a produces a transformation of the block A of the Hamiltonian matrix to the diagonal form at $\boldsymbol{k} = 0$.

In the same way, the set of permutations of twelve d sublattices generates a twelve-dimensional reducible representation of the point group O_h. This representation is constructed of two one-dimensional irreducible representations: τ_1 and τ_4, two two-dimensional ones: τ_5 and τ_6, and two three-dimensional ones: τ_8 and τ_9. The basis of the reducible 12-dimensional representation can be written as

$$U_d = \frac{1}{\sqrt{12}} \begin{pmatrix}
1 & 1 & 1 & 1 & 1 & 1 & 1 & 1 & 1 & 1 & 1 & 1 \\
1 & 1 & 1 & 1 & 1 & 1 & -1 & -1 & -1 & -1 & -1 & -1 \\
1 & \lambda^2 & \lambda & 1 & \lambda^2 & \lambda & 1 & \lambda^2 & \lambda & 1 & \lambda^2 & \lambda \\
1 & \lambda & \lambda^2 & 1 & \lambda & \lambda^2 & 1 & \lambda & \lambda^2 & 1 & \lambda & \lambda^2 \\
1 & \lambda^2 & \lambda & 1 & \lambda^2 & \lambda & 1 & \lambda^2 & \lambda & 1 & \lambda^2 & \lambda \\
1 & \lambda & \lambda^2 & 1 & \lambda & \lambda^2 & 1 & \lambda & \lambda^2 & 1 & \lambda & \lambda^2 \\
1 & 1 & 1 & -1 & -1 & -1 & 1 & 1 & 1 & -1 & -1 & -1 \\
1 & \lambda^2 & \lambda & -1 & -\lambda^2 & -\lambda & 1 & \lambda^2 & \lambda & -1 & -\lambda^2 & -\lambda \\
1 & \lambda & \lambda^2 & -1 & -\lambda & -\lambda^2 & 1 & \lambda & \lambda^2 & -1 & -\lambda & -\lambda^2 \\
1 & 1 & 1 & -1 & -1 & -1 & -1 & -1 & -1 & 1 & 1 & 1 \\
1 & \lambda^2 & \lambda & -1 & -\lambda^2 & -\lambda & -1 & -\lambda^2 & -\lambda & 1 & \lambda^2 & \lambda \\
1 & \lambda & \lambda^2 & -1 & -\lambda & -\lambda^2 & -1 & -\lambda & -\lambda^2 & 1 & \lambda & \lambda^2
\end{pmatrix} \tag{1.33}$$

The matrix U_d makes the (12×12) block D of the Hamiltonian matrix diagonal.

Our goal in this section, which is of a preparatory nature, is to write the quadratic Hamiltonian H_k (for any $\boldsymbol{k}$) in the irreducible (for $\boldsymbol{k} = 0$) representation (i.e., after the transformation to the new basis by formula (1.18)), in which

$$u_{ij}^{(1)} = u_{aij}\,, \quad u_{ij}^{(2)} = u_{dij}\,, \quad v_{ij} = 0\,. \tag{1.34}$$

The Hamiltonian is specified by the matrices $A^{(1)}(\boldsymbol{k})$, $D^{(1)}(\boldsymbol{k})$, and $B^{(1)}(\boldsymbol{k})$ with the aid of the relations

$$\begin{aligned} &A^{(1)}(\boldsymbol{k}) = U_a A(\boldsymbol{k}) U_a^{-1}\,, \quad D^{(1)}(\boldsymbol{k}) = U_d D(\boldsymbol{k}) U_d^{-1}\,, \\ &B^{(1)}(\boldsymbol{k}) = U_a B(\boldsymbol{k}) U_d^{-1}\,. \end{aligned} \tag{1.35}$$

In writing the results of the matrix multiplication, we shall assign double indices to the rows and columns: $A^{(1)}_{mj,nl}$, $D^{(1)}_{mj,nl}$, and $B^{(1)}_{mj,nl}$. The first indices m and n give the irreducible representations, and i and j give the number of the basis function within a single representation, if it is not one-dimensional. Further, we shall separate out the diagonal terms in the matrices $A^{(1)}$ and $D^{(1)}$ and reduce the remaining terms to dimensionless form,

$$\begin{aligned} &A^{(1)}_{mj,nl} = \omega_a \delta_{m,n}\delta_{j,l} + 20|J_{aa}|a_{mj,nl}\,, \quad D^{(1)}_{mj,nl} = \omega_d \delta_{m,n}\delta_{j,l} + 10|J_{dd}|d_{mj,nl}\,, \\ &B^{(1)}_{mj,nl} = -10\sqrt{6}\,|J_{ad}|b_{mj,nl}\,, \quad \omega_a = 30\,|J_{ad}| - 40|J_{aa}|\,, \quad \omega_d = 20(|J_{ad}| - |J_{dd}|)\,. \end{aligned} \tag{1.36}$$

In this normalization the maximum values of the matrix elements a, b, and d which do not vanish as $\boldsymbol{k} \to 0$ are equal to unity. The matrices we seek are expressed in terms of combinations of trigonometric functions. Some of these combinations, $\alpha, \gamma, \eta, \chi, \rho$, and ν were already defined by formulas (2) and (3) in the introduction. The full list of the functions is

$$\alpha_{ijl} = \cos 2q_i \cos q_j \cos q_l\,, \quad \gamma_{ijl} = \cos 2q_i \sin q_j \sin q_l\,, \quad \eta_{ijl} = \cos 2q_i \cos q_j\,,$$
$$\chi_{ijl} = \sin 2q_i \sin q_j\,, \quad \nu_{ijl} = \cos 2q_i \cos 2q_j \cos 2q_l\,, \quad \rho_{ijl} = \cos 2q_i \sin 2q_j \sin 2q_l\,, \tag{1.37a}$$

$$\beta_{ijl} = \sin 2q_i \sin q_j \sin q_l\,, \quad \delta_{ijl} = \sin 2q_i \cos q_j \cos q_l\,, \quad \varepsilon_{ijl} = \cos 2q_i \sin q_j \cos q_l\,,$$
$$\zeta_{ijl} = \sin 2q_i \cos q_j \sin q_l\,, \quad \theta_{ijl} = \cos 2q_i \sin q_j\,, \quad \mu_{ijl} = \sin 2q_i \cos q_j\,. \tag{1.37b}$$

Here, as before, the indices i, j, and l take on the values x, y, and z, $q = ak/8$, and $i \neq j \neq l \neq i$. The functions (1.37), like the functions (2), are combined into symmetric combinations $\beta_\pm, \delta_\pm, \ldots$ according to rule (3). In addition, a new type of symmetric combinations arises: $\tilde{\alpha}_\pm, \tilde{\beta}_\pm, \tilde{\gamma}_\pm$, etc., which are the sums over the even and odd permutations of x, y, and z with weight factors of $1, \lambda = \exp(2i\pi/3)$, and λ^2. For example,

$$\tilde{\alpha}_\pm = (\lambda^2 \alpha_{xyz} + \lambda \alpha_{zxy} + \alpha_{yzx})/3\,, \quad \tilde{\alpha}_- = (\lambda^2 \alpha_{zyx} + \lambda \alpha_{yxz} + \alpha_{xzy})/3\,, \quad \tilde{\alpha} = (\tilde{\alpha}_+ + \tilde{\alpha}_-)/2\,. \tag{1.38}$$

The remaining definitions ($\tilde{\beta}_\pm, \tilde{\gamma}_\pm$, etc.) differ only by replacement of the Greek letter.

To describe the Hamiltonian matrix in the irreducible basis we begin with the most awkward matrix D. Its diagonal blocks with respect to the irreducible representation are of the form

$$d_{11} = -d_{44} = 2\alpha(\boldsymbol{k})\,, \quad d_{66} = -d_{55} = \begin{pmatrix} \alpha & -\tilde{\alpha}^* \\ -\tilde{\alpha}^* & \alpha \end{pmatrix},$$
$$d_{88} = d_{99} = \begin{pmatrix} -2\gamma & \tilde{\gamma}^* & \tilde{\gamma} \\ \tilde{\gamma} & \gamma & -2\tilde{\gamma}^* \\ \tilde{\gamma}^* & -2\tilde{\gamma} & \gamma \end{pmatrix}, \tag{1.39}$$

$$d_{14} = d_{41}^* = 2i\beta\,, \quad d_{46} = -d_{45} = (\tilde{\alpha}^*, \tilde{\alpha})\,, \quad d_{15} = -d_{16} = i(\tilde{\beta}^*, \tilde{\beta})\,,$$

$$d_{56} = i\begin{pmatrix} \beta & -\tilde{\beta} \\ -\tilde{\beta}^* & \beta \end{pmatrix},$$
$$d_{89} = i\begin{pmatrix} -2\delta & \tilde{\delta}^* & \tilde{\delta} \\ \tilde{\delta} & \delta & -2\tilde{\delta}^* \\ \tilde{\delta}^* & -2\tilde{\delta} & \delta \end{pmatrix}. \tag{1.40}$$

The blocks which intermix the three-dimensional representations with one- and two-dimensional representations have the most complicated appearance. They can be written in the form

$$
\begin{aligned}
&d_{mn} = d^{\dagger}_{mn} - d^{-}_{mn}\,, \quad m = 1,4,5,6, \quad n = 8,9\,,\\
&d^{\pm}_{18} = -d^{\pm}_{19} = \mathrm{i}(\varepsilon_{\pm}, \lambda^2\tilde{\varepsilon}^{*}_{\pm}, \lambda\tilde{\varepsilon}_{\pm})\,, \quad d^{\pm}_{18} = -d^{\pm}_{19} = (\zeta_{\pm}, \tilde{\zeta}^{*}_{\pm}, \tilde{\zeta}_{\pm})\,,\\
&d^{\pm}_{58} = -d^{\pm}_{69} = \mathrm{i}\begin{pmatrix} \tilde{\varepsilon}_{\pm} & \lambda^{\pm 1}\varepsilon_{\pm} & \lambda^2\tilde{\varepsilon}^{*} \\ \tilde{\varepsilon}^{*}_{\pm} & \lambda\tilde{\varepsilon}_{\pm} & \lambda^{\mp 1}\varepsilon_{\mp} \end{pmatrix}, \quad d^{\pm}_{68} = -d^{\pm}_{59} = \begin{pmatrix} \tilde{\zeta} & \lambda^{\pm 1}\zeta_{\pm} & \lambda^2\tilde{\zeta}^{*}_{\pm} \\ \tilde{\zeta}^{*}_{\pm} & \lambda\tilde{\zeta}_{\pm} & \lambda^{\mp 1}\zeta_{\pm} \end{pmatrix}.
\end{aligned}
\tag{1.41}
$$

The matrix B, which describes the interaction of the a ions with the d ions, has the form

$$
\begin{aligned}
&b_{14} = b_{16} = b_{19} = b_{34} = b_{36} = b_{39} = 0\,, \quad b_{11} = (\eta_{+} + \eta)/2 \equiv \eta\,,\\
&b_{15} = (\tilde{\eta}_{+} + \tilde{\eta}_{-}, \tilde{\eta}^{*}_{+} + \tilde{\eta}^{*}_{-})/2\,, \quad b_{18} = -i\tfrac{1}{2}(\theta_{+} - \theta_{-}, \tilde{\theta}_{+} - \tilde{\theta}_{-}, \tilde{\theta}^{*}_{+} - \tilde{\theta}^{*}_{-})\,.
\end{aligned}
\tag{1.42}
$$

The matrices b_{3m} can be obtained from b_{1m} by changing the signs in front of the terms $\eta_{-}, \tilde{\eta}_{-}, \theta_{-}$ and $\tilde{\theta}_{-}$. In precisely the same way, the matrices b_{7m} and b_{9m} differ by the sign in front of the combinations having a minus sign as subscript: $\chi_{-}, \tilde{\chi}_{-}, \theta_{-}$ etc. We shall therefore give only the blocks of b_{9m},

$$
\begin{aligned}
&b_{91} = \frac{1}{2\sqrt{3}}\begin{pmatrix} (\chi_{+} - \chi_{-}) \\ (\tilde{\chi}_{+} - \lambda\tilde{\chi})^{*} \\ (\tilde{\chi}_{+} - \lambda\tilde{\chi}_{-}) \end{pmatrix}, \quad b_{95} = \frac{1}{2\sqrt{3}}\begin{pmatrix} (\tilde{\chi}_{+} - \tilde{\chi}_{-}) & (\tilde{\chi}_{+} - \tilde{\chi}_{-})^{*} \\ (\chi_{+} - \lambda^2\chi_{-})^{*} & (\tilde{\chi}_{+} - \lambda^2\tilde{\chi}_{-}) \\ (\tilde{\chi}_{+} - \lambda^2\tilde{\chi}_{-}) & (\chi_{+} - \lambda\chi_{-}) \end{pmatrix},\\
&b_{98} = \frac{\mathrm{i}}{2\sqrt{3}}\begin{pmatrix} (\mu_{+} + \mu_{-}) & (\tilde{\mu}_{+} + \tilde{\mu}_{-}) & (\tilde{\mu}_{+} + \tilde{\mu}_{-})^{*} \\ (\tilde{\mu}_{+} + \lambda\tilde{\mu}_{-})^{*} & (\mu_{+} + \lambda\mu_{-}) & (\tilde{\mu}_{+} + \lambda^2\tilde{\mu}_{-}) \\ (\tilde{\mu}_{+} + \lambda\tilde{\mu}_{-}) & (\tilde{\mu}_{+} + \lambda^2\tilde{\mu}_{-})^{*} & (\mu_{+} + \lambda^2\mu_{-}) \end{pmatrix},\\
&b_{94} = b^{(1)}_{94} + b^{(2)}_{94}\,, \quad b_{96} = b^{(1)}_{96} + b^{(2)}_{96}\,, \quad b_{99} = b^{(1)}_{99} + b^{(2)}_{99}\,,\\
&b^{(1)}_{94} = \frac{\mathrm{i}}{2\sqrt{3}}\begin{pmatrix} \theta_{+} - \theta \\ \lambda(\tilde{\theta}_{+} - \tilde{\theta}_{-})^{*} \\ \lambda^2(\tilde{\theta}_{+} - \tilde{\theta}_{-}) \end{pmatrix}, \quad b^{(1)}_{96} = \frac{\mathrm{i}}{2\sqrt{3}}\begin{pmatrix} (\tilde{\theta}_{+} - \tilde{\theta}_{-}) & (\tilde{\theta}_{+} - \tilde{\theta}_{-})^{*} \\ \lambda(\theta_{+} - \theta_{-}) & \lambda(\tilde{\theta}_{+} - \tilde{\theta}_{-})^{*} \\ \lambda^2(\tilde{\theta}_{+} - \tilde{\theta}_{-})^{*} & \lambda^2(\theta_{+} - \theta_{-}) \end{pmatrix},\\
&b^{(2)}_{94} = -\frac{\mathrm{i}}{2\sqrt{3}}\begin{pmatrix} (\mu_{+} - \mu_{-}) \\ \lambda^2(\tilde{\mu}_{+} - \tilde{\mu}_{-})^{*} \\ \lambda(\tilde{\mu}_{+} - \tilde{\mu}_{-}) \end{pmatrix}, \quad b^{(2)}_{96} = -\frac{\mathrm{i}}{2\sqrt{3}}\begin{pmatrix} (\tilde{\mu}_{+} - \tilde{\mu}_{-}) & (\tilde{\mu}_{+} - \tilde{\mu}_{-})^{*} \\ (\lambda^2\mu_{+} - \mu_{-}) & (\lambda^2\tilde{\mu}_{+} - \tilde{\mu}_{-}) \\ (\lambda^2\tilde{\mu}_{+} - \tilde{\mu}_{-})^{*} & (\lambda\mu_{+} - \mu_{-}) \end{pmatrix},\\
&b^{(1)}_{99} = -\frac{1}{2\sqrt{3}}\begin{pmatrix} (\eta_{+} + \eta_{-}) & (\tilde{\eta}_{+} + \tilde{\eta}_{-}) & (\tilde{\eta}_{+} + \tilde{\eta}_{-})^{*} \\ \lambda(\tilde{\eta}_{+} + \tilde{\eta}_{-})^{*} & \lambda(\eta_{+} + \eta_{-}) & \lambda(\tilde{\eta}_{+} + \tilde{\eta}_{-}) \\ \lambda^2(\tilde{\eta}_{+} + \tilde{\eta}_{-}) & \lambda^2(\tilde{\eta}_{+} + \tilde{\eta}_{-})^{*} & \lambda^2(\eta_{+} + \eta_{-}) \end{pmatrix},\\
&b^{(2)}_{99} = \frac{1}{2\sqrt{3}}\begin{pmatrix} (\chi_{+} + \chi_{-}) & (\tilde{\chi}_{+} + \tilde{\chi}_{-}) & (\tilde{\chi}_{+} + \tilde{\chi}_{-})^{*} \\ (\lambda\tilde{\chi}_{+} + \chi_{-})^{*} & (\lambda^2\chi_{+} + \chi_{-}) & (\lambda^2\tilde{\chi}_{+} + \tilde{\chi}_{-}) \\ (\lambda\tilde{\chi}_{+} + \chi_{-}) & (\lambda^2\tilde{\chi}_{+} + \chi_{-})^{*} & (\lambda\chi_{+} + \chi_{-}) \end{pmatrix}.
\end{aligned}
\tag{1.43}
$$

One should not be frightened by the cumbersome form of the matrix b_{mn}. At $\boldsymbol{k} = 0$ it simplifies to the utmost, with all of its blocks vanishing except b_{11} and $b_{99}^{(1)}$, which intermix identical representations. The diagonal elements of these blocks will be taken into account exactly. Next in importnce are the blocks which are linear in $\boldsymbol{k}$. These are b_{38}, b_{78}, b_{98}, $b_{74}^{(1)}$, $b_{76}^{(1)}$, $b_{74}^{(2)}$, $b_{76}^{(2)}$, $b_{94}^{(1)}$, and $b_{96}^{(2)}$. The expansion of the matrix elements of the remaining blocks in a series in $\boldsymbol{k}$ begins at the second order in $\boldsymbol{k}$ or higher. As a rule, it is sufficient to take them into account in the lowest order of perturbation theory over the entire Brillouin zone.

The A matrix, of dimension 8×8, is constructed rather simply:

$$a_{11} = -a_{33} = 2v(\boldsymbol{k}) \,, \; a_{1m} = 0 \quad \text{for} \quad m \neq 1 \,, \; a_{3m} = 0 \quad \text{for} \quad m \neq 3 \,,$$

$$a_{77} = -a_{99} = \begin{pmatrix} -2\rho & \tilde{\rho} & \tilde{\rho}^* \\ \tilde{\rho}^* & \rho & -2\tilde{\rho} \\ \tilde{\rho} & -2\tilde{\rho}^* & \rho \end{pmatrix} . \tag{1.44}$$

Here only a_{11} and a_{33} are large at small k. The expansion of the remaining coefficients begins with terms of at least second order and, as a rule, can be taken into account by perturbation theory.

1.5.2. Quasinormal basis

We recall that in the "irreducible" basis of the Hamiltonian matrix, four pairs of off-diagonal elements remained in the matrix B at $\boldsymbol{k} = 0$. These were $b_{11}(0) = I$ and $b_{9j,9l} = -\delta_{j,l}/\sqrt{3}$. These elements can easily be eliminated with the aid of four independent u–v transformations, each of which involves only a single pair of eigenvectors. The coefficients of these transformations can be written in the form

$$u_p(\boldsymbol{k}) = \tfrac{1}{2}(\sqrt{C_p + 2|B_p|} + \sqrt{C_p - 2|B_p|})(C_p^2 - 4|B_p|^2)^{-1/4} \,,$$

$$v_p(\boldsymbol{k}) = -(B_p/2|B_p|)(\sqrt{C_p + 2|B_p|} - \sqrt{C_p - 2|B_p|})(C_p^2 - 4|B_p|^2)^{-1/4} \,, \tag{1.45}$$

$$C_p = A_p + D_p \,.$$

Here $B_p \equiv B_{pp}^{(1)}$ is a nonzero element of the matrix $B^{(1)}(p = 1, p = 9.1; 9.2; 9.3)$, $A_p \equiv \mathrm{A}_{pp}^{(1)}(\boldsymbol{k})$, and $D_p \equiv D_{pp}^{(1)}(\boldsymbol{k})$. In the new basis the Hamiltonian matrix is diagonal at $k = 0$ and is nearly diagonal in a significant portion of the Brillouin zone. It is natural to call such a basis "quasinormal". The diagonal elements of the Hamiltonian matrix in this basis give the approximate expressions for the spin-wave frequencies given in formulas (4)–(7) of the introduction.

1.6. Perturbation theory for nondegenerate modes

1.6.1. Ferromagnetic mode

The dispersion relation of the ferromagnetic mode in the "quasinormal" approximation is given by the expressions (6), which were obtained in section 1.4.2 from simple considerations. This expression gives a good approximation for the frequency $\omega_{d1}^0(\boldsymbol{k})$ of the ferromagnons over the

entire Brillouin zone. Expanding ω_{d1}^0 as $k \to 0$, we find

$$\omega_{d1}^0(\boldsymbol{k}) = \omega_{ex}(ak)^2 + [E^0 + F^0 f_4(\boldsymbol{n})](ak)^4 , \tag{1.46}$$

$$E^0 = \tfrac{5}{4096}|J_{ad}|(-214 + 103J_{dd}/J_{ad} + 410\tfrac{2}{3}J_{aa}/J_{ad} - 50J_{dd}^2/J_{ad}^2 - 800J_{aa}^2/J_{ad}^2) ,$$

$$F^0 = \tfrac{5}{4096}|J_{ad}|(\tfrac{10}{9} + J_{dd}/J_{ad} + \tfrac{128}{9}J_{aa}/J_{ad}) . \tag{1.47}$$

The coefficient ω_{ex} agrees with the exact expression (1). The coefficient E_0 is 2% smaller than that obtained by Harris [2] from consistent expansion of the ferromagnon frequency in series in the wave vector powers. The ratio $F^0/E^0 \sim 10^{-2}$ for the chosen exchange integrals, while Harris obtained $F = 0$. The ferromagnon frequency expansion of the fourth order in power of $\boldsymbol{k}$ obtained by Harris deviates from the exact frequency about 10% at $ak = 1$, i.e., at $k \approx k_m/5$, where k_m is the wave vector at the edge of the Brillouin zone. As for the approximate formula (6), the deviation is $< 1\%$ at $k \simeq k_m/5$, and it gives the frequency to within an error of 5% at the edge of the Brillouin zone. Of course, in discussing the degree of accuracy we are comparing the approximate expressions not with the true values of the spin-wave frequencies in YIG but with the values that can be obtained by exactly solving the equations of motion (by computer, for instance). With the same accuracy one can expand the trigonometric functions in (2) to order q^4 and obtain a "practical" formula for the frequency from which the small terms have been dropped:

$$\omega_{pr}(\boldsymbol{k}) = 5|J_{ad}|\{[1 + 40(1 - K/2 - 2L)q^2 - (28 - 2f_4(\boldsymbol{n}))q^4]^{1/2} - 1 - 2(K - 4L)q^2\} , \tag{1.48}$$

$$\boldsymbol{q} = a\boldsymbol{k}/8 , \quad \boldsymbol{n} = \boldsymbol{k}/k , \quad K = J_{dd}/J_{ad} , \quad L = J_{aa}/J_{ad} , \quad f_4(n) = 3(n_x^2 n_y^2 + n_x^2 n_z^2 + n_y^2 n_z^2) .$$

In this formula one can readily see the linear part of the k dependence and the low degree of crystallographic anisotropy that appear in the numerical calculation. We note that the linear part of the spectrum is due to the circumstance that YIG is almost an antiferromagnet: For every three d spins there are two a spins with the opposite equilibrium orientation.

In the second order of perturbation theory the correction to the frequency is

$$\omega_{d1}^{(2)}(\boldsymbol{k}) = \omega_{d1}^0(\boldsymbol{k}) - \sum_{m \neq 1, j} \frac{|D_{1,mj}^{(2)}|^2}{\omega_{dmj}^0(\boldsymbol{k}) - \omega_{d1}^0(\boldsymbol{k})} - \sum_{n \neq 1, l} \frac{|B_{nl,1}^{(2)}|^2}{\omega_{an1}^0(\boldsymbol{k}) + \omega_{d1}^0(\boldsymbol{k})} . \tag{1.49}$$

Here the matrix elements $D_{1,mj}^{(2)}$ and $B_{nl,1}^{(2)}$ are obtained after an u–v transformation (1.45) of the original matrices (1.36). The first group of terms, proportional to $|D|^2$, arises as a result of the mixing in of the d modes; the second group, proportional to $|B|^2$, from the mixing in of the a modes. All of these terms are nonzero, but the main correction to the frequency ω_{d1}^0 is from the matrix elements proportional to k^2 at small k, namely $D_{1,5j}^{(2)}$ $(j = 1, 2)$ and $B_{71,1}^{(2)}$ $(l = 1, 2, 3)$. Taking only these modes into account, we obtain from (1.49).

$$\omega_{d1}^{(2)}(\boldsymbol{k}) = \omega_{d1}^0(\boldsymbol{k}) - \frac{5[J_{dd}u_1(\boldsymbol{k}) - J_{ad}v_1(\boldsymbol{k})]^2}{\omega_{d5}(0) + \omega_{d1}^0(\boldsymbol{k})}[1 - f_4(\boldsymbol{n})]q^4$$

$$- \frac{40}{27}\frac{J_{ad}^2 u_1^2(\boldsymbol{k})}{\omega_{a7}(0) + \omega_{d1}(\boldsymbol{k})} f_4(\boldsymbol{n})q^4 . \tag{1.50}$$

The next largest matrix elements are $D_{1,8j}$ ($j = 1, 2, 3$), whose expansion begins with terms cubic in $\boldsymbol{k}$. Their contribution to $\omega_{d1}^{(2)}$ is proportional to $(ak)^6$ and falls off rapidly with decreasing k. Furthermore, their contribution goes to zero for $\boldsymbol{k} \parallel [111]$ or $[100]$ and, hence, has an additional, angular smallness. Estimates show that this contribution does not exceed 1%, and we shall not even write it out.

1.6.2. Antiferromagnetic mode

The frequency $\omega_{a1}^0(\boldsymbol{k})$ of the antiferromagnetic mode in the quasinormal approximation is given by the second of expressions (6). The accuracy of this formula is not worse that 1% at the edge of the Brillouin zone. In the second order of perturbation theory

$$\omega_{a1}^{(2)}(\boldsymbol{k}) = \omega_{a1}^0(\boldsymbol{k}) - 5\frac{[J_{ad}u_1(\boldsymbol{k}) - J_{dd}v_1(\boldsymbol{k})]^2}{\overline{\omega_{ds}^0(0)} + \overline{\omega_{a1}^0(0)}}[1 - f_4(\boldsymbol{n})]q^4 . \tag{1.51}$$

1.6.3. Soft d modes

The soft d mode ω_{d4} has a minimal gap ≈ 260 K for the standard choice of exchange integrals (1.28). The formula for the correction to the frequency of this mode is obtained from (1.49) by replacing the index 1 with 4. The largest contribution to the correction is due to the interaction with the ω_{a7} mode:

$$\omega_{d4}^{(2)}(\boldsymbol{k}) = \omega_{d4}^0(\boldsymbol{k}) - \frac{|B_{71.4}|^2 + 2|B_{12.4}|^2}{\omega_{a7}^0(\boldsymbol{k}) + \omega_{d1}(\boldsymbol{k})} = \omega_{di}^0(\boldsymbol{k}) - 10\frac{J_{ad}^2 q^2}{\omega_{a7}^0 + \omega_{d4}^0(\boldsymbol{k})} . \tag{1.52}$$

It is seen that the correction to the frequency amounts to 30% of the dispersion of the mode; allowance for this correction reduces the disagreement between the analytical expression for $\omega_{d4}^{(2)}$ and the numerical results to 10%.

We note that the $\omega_{d4}(\boldsymbol{k})$ branch crosses the ferromagnetic branch $\omega_{d1}(\boldsymbol{k})$ at $ak \simeq 2$. The matrix element $|D_{1.4}^{(2)}|$ for the interaction of these oscillations at such values of k is approximately equal to 3 K. The behavior of the functions $\omega_{d1}(\boldsymbol{k})$ and $\omega_{d4}(\boldsymbol{k})$ near the crossing is described by the usual formula (see, for example, section 39 in ref. [40]). The splitting $2|D_{14}^{(2)}|$ of the spectra is small, and this effect may, as a rule, be neglected.

The last of the nondegenerate modes, ω_{a3}, has an energy of the order of 1000 K and is never excited at temperatures $T < T_c = 560$ K. We shall therefore not write out the correction to the frequency of this mode.

1.7. Approximate calculation of the spectra

The procedure described in the previous section for approximate calculations of the spectra is efficient if the off-diagonal matrix elements are small in comparison with the difference (or sum) of the corresponding frequencies. For the majority of matrix elements this condition does in fact hold. However, for frequencies which are close together or degenerate this condition can be violated, and simple perturbation theory is inapplicable. Since the "large" matrix elements are not too great in number, one can use an approximate procedure for diagonalizing the matrices by a sequence of two-dimensional rotations.

To do this we associate with each off-diagonal matrix element through formula (1.45) a coefficient $v_{pp'}$ which characterizes the size of the elementary "rotation" that would cause this element to vanish. We then do the "rotation" corresponding to the maximum $|v_{pp'}|$ and again analyze the resulting Hamiltonian matrix in the same way as before. Then we can again perform the next "largest" rotation. After several rotations the Hamiltonian matrix is almost diagonal and then one may use standard perturbation theory. Such a program of analytical calculations will be constructive if the number of large rotations is not too large, so that the expressions obtained for the frequencies are not too unwieldy.

1.7.1. Magnon spectra for $\boldsymbol{k} \parallel [100]$ *and* $[111]$

We have carried out this program for the symmetric wave-vector directions $\boldsymbol{k} \parallel [100]$ and [111]. Here we shall only describe the sequence of two-dimensional rotations, as the reader may find detailed results for the evaluated spectra in our blueprint [41].

For the direction $\boldsymbol{k} \parallel [111]$ the Hamiltonian matrix decomposes into two 4×4 and two 6×6 blocks. One of the small blocks couples the oscillations of the ferromagnetic, antiferromagnetic, and soft $d(\tau_{d4})$ modes and also the a mode τ_{a71}, which is triply degenerate at $\boldsymbol{k} = 0$. This block becomes almost diagonal after a rotation that defines the ferro- and antiferromagnetic oscillations in terms of the vectors τ_{a1} and τ_{d1}. The other small block couples the vectors τ_{a3}, τ_{d81}, and τ_{d91}. With the aid of a rotation that intermixes τ_{a91} and τ_{d91} and a second rotation that intermixes τ_{d81} with the new a–d oscillation τ_{d1}, this block is reduced to an almost diagonal form.

The 6×6 blocks are complex conjugate, so it is sufficient to consider one of them, say, that which mixes the vectors τ_{a72}, τ_{a92}, τ_{d51}, τ_{d61}, τ_{d82}, and τ_{d92}. To diagonalize this block one must perform four exact rotations. The first of these intermixes the vector of identical representations τ_{a92} and τ_{d92} and gives a pair of a–d modes. The next rotation mixes the vectors τ_{d82} and τ_{d92}. Finally, the last two rotations intermix the pairs of vectors τ_{d51} and τ_{d92} and τ_{d61} and τ_{d82}.

After these transformations, all of the frequencies except ω_{d62} are given to within 10% over the entire Brillouin zone. To evaluate ω_{d62} to the same accuracy one must obtain corrections using perturbation theory.

For the direction $\boldsymbol{k} \parallel [100]$ it is more convenient to use a different choice of bases for the two-dimensional and three-dimensional representations.

$$U_a = \frac{1}{\sqrt{8}} \begin{pmatrix} 1 & 1 & 1 & 1 & 1 & 1 & 1 & 1 \\ 1 & 1 & 1 & 1 & -1 & -1 & -1 & -1 \\ -1 & -1 & 1 & 1 & -1 & -1 & 1 & 1 \\ -1 & 1 & -1 & 1 & -1 & 1 & -1 & 1 \\ -1 & 1 & 1 & -1 & -1 & 1 & 1 & -1 \\ -1 & -1 & 1 & 1 & 1 & 1 & -1 & -1 \\ -1 & 1 & -1 & 1 & 1 & -1 & 1 & -1 \\ -1 & 1 & 1 & -1 & 1 & -1 & -1 & 1 \end{pmatrix}, \tag{1.53}$$

$$A = 1/\sqrt{2}, \quad B = \sqrt{2}, \quad C = \sqrt{3},$$

$$U_d = \frac{1}{\sqrt{12}}$$

$$\times \begin{pmatrix} 1 & 1 & 1 & 1 & 1 & 1 & 1 & 1 & 1 & 1 & 1 & 1 \\ 1 & 1 & 1 & 1 & 1 & 1 & -1 & -1 & -1 & -1 & -1 & -1 \\ A & A & -B & A & A & -B & A & A & -B & A & A & -B \\ A & -A & 0 & A & -A & 0 & A & -A & 0 & A & -A & 0 \\ A & A & -B & A & A & -B & -A & -A & B & -A & -A & B \\ A & -A & 0 & A & -A & 0 & -A & A & 0 & -A & A & 0 \\ 0 & C & 0 & 0 & -C & 0 & 0 & C & 0 & 0 & -C & 0 \\ 0 & 0 & C & 0 & 0 & -C & 0 & 0 & C & 0 & 0 & -C \\ C & 0 & 0 & -C & 0 & 0 & C & 0 & 0 & -C & 0 & 0 \\ 0 & C & 0 & 0 & -C & 0 & 0 & -C & 0 & 0 & C & 0 \\ 0 & 0 & C & 0 & 0 & -C & 0 & 0 & -C & 0 & 0 & C \\ C & 0 & 0 & -C & 0 & 0 & -C & 0 & 0 & C & 0 & 0 \end{pmatrix} \tag{1.54}$$

After the transforming to the new basis the Hamiltonian matrix decomposes into four 3×3 and two 4×4 blocks.

In the first of the 3×3 blocks, which couples vectors τ_{a1}, τ_{d1}, and τ_{d51}, it is sufficient to do a rotation between the vectors τ_{a1} and τ_{da} of the same representation. As a result, the FM and AFM oscillations will be weakly coupled with τ_{d51}. In the second block, which mixes the vectors τ_{a3}, τ_{d52}, and τ_{d81}, it is necessary to rotate the vectors τ_{d52} and τ_{d81}. The third block couples the vectors τ_{a91}, τ_{d91}, and τ_{d62}. The first rotation is done in the (τ_{a91}, τ_{d91}) plane, and the second rotation in the (τ_{d91}, τ_{d62}) plane.

The last 3×3 block couples the vectors τ_{a71}, τ_{d4}, and τ_{d61}. Here it is sufficient to rotate the vectors τ_{a71} and τ_{d61}.

The first 4×4 block couples the vectors τ_{a73}, τ_{a93}, τ_{d82} and τ_{d93}. In this block one should perform a rotation in the plane (τ_{a93}, τ_{d93}) of the vectors of the same representation and a rotation of the vectors τ_{d93} and τ_{d82}. The second 4×4 block couples the vectors τ_{a72}, τ_{a92}, τ_{d82} and τ_{d92} and it is complex conjugate to the first one.

1.7.2. Perturbation theory for highly degenerate a–d modes of the d type

Of particular interest are the three a–d branches of the d type with activation energy 290 K, which lie next above the soft d mode ω_{d4}. These magnons contribute significantly to the thermodynamics of YIG and to the kinetics of the spin waves of the ferromagnetic branch with $\boldsymbol{k} \to 0$. Unfortunately, one is unable to calculate the spectrum of these three branches for an arbitrary direction of $\boldsymbol{k}$ with reasonable accuracy and simplicity. The analytical formulas which arise are even more unwieldy than in the case of the symmetric direction [111]. For quantitative treatment we therefore consider only two particular cases. The first – for any value of k but with $\boldsymbol{k} \parallel [100]$ or [111] – was considered above. The second – for any direction of $\boldsymbol{k}$ but with $ak \lesssim 1$ – we shall consider now. Here we may drop terms higher than second order in k from the expressions for the frequencies. Because of the degeneracy the eigenvectors and $\omega_j(\boldsymbol{k})$ will not, of course, be analytic functions of $\boldsymbol{k}$ at $\boldsymbol{k} = 0$. The τ_9 block of the Hamiltonian matrix in

the quasinormal basis is

$$G = \begin{matrix} \tau_{9x} \\ \tau_{9y} \\ \tau_{9z} \end{matrix} \begin{pmatrix} \Omega_{x,q} & u^2\mu_z + uv(\sigma_{yx} + \sigma_{xy}) & u^2\mu_y + uv(\sigma_{zx} + \sigma_{xz}) \\ u^2\mu_z + uv(\sigma_{yx} + \sigma_{xy}) & \Omega_{y,q} & u^2\mu_x + uv(\sigma_{zy} + \sigma_{yz}) \\ u^2\mu_y + uv(\sigma_{zx} + \sigma_{xz}) & u^2\mu_x + uv(\sigma_{zy} + \sigma_{yz}) & \Omega_{z,q} \end{pmatrix} \begin{matrix} \\ \\ \\ \end{matrix} . \qquad (1.55)$$

$$\qquad\qquad \tau_{9x} \qquad\qquad \tau_{9y} \qquad\qquad \tau_{9z}$$

Here

$$\Omega_{x,q} = 5J_{ad}[1 + 2K - \sqrt{(5-2K)^2 - 2\cos^2 q_x(\cos^2 q_y + \cos 2q_z)^2}] ,$$
$$\mu_x = -10J_{dd}\cos 2q_x \sin q_y \sin q_z , \quad \sigma_{xy} = (10/\sqrt{2})J_{ad}\sin q_x \sin 2q_2 . \qquad (1.56)$$

The parameters u and v are taken at $\boldsymbol{k} = 0$.

Expansion of the matrix G in powers of q up to q^2 gives

$$G = \Omega_0 I_3 - q^2 \mathscr{L}(\boldsymbol{n}) , \quad \Omega_0 = \Omega_{x0} = \Omega_{y0} = \Omega_{z0} , \quad \boldsymbol{n} = \boldsymbol{q}/q , \qquad (1.57)$$

I_m is the $(m \times m)$ unit matrix. The matrix $\mathscr{L}(\boldsymbol{n})$ can be written as

$$\mathscr{L}(\boldsymbol{n}) = \xi I_3 + \eta F(\boldsymbol{n}) - \zeta Q(\boldsymbol{n}) , \quad F(\boldsymbol{n}) = \begin{pmatrix} n_y^2 + n_z^2 & -n_x n_y & -n_x n_z \\ -n_x n_y & n_x^2 + n_z^2 & -n_z n_y \\ -n_x n_z & -n_z n_y & n_x^2 + n_y^2 \end{pmatrix} ,$$
$$Q(\boldsymbol{n}) = \begin{pmatrix} n_y^2 + n_z^2 & 0 & 0 \\ 0 & n_x^2 + n_z^2 & 0 \\ 0 & 0 & n_x^2 + n_y^2 \end{pmatrix} , \qquad (1.58)$$

where

$$\zeta = 20J_{ad}^2/R , \quad \eta = [40J_{ad}^2 - J_{dd}(30J_{ad} - \Omega_0)]/R ,$$
$$\xi = [20J_{ad}^2 - J_{dd}(30J_{ad} - \Omega_0)]/R , \quad R = J_{ad} + 2J_{dd} - 2\Omega_0/10 . \qquad (1.59)$$

There is no small parameter in the expression for the matrix $\mathscr{L}(\boldsymbol{n})$, therefore it is necessary to transform this matrix to the diagonal form using the exact transformation $T_1(\boldsymbol{n})$.

$$T_1(\boldsymbol{n}) = \begin{pmatrix} n_x & 0 & (n_y^2 + n_z^2)/D \\ n_y & -n_z/D & -n_x n_y/D \\ n_z & n_y/D & -n_x n_z/D \end{pmatrix} , \quad D = \sqrt{n_x^2 + n_y^2} \qquad (1.60)$$

transforms the matrix F into the diagonal form

$$T_1^{-1}(\boldsymbol{n})F(\boldsymbol{n})T_1(\boldsymbol{n}) = \begin{pmatrix} 0 & 0 & 0 \\ 0 & 1 & 0 \\ 0 & 0 & 1 \end{pmatrix} . \qquad (1.61)$$

The same transformation of the matrix $Q(\boldsymbol{n})$ gives:

$$\tilde{Q}_{\mathrm{T}}(\boldsymbol{n}) = T_1^{-1}(\boldsymbol{n}) Q(\boldsymbol{n}) T_1(\boldsymbol{n})$$

$$= \begin{pmatrix} 1-n^4 & n_y n_z (n_y^2 - n_z^2)/D & n_x (n^4 - n_x^2)/D \\ n_y n_z (n_y^2 - n_z^2)/D & 1 - (2 n_z^2 n_y^2)/D^2 & n_x n_y n_z (n_z^2 - n_y^2)/D \\ n_x (n^4 - n_x^2)/D & n_x n_y n_z (n_z^2 - n_y^2)/D & n^4 + 2 n_y^2 n_z^2 D^2 \end{pmatrix}, \tag{1.62}$$

Here $n^4 = n_x^4 + n_y^4 + n_z^4$. The off-diagonal elements of the matrix $\tilde{Q}_{\mathrm{T}}(\boldsymbol{n})$ have an angular smallness, therefore only elements $(\tilde{Q}_{\mathrm{T}})_{2,3}$ should be taken into account. An appropriate two-dimensional rotation gives

$$Q_{\mathrm{T}}(\boldsymbol{n}) = T_2^{-1} \tilde{Q}_{\mathrm{T}}(n) T_2$$

$$= \begin{pmatrix} \frac{2}{3} f_4(\boldsymbol{n}) & 0 & 0 \\ 0 & 1 + \frac{1}{3}[\sqrt{f_4^2(\boldsymbol{n}) - f_6(\boldsymbol{n})} - f_4(\boldsymbol{n})] & 0 \\ 0 & 0 & 1 - \frac{1}{3}(\sqrt{f_4^2 - f_6} + f_4) \end{pmatrix}. \tag{1.63}$$

Here $f_4(\boldsymbol{n})$ and $f_6(\boldsymbol{n})$ are normalized cubic invariant functions,

$$f_4(\boldsymbol{n}) = 3(n_x^2 n_y^2 + n_x^2 n_z^2 + n_y^2 n_z^2), \quad f_6(\boldsymbol{n}) = 27 n_x^2 n_y^2 n_z^2 . \tag{1.64}$$

Thus the orthogonal transformation

$$T(\boldsymbol{n}) = T_1(\boldsymbol{n}) T_2(\boldsymbol{n}) \tag{1.65}$$

together with neglecting angular small element results in the diagonal form of the matrix $\mathscr{L}(\boldsymbol{n})$,

$$\mathscr{L}_{\mathrm{T}}(\boldsymbol{n}) = T^{-1}(\boldsymbol{n}) \mathscr{L}(\boldsymbol{n}) T(\boldsymbol{n})$$

$$= \begin{pmatrix} \zeta - \frac{2}{3}\xi f_4(\boldsymbol{n}) & 0 & 0 \\ 0 & 2\zeta + \frac{1}{3}\xi(f_4 - \sqrt{f_4^2 - f_6}) & 0 \\ 0 & 0 & 2\zeta + \frac{1}{3}\xi(f_4 + \sqrt{f_4^2 - f_6}) \end{pmatrix}. \tag{1.66}$$

The next step in the calculations is to take small perturbations, which mix the representation τ_9 with representations τ_8 and τ_6, into account. The diagonal matrix Ω with diagonal elements $\omega_{d9(x,y,z)}$ can be written as

$$\Omega = I_3 \Omega_0 - q^2 R(\boldsymbol{n}), \tag{1.67}$$

where

$$R(\boldsymbol{n}) = \mathscr{L}_{\mathrm{T}}(\boldsymbol{n}) + R_8(\boldsymbol{n}) + R_6(\boldsymbol{n}). \tag{1.68}$$

Here the matrices $R_m(\boldsymbol{n})$ are due to the influence of representations τ_m involved in the Hamiltonian matrix. Some transformations result in the following matrices $R_m(\boldsymbol{n})$:

$$R_8(\boldsymbol{n}) = -r_8 \begin{pmatrix} \frac{4}{3}f_4 & 0 & 0 \\ 0 & 1-\frac{2}{3}(f_4-\sqrt{f_4^2-f_6}) & 0 \\ 0 & 0 & f_4+\sqrt{f_4^2-f_6} \end{pmatrix},$$

$$R_6(\boldsymbol{n}) = -r_6 \begin{pmatrix} 2(1-f_4) & 0 & 0 \\ 0 & f_4-\sqrt{f_4^2-f_6} & 0 \\ 0 & 0 & f_4+\sqrt{f_4^2-f_6} \end{pmatrix}, \tag{1.69}$$

where

$$\begin{aligned} r_6 &= 100(uJ_{dd}-\sqrt{2}vJ_{ad})^2[10J_{dd}-20J_{ad}-\omega_{d9}(0)]^{-1}, \\ r_8 &= 200(vJ_{ad}-\sqrt{2}uJ_{dd})^2[20(J_{dd}-J_{ad})-\omega_{d9}(0)]^{-1}, \\ \begin{pmatrix} u \\ v \end{pmatrix} &= \frac{\sqrt{F\pm 1}}{\sqrt{2}}, \quad F = \frac{5-2K}{\sqrt{(5-2K)^2-8}}. \end{aligned} \tag{1.70}$$

The final expressions for the frequencies $\omega_{d9j}(\boldsymbol{k})$ up to terms $\sim q^2$ are

$$\begin{aligned} \omega_{d9x} &= \omega_{d9}(0) + q^2[X - 2Zf_4(\boldsymbol{n})], \\ \omega_{d9y} &= \omega_{d9}(0) + q^2\{Y + Z[f_4(\boldsymbol{n}) - \sqrt{f_4^2(\boldsymbol{n}) - f_6(\boldsymbol{n})}]\}, \\ \omega_{d9}(0) &= 5|J_{ad}|[\sqrt{(5-2K)^2-8} - 1 - 2K], \end{aligned} \tag{1.71}$$

where

$$\begin{aligned} &X = \zeta - 2r_6, \quad Y = 2\zeta - r_8, \quad Z = (\xi + 2r_8 - 3r_6)/3, \quad \zeta = 20J_{ad}^2R^{-1}, \\ &\xi = \{20J_{ad}^2 - J_{dd}[30J_{ad} - \omega_{d9}(0)]\}R^{-1}, \quad R = \omega_{d9}(0)/5 - J_{ad} - 2J_{dd}. \end{aligned} \tag{1.72}$$

A comparison with the numerical calculation shows that expressions (1.71) have an accuracy not worse that 5% of the dispersion up to $ak \simeq 1.2$. This is a small part of the Brillouin zone, but it is important in ferromagnon relaxation. In conclusion of the section we point out that the transformation (1.65) gives the eigenvectors of the Hamiltonian matrix (i.e. magnon modes) at $\boldsymbol{k} \to 0$.

1.8. Determination of the exchange integrals in YIG

The magnetic spectra in YIG have been studied in detail in sections 1.6 and 1.7. Now it is time to obtain the values of the exchange integrals from a comparison of inelastic neutron scattering data with the spectra. Plant [4] reported low-temperature neutron-diffraction measurements of the frequencies $\omega_1(\boldsymbol{k})$ and $\omega_{a1}(\boldsymbol{k})$ of the ferromagnetic and antiferromagnetic modes, respectively, and the frequency $\omega_x(\boldsymbol{k})$ of another optical magnon mode in YIG with an undetermined pattern of oscillation (see section 1.2.2). From the antiferromagnetic gap $\omega_{a1}(0) = 10J_{ad}$, Plant found $J_{ad} = -39.8$ K. From a comparison of formula (1.45) for the ferromagnon spectrum $\omega_{d1}(\boldsymbol{k})$ with

the experimental data in the directions $\boldsymbol{k} \parallel [110]$ and [100], with $\boldsymbol{k}$ varying from 0 to the Brillouin zone boundary, we obtained the value of the combination of exchange integrals in eq. (1.3) as $\omega_{ex} = 40.0 \pm 1.0$ K and found $J_{aa} = -4 \pm 1$ K. Using this set of J values to calculate the gaps of all the optical modes, we became convinced that the role of $\omega_x(\boldsymbol{k})$ could be played by only one of the triad of zone-center-degenerate modes $\omega_{d8j}, j = 1, 1, 3$. By comparing $\omega_{d8j}(0) = 20(J_{dd} - J_{ad})$ with the experimental value $\omega_x(0) = 530$ K, we find $J_{dd} = -13.4 \pm 0.2$ K, and then we get the refined value $J_{aa} = -3.8 \pm 0.2$ K. Finally, we put

$$J_{ad} = -39.8 \text{ K}, \quad J_{dd} = -13.4 \text{ K}, \quad J_{aa} = -3.8 \text{ K}. \tag{1.73}$$

Fortunately, all other choices of optical branches as observed in the inelastic neutron scattering experiment [4] either provide a poor agreement with the experimental results for ferromagnetic and antiferromagnetic branches in the whole Brillouin zone or give a negative magnon energy for one of the other optical branches. The latter would mean an instability of the YIG magnetic structure. The set of the exchange integral values (1.73) differs from that obtained by Plant himself [4] from the same experimental data. The reason for such contradiction is that he considered the only optical branch, except the antiferromagnetic one, found in the experimental research as one of the two $\omega_{d6}(\boldsymbol{k})$ branches. This resulted in a poor agreement of the energies of the ferromagnetic and antiferromagnetic branches calculated with that set of three exchange constants, and therefore Plant was forced to take the exchange interaction with further neighbours into account.

1.9. Temperature dependence of the magnetization and the exchange integrals

With the spectrum of the spin waves and the corresponding eigenvectors, one can determine all the thermodynamic properties of the magnetic subsystem of YIG for temperatures not too close to the Curie temperature, i.e., when the interaction between magnons is small. The temperature dependence of the magnetization is the property which has been the most thoroughly studied in experiment [7, 8], so that a "first-principles" calculation (in the theory of magnetism) of this characteristic is of greater interest.

The magnetization of M is proportional to the average values of the density of the z component S_i of the spin,

$$M = 2\mu_B \langle S_i \rangle, \tag{1.74}$$

where μ_B is the Bohr magneton and

$$\langle S_i \rangle = \frac{1}{N v_0} \sum_n \left(\sum_{j=9}^{20} (S_0 - \langle a_{jn}^\dagger a_{jn} \rangle) - \sum_{j=1}^{8} (S_0 - \langle a_{jn}^\dagger a_{jn} \rangle) \right). \tag{1.75}$$

Here v_0 is the volume of the primitive cell, n is the number of the cell, and N is the number of such cells in the crystal. After the Fourier transformations (1.14) we have

$$\langle S_z \rangle = \frac{1}{v_0} \left[4S_0 - \sum_k \left(\sum_{j=1}^{8} \langle a_{jk}^\dagger a_{jk} \rangle - \sum_{j=9}^{20} \langle a_{jk}^\dagger a_{jk} \rangle \right) \right]. \tag{1.76}$$

One is readily convinced that the canonical transformations (1.18) leave invariant the form of

$$\sum_{j=1}^{8} a_{jk}^\dagger a_{jk} - \sum_{j=9}^{20} a_{jk}^\dagger a_{jk}. \tag{1.77}$$

Therefore

$$\Delta S_z = \langle S_z \rangle_0 - \langle S_z \rangle = \frac{1}{v} \sum_k \left(\sum_{j=9}^{20} n_{jk} - \sum_{j=1}^{8} n_{jk} \right) , \tag{1.78}$$

where $\langle S_z \rangle_0$ is the value of $\langle S_z \rangle$ at $T = 0$, and

$$n_{jk} \equiv \langle b_{jk}^{\dagger} b_{jk} \rangle = \{ \exp [\omega_j(\boldsymbol{k})/T] - 1 \}^{-1} . \tag{1.79}$$

At low temperatures, only the magnons of the lowest, "ferromagnetic" branch are excited. At very low temperatures $T < 25$ K the dispersion relation for these magnons is quadratic, and obviously, $\Delta S_z \propto T^{3/2}$:

$$\Delta S_z = 0.029 (T/\omega_{ex})^{3/2} . \tag{1.80}$$

For temperatures in the region $25 \text{ K} \lesssim T \lesssim 20(|J_{ad}| - 2|J_{dd}|) \approx 250$ K only magnons of the lowest branch are excited, but most of them are concentrated in the linear region of the dispersion relation, $\omega_k = \omega_l(ak)$, and so $\Delta S_z \propto T^3$, in analogy with the temperature dependence of the number of phonons,

$$\Delta S_z = [\zeta(3)/2\pi^3](T/\omega_l)^3 , \tag{1.81}$$

where $\omega_l \simeq 2\omega_{ex}$, in accordance with (1.48).

To determine the temperature dependence of ΔS_z at higher temperatures we used a computer. Starting from the approximate analytical expressions for the frequencies as obtained in the previous sections, the computer performed calculations for any specified set of exchange integrals J_{ad}, J_{dd}, and J_{aa}.

The results of the computations for the set of exchange integrals (1.73) are presented in fig. 5. The calculated function $M(T)$ is extremely sensitive to the values of the exchange integrals and it had little in common with the experimental curve even for the values of the exchange integrals which differ by 1–3 K from the values in eqs. (1.73). The reason for such strong dependence is that the magnetization depends on the optical magnon frequencies which are proportional to a large factor, e.g. $(20|J_{ad}| - 40|J_{dd}|)$ for the lowest optical branch.

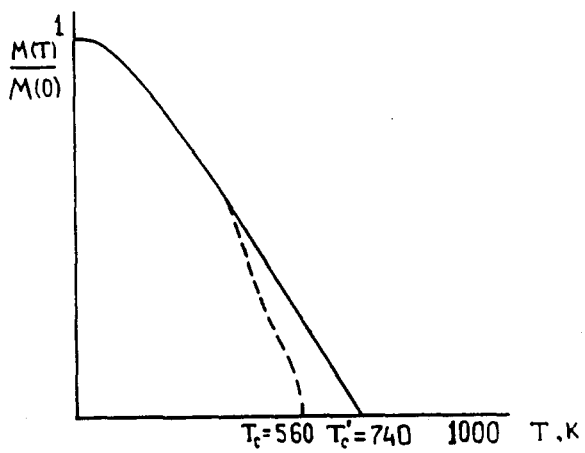

Fig. 5. Temperature of the magnetization for the values of the exchange integrals given in (1.73). The dashed curve shows the experimental results.

It should be pointed out that the magnetization calculated with the values (1.73) found for the exchange integrals (see fig. 5) agrees with the experimentally measured value to within 2% at $T = 400$ K, but gives a Curie temperature $T_C = 740$ K that differs from the actual value by 30%. This evidently means that the spin-wave approximation is valid for YIG in the temperature region $0 \leq T \lesssim \frac{2}{3} T_C$.

2. Magnon interaction and relaxation in YIG

The YIG magnon spectra have been studied in detail in the previous chapter. The magnon spectra have been obtained from a Hamiltonian that is quadratic in the creation and annihilation operators, i.e., from linear dynamical equations for the operators. Magnons are considered as noninteracting quasiparticles which propagate independently in this approximation. Here, in chapter 2, we are dealing with problems arising from magnon interaction, i.e., with their scattering and relaxation. Magnon–magnon interactions of diverse nature in magnetic insulators and the kinetic equation for magnons are discussed in section 2.1. The magnon relaxation rates in a simple cubic ferromagnet resulting from these interactions are presented in this section as well. The unique role of YIG in the physics of magnetic systems is due predominantly to its microwave properties. The ferromagnon relaxation in YIG in the microwave frequency range has been investigated extensively in numerous experimental studies (see, e.g. refs. [9–11, 42]). The results of these studies are discussed briefly in section 2.2. Section 2.3 is devoted to the ferromagnon scattering and relaxation in YIG caused by the magnon–magnon exchange interaction. This interaction is the strongest one for most of the magnons in the Brillouin zone. However, the amplitude of the exchange magnon–magnon interaction tends to zero for magnons with $\boldsymbol{k} \to 0$, because the exchange interaction is invariant with respect to any homogeneous rotation of all the spins. There is a weaker, magnetic dipole interaction in YIG. It is a long-range interaction and therefore it is very important for nonlinear processes involving long-wavelength magnons. The relaxation of the ferromagnons caused by the magnetic dipole interaction is studied in section 2.4. The magnetic dipole relaxation frequency in YIG differs essentially from that in a simple cubic ferromagnet. For very long wavelengths, $k \lesssim 10^3$–10^4 cm^{-1}, the magnetic dipole relaxation is also very small because the energy and momentum conservation conditions forbid relatively strong three-magnon magnetic dipole interaction in this wave number range. The ferromagnetic relaxation for such small k is caused by scattering of ferromagnon on almost degenerate optical magnons owing to a weak magnetic anisotropy. This relaxation mechanism is studied in section 2.5.

2.1. Magnon interaction and relaxation theory

2.1.1. Magnon–magnon interactions

There are two ways of classifying quasiparticle interactions: (i) according to the characteristic energy of an interaction, and (ii) according to the number of quasiparticles involved in an interaction process. We will see later that the relaxation frequency owing to a certain interaction process is, very roughly, a product of the square characteristic energy and the probability of this process. The probability depends on the number of quasiparticles involved in the process. Therefore, both the characteristic energy and the number of interacting magnons are important for magnon relaxation.

There are three magnetic interactions of different nature which are responsible for magnon relaxation in YIG. The strongest one is the exchange interaction discussed in section 1.1.2. Its characteristic energy per spin is of order of 10^3 K in YIG. The second interaction is the magnetic

dipole interaction with the Hamiltonian

$$H_{\mathrm{d}} = 2\mu_{\mathrm{B}}^2 \sum_{i \neq j} \frac{R_{ij}^2(\boldsymbol{S}_i \boldsymbol{S}_j) - (\boldsymbol{R}_j \boldsymbol{S}_i)(\boldsymbol{R}_{ij} \boldsymbol{S}_j)}{R_{ij}^5} \,. \tag{2.1}$$

Here μ_{B} is Bohr magneton, $\boldsymbol{R}_{ij} = \boldsymbol{R}_i - \boldsymbol{R}_j$ is the distance between spins in the sites i and j, i and j number all the spins. The characteristic energy of the magnetic dipole interaction is of order of 1 K. The third interaction is the spin–orbit interaction which results in a relatively small magnetic anisotropy. The energy of this interaction is about 0.3 K. The term in the Hamiltonian resulting from the magnetic anisotropy is discussed in section 2.5.

In general, the Hamiltonian can be represented as a series in magnon operator powers,

$$H = H^{(2)} + H^{(3)} + H^{(4)} + \cdots \,, \tag{2.2}$$

where $H^{(2)}$ is the quadratic term, $H^{(3)}$ is the term of the third-order, etc. The Hamiltonian $H^{(3)}$ describes three-magnon processes,

$$H^{(3)} = \frac{1}{2} \int (V_q b_1^\dagger b_2 b_3 + \text{h.c.}) \delta(\boldsymbol{k}_1 - \boldsymbol{k}_2 - \boldsymbol{k}_3) \, \mathrm{d}\boldsymbol{k}_1 \, \mathrm{d}\boldsymbol{k}_2 \, \mathrm{d}\boldsymbol{k}_3$$

$$+ \frac{1}{6} \int (U_q b_1^\dagger b_2^\dagger b_3^\dagger + \text{h.c.}) \delta(\boldsymbol{k}_1 + \boldsymbol{k}_2 + \boldsymbol{k}_3) \, \mathrm{d}\boldsymbol{k}_1 \, \mathrm{d}\boldsymbol{k}_2 \, \mathrm{d}\boldsymbol{k}_3 \,. \tag{2.3}$$

Here and below a shorthand notation is used:

$$b_1 = b_{j_1, \boldsymbol{k}_1}(t) \,, \quad b_2 = b_{j_2, \boldsymbol{k}_2}(t) \,, \quad q = (j_1, \boldsymbol{k}_1; j_2, \boldsymbol{k}_2; j_3, \boldsymbol{k}_3) \,, \quad V_q = V_{123} = V^{j_1 j_2 j_3}_{\boldsymbol{k}_1 \boldsymbol{k}_2 \boldsymbol{k}_3} \,, \tag{2.4}$$

where j denotes the number of the magnon branch and $\boldsymbol{k}$ is the wavevector of a magnon. The first term in (2.3) describes the decay processes: 1 magnon → 2 magnons, and the reversal confluence process: 2 magnons → 1 magnon. The second term describes mutual annihilation of three magnons and their creation from the vacuum.

The Hamiltonian $H^{(4)}$ describes processes involving four magnons,

$$H^{(4)} = \frac{1}{4} \int W_p b_1^\dagger b_2^\dagger b_3 b_4 \delta(\boldsymbol{k}_1 + \boldsymbol{k}_2 - \boldsymbol{k}_3 - \boldsymbol{k}_4) \, \mathrm{d}\boldsymbol{k}_1 \, \mathrm{d}\boldsymbol{k}_2 \, \mathrm{d}\boldsymbol{k}_3 \, \mathrm{d}\boldsymbol{k}_4$$

$$+ \int (G_p b_1^\dagger b_2 b_3 b_4 + \text{h.c.}) \delta(\boldsymbol{k}_1 - \boldsymbol{k}_2 - \boldsymbol{k}_3 - \boldsymbol{k}_4) \, \mathrm{d}\boldsymbol{k}_1 \, \mathrm{d}\boldsymbol{k}_2 \, \mathrm{d}\boldsymbol{k}_3 \, \mathrm{d}\boldsymbol{k}_4$$

$$+ \frac{1}{4} \int (R_p^* b_1 b_2 b_3 b_4 + \text{h.c.}) \delta(\boldsymbol{k}_1 + \boldsymbol{k}_2 + \boldsymbol{k}_3 + \boldsymbol{k}_4) \, \mathrm{d}\boldsymbol{k}_1 \, \mathrm{d}\boldsymbol{k}_2 \, \mathrm{d}\boldsymbol{k}_3 \, \mathrm{d}\boldsymbol{k}_4 \,,$$

$$p = (j_1, \boldsymbol{k}_1; j_2, \boldsymbol{k}_2; j_3, \boldsymbol{k}_3; j_4, \boldsymbol{k}_4) \,. \tag{2.5}$$

The expansion (2.2) is suitable when the magnon occupation numbers are small compared to S. It takes place at low temperature, $T < T_{\mathrm{C}}$. As a rule, the terms $H^{(3)}$ and $H^{(4)}$ in (2.2) are sufficient to describe the dynamical and kinetic properties of magnons in a wide temperature range from the zero temperature to a vicinity of the Curie temperature where the critical behaviour of the magnet takes place.

Formally, at low temperature the term $H^{(3)}$ is larger than $H^{(4)}$ for the general kind of magnon–magnon interaction because of the smallness of the magnon amplitudes. However, there

are two reasons for the four-magnon interaction being comparable or even stronger than the three-magnon one in many cases. The first reason is that there are only even terms in the magnon amplitudes in the expansion of the exchange interaction Hamiltonian because of the symmetry of the exchange interaction. So the strongest exchange interaction originates only from $H^{(2)}$ and $H^{(4)}$ terms in the Hamiltonian expansion. The second reason is that the three-magnon processes can be forbidden by the energy and momentum conservation conditions for some wave vectors. As for the four-magnon interaction (2 magnons $\rightarrow$ 2 magnons), it cannot be forbidden, except in some very special cases. Thus, in region of the Brillouin zone where the three-magnon processes are forbidden, one has to take into account the four-magnon processes. It should be noted that the three-magnon interaction yields some additional terms in the amplitude of the four-magnon interaction in the second order of the perturbation theory [36, 43].

2.1.2. Kinetic equation for magnons

A full description of properties of a system of interacting particles or quasiparticles is given by the density matrix. However, if the interaction is small compared to the quasiparticle energies, the influence of this interaction on the system's evolution can be considered as a perturbation. The phases of the quasiparticles are almost random and in this case all information about the system's evolution can be obtained from the one-particle distribution function. In this approximation the many-particle distribution function is a product of one-particle functions. The evolution of the one-particle distribution function, n_k which is called the distribution function further on, is described by the kinetic equation. This equation is obtained in the second order in the amplitude of the quasiparticle interaction. It can be written as

$$\partial n_k/\partial t = I\{n_k\}\,, \tag{2.6}$$

where $I\{n_k\}$ is the collision term. The form of the collision term depends on the type of the quasiparticle interaction. If only three- and four-magnon processes are significant, the collision term is

$$I\{N_k\} = I^{(3)}\{n_k\} + I^{(4)}\{n_k\}\,. \tag{2.7}$$

Here $I^{(3)}\{n_k\}$ and $I^{(4)}\{n_k\}$ are collision terms due to the three- and four-magnon processes respectively. It is convenient to divide the collision term into departure and arrival terms,

$$I_k\{n_k\} = -2\gamma_k n_k + J_k\{n_k\}\,. \tag{2.8}$$

The departure term, $-2\gamma_k n_k$, describes the number of magnons leaving the point of $\boldsymbol{k}$-space per unit time. The arrival term, $J\{n_k\}$, is the number of magnons arriving at the point $\boldsymbol{k}$ of the $\boldsymbol{k}$-space because of magnon–magnon interaction per unit time. The quantities γ_k and $J_k\{n_k\}$ can be expressed in terms of the amplitudes of three- and four-magnon processes, V_q and W_p, the occupation number n_{jk}, and the magnon spectra ω_{jk},

$$J_{jk}^{(3)}\{n_k\} = \frac{v_0}{(2\pi)^2}\sum_{g,\,j_1,\,j_2}\int\left[\tfrac{1}{2}|V_{k12}^{jj_1j_2}|^2 n_1 n_2\delta(\omega_{jk}-\omega_1-\omega_2)\delta(\boldsymbol{k}-\boldsymbol{k}_1-\boldsymbol{k}_2-\boldsymbol{g})\right.$$
$$\left.+\,|V_{1k2}|^2 n_1(n_2+1)\delta(\omega_1-\omega_{jk}-\omega_2)\delta(\boldsymbol{k}_1-\boldsymbol{k}-\boldsymbol{k}_2-\boldsymbol{g})\right]\mathrm{d}\boldsymbol{k}_1\,\mathrm{d}\boldsymbol{k}_2\,, \tag{2.9}$$

$$\gamma_{jk}^{(3)} = \pi \frac{v_0}{(2\pi)^3} \sum_{g, j_1, j_2} \int [\tfrac{1}{2} |V_{k12}^{jj_1j_2}|^2 (n_1 + n_2 + 1)\delta(\omega_{jk} - \omega_1 - \omega_2)\delta(\boldsymbol{k} - \boldsymbol{k}_1 - \boldsymbol{k}_2 - \boldsymbol{g})$$

$$+ |V_{1k2}|^2 (n_2 - n_1)\delta(\omega_1 - \omega_{jk} - \omega_2)\delta(\boldsymbol{k}_1 - \boldsymbol{k} - \boldsymbol{k}_2 - \boldsymbol{g})] \, \mathrm{d}\boldsymbol{k}_1 \, \mathrm{d}\boldsymbol{k}_2 , \tag{2.10}$$

$$J_{jk}^{(4)}\{n_k\} = \frac{\pi v_0^2}{(2\pi)^5} \sum_{g} \int |T_{k123}^{jj_1j_2j_3}|^2 (n_1 + 1) n_2 n_3 \delta(\omega_{jk} + \omega_1 - \omega_2 - \omega_3)\delta(\boldsymbol{k} + \boldsymbol{k}_1 - \boldsymbol{k}_2 - \boldsymbol{k}_3 - \boldsymbol{g})$$

$$\times \mathrm{d}\boldsymbol{k}_1 \, \mathrm{d}\boldsymbol{k}_2 \mathrm{d}\boldsymbol{k}_3 , \tag{2.11}$$

$$\gamma_{jk}^{(4)} = \pi \frac{v_0^2}{(2\pi)^6} \sum_{g} \int |T_{k123}^{jjj_2j_3}|^2 [n_1(n_2 + n_3 + 1) - n_2 n_3] \delta(\omega_k^j + \omega_1 - \omega_2 - \omega_3)$$

$$\times \delta(\boldsymbol{k} + \boldsymbol{k}_1 - \boldsymbol{k}_2 - \boldsymbol{k}_3 - \boldsymbol{g}) \, \mathrm{d}\boldsymbol{k}_1 \, \mathrm{d}\boldsymbol{k}_2 \mathrm{d}\boldsymbol{k}_3 , \tag{2.12}$$

$$J_{jk}\{n_k\} = J_{jk}^{(3)}\{n_k\} + J_{jk}^{(4)}\{n_k\} , \quad \gamma_{jk} = \gamma_{jk}^{(3)} + \gamma_{4k}^{(4)} . \tag{2.13}$$

Here v_0 is the volume of a unit cell, $\boldsymbol{g}$ are reciprocal lattice vectors, $\boldsymbol{k}, \boldsymbol{k}_1, \boldsymbol{k}_2$ and $\boldsymbol{k}_3$ are situated in the first Brillouin zone, and j, j_1, j_2 and j_3 number the magnon branches.

The magnon kinetic equation is derived in numerous books and review papers (see, e.g. refs. [44–46, 10]), therefore we do not present a derivation of the magnon kinetic equation. It should be pointed out that the magnon kinetic equation has a class of stationary solutions,

$$n_{jk}^0 = [\exp(\beta\omega_{jk}) - 1]^{-1} , \tag{2.14}$$

with an arbitrary parameter $\beta = 1/T$. These solutions correspond to a thermodynamical equilibrium with temperature T. The quantity γ_{jk}^{-1} is the relaxation time of a magnon packet which is narrow in the k-space with a small number of magnons, δn_{jk}, against a wide equilibrium background n_{jk}^0. The smallness of the number δn_{jk} means that

$$\frac{v_0}{(2\pi)^3} \int \sum_j \delta n_{jk} \, \mathrm{d}\boldsymbol{k} \ll \frac{v_0}{(2\pi)^3} \sum_j \int n_{jk}^0 \, \mathrm{d}\boldsymbol{k} . \tag{2.15}$$

The number of the nonequilibrium magnons departing from the area in the $\boldsymbol{k}$-space originally occupied by the narrow packet is $2\gamma_{jk}\delta n_{jk}$. The number of nonequilibrium magnons arriving in this area is much smaller because the nonequilibrium magnons are scattered over a wider area as a result of their interaction with equilibrium magnons. Thus the kinetic equation for a narrow nonequilibrium magnon packet takes the form

$$(\partial/\partial t + 2\gamma_{jk})\delta n_{jk} = 0 . \tag{2.16}$$

The solution of this equation,

$$\delta n_{jk}(t) = \delta n_{jk}(0) \exp(-2\gamma_{jk} t) , \tag{2.17}$$

describes the exponential decay of the packet. It should be noted that eq. (2.16) is approximate; it is correct as far as the packet can be considered narrow.

The magnon relaxation frequency, or decrement, γ_{jk} is a very important parameter which characterizes evolution of nonequilibrium magnons. As a rule, magnon relaxation in magnetic dielectrics is due to their interaction with thermal magnons.

2.1.3. Temperature dependence of the magnon spectra

There is another important quantity due to the magnon–magnon interaction, the temperature dependent shift of the magnon frequencies. This shift has the same nature as the frequency shift in a nonlinear pendulum: the eigenfrequencies in nonlinear systems depend upon the squared amplitudes of the oscillations. In a system of interacting magnons this shift can be obtained in the first order in the four-magnon interaction amplitude [44],

$$\Delta\omega^j(\boldsymbol{k}) = 2\sum_{\boldsymbol{q}} T^{jjjj}_{\boldsymbol{k}\boldsymbol{q}\boldsymbol{k}\boldsymbol{q}} n^j_{\boldsymbol{q}} + \frac{1}{2}\sum_{\boldsymbol{q},l} T^{jljl}_{\boldsymbol{k}\boldsymbol{q}\boldsymbol{k}\boldsymbol{q}} n^l_{\boldsymbol{q}} (1-\delta_{jl}) . \tag{2.18}$$

Here $n^l_{\boldsymbol{q}}$ is the occupation number of magnons with the quasimomentum $\boldsymbol{q}$ in the lth branch. The main contribution into the magnon frequency shift is due to the exchange interaction. This results in a very special behavior of the frequency shift for the ferromagnon spectrum: it tends to zero at $\boldsymbol{k} \to 0$, because the magnon with $\boldsymbol{k} \to 0$ is simply a homogeneous spin rotation, and the exchange interaction is invariant with respect to such a rotation. Thus, the shift of the ferromagnon frequency is proportional to k^2. This leads to a temperature dependence of the magnon stiffness ω_{ex}.

2.1.4. Magnon interactions and relaxation in a cubic ferromagnet

(1) There is only one magnetic lattice in a ferromagnet, and, consequently, there is only one magnon branch in the magnon spectrum. The Hamiltonian of the ferromagnet consists of three terms resulting from the most important interactions,

$$H = H_{ex} + H_d + H_a . \tag{2.19}$$

H_{ex} is the Hamiltonian of the exchange interaction. It can be expanded up to the fourth order in magnon amplitudes as

$$H_{ex} = \sum_{k} \varepsilon_k a^\dagger_k a_k + \tfrac{1}{2}\sum_{12,34} T_{12,34} a^\dagger_1 a^\dagger_2 a_3 a_4 \Delta(\boldsymbol{k}_1 + \boldsymbol{k}_2 - \boldsymbol{k}_3 - \boldsymbol{k}_4) ,$$

$$\varepsilon_k = gH_0 + S(J_0 - J_k) , \tag{2.20}$$

$$T_{12,34} = \tfrac{1}{4}(J_{k_1-k_3} + J_{k_1-k_4} + J_{k_2-k_3} + J_{k_2-k_4} - J_{k_1} - J_{k_2} - J_{k_3} - J_{k_4}) ,$$

where H_0 is the magnetic field and J_k is the Fourier transform of the exchange integral,

$$J_k = \frac{1}{N}\sum_{n,m} J_{n,m} \exp[i\boldsymbol{k}\cdot(\boldsymbol{r}_n - \boldsymbol{r}_m)] . \tag{2.21}$$

The Hamiltonian of the magnetic dipole interaction (2.1) expressed in terms of the magnon amplitudes is

$$H_{\mathrm{d}} = \sum_k [|B_k| a_k^\dagger a_k + \tfrac{1}{2}(B_k^* a_k a_{-k} + B_{-k} a_k^\dagger a_{-k}^\dagger)] + \frac{1}{2}\sum_{12,3} (V_{123} a_1^\dagger a_2 a_3 + \text{h.c.})$$

$$+ \frac{1}{2}\sum_{12,34} P_{1234} a_1^\dagger a_2^\dagger a_3 a_4 ,$$

$$B_k = \tfrac{1}{2}\omega_{\mathrm{M}} \frac{k_+^2}{k^2} , \quad k_+ = k_x + \mathrm{i}k_y , \quad \omega_{\mathrm{M}} = 4\pi g M ,$$

$$V_{123} = \tfrac{1}{2}(V_2 + V_3) , \quad V_k = -(\omega_{\mathrm{M}}/\sqrt{2S})\, k_z k_+ / k^2 , \tag{2.22}$$

$$P_{1234} = \tfrac{1}{4}(C_{k_1 - k_3} + C_{k_1 - k_1} + C_{k_2 - k_3} + C_{k_2 - k_4} - D_{k_1} - D_{k_2} - D_{k_3} - D_{k_4}) ,$$

$$C_k = (\omega_{\mathrm{M}}/S) k_z^2 / k^2 , \quad C_0 = \omega_{\mathrm{M}}/3S , \quad D_k = |B_k|/S .$$

It is assumed that the z axis is parallel to the magnetic field. The last term in the Hamiltonian (2.19) describes the magnetic anisotropy. In a cubic ferromagnet it takes the form

$$H_{\mathrm{a}} = -\frac{\omega_{\mathrm{a}}}{4S^4} \sum_n (S_{nx'}^4 + S_{ny'}^4 + S_{nz'}^4) . \tag{2.23}$$

Here ω_{a} is the energy of the anisotropic interaction, x', y' and z' are the crystallographic axes of the ferromagnet. The Hamiltonian H_{a} can be expanded as

$$H_{\mathrm{a}} = \alpha \sum_k \omega_{\mathrm{a}} a_k^\dagger a_k + \beta \sum_{1,2,3,4} (\omega_{\mathrm{a}}/S) a_1^\dagger a_2^\dagger a_3 a_4 \Delta(\boldsymbol{k}_1 + \boldsymbol{k}_2 - \boldsymbol{k}_3 - \boldsymbol{k}_4) . \tag{2.24}$$

The coefficients α and β depend on the angles between the magnetic field and the crystallographic axes. In particular,

$$\alpha = 1 , \quad \beta = -9 , \quad \text{if } \boldsymbol{H} \parallel [100] , \quad \alpha = -2/3 , \quad \beta = 6 , \quad \text{if } \boldsymbol{H} \parallel [111] . \tag{2.25}$$

In order to find the magnon spectrum one has to perform the linear transformation (1.18) [33]

$$a_k = u_k b_k + v_k b_k^\dagger , \quad a_k^\dagger = u_k^* b_k^\dagger + v_k^* b_{-k} , \quad |u_k|^2 - |v_k|^2 = 1 , \tag{2.26}$$

where

$$u_k = [(A_k + \omega_k)/2\omega_k]^{1/2} , \quad v_k = -(B_k/|B_k|)[(A_k - \omega_k)/2\omega_k]^{1/2} ,$$

$$A_k = \varepsilon_k + \alpha\omega_{\mathrm{a}} + |B_k| , \quad \omega_k = \sqrt{A_k^2 - |B_k|^2} , \tag{2.27}$$

and B_k is defined by eq. (2.22); ω_k is the spectrum of magnons in the ferromagnet. For the most magnons in the Brillouin zone the coefficient v_k is negligibly small because of the smallness of the magnetic dipole interaction. Only for small $\boldsymbol{k}$ and a not very strong magnetic field the transformation (2.25) is essential and the magnon spectrum differs significantly from ε_k.

(2) As a rule, magnons with relatively small energies are excited in ferrites ($\omega_k \ll SJ_0$). These energies are smaller than all the energies of optical magnons. The magnon dynamics in this energy range coincides with that of magnons in a ferromagnet with the same magnetization and the same exchange frequency ω_{ex}. The reason for the coincidence is that only magnetization oscillates with relatively low frequency; these oscillations can be considered in the continuous medium approximation, when

$$\omega_k = \omega_0 + \omega_{ex}(ak)^2 , \quad \omega_0 = gH_0 , \quad \omega_{ex}a^2 = \tfrac{1}{2}\partial^2 J/\partial^2 k|_{k=0} . \tag{2.28}$$

This approximation is correct when $\omega_k \ll SJ_0$ or, in other words, when $ka \ll \pi$. The amplitude of the magnetic dipole interaction depends mostly on the macroscopic magnetization and therefore the continuous medium approximation is a very reasonable approximation for magnon dynamics in the microwave frequency range.

The interaction and relaxation of magnons with $ak \ll \pi$ in a cubic ferromagnet has been studied in detail (see, e.g. refs. [10, 44–46]). We present the results of these studies briefly. The exchange relaxation frequency in the cubic ferromagnet is [34, 47]

$$\gamma_{ex}(k) = \frac{T^2\omega_k(ak)^2}{24\pi^3\omega_{ex}^2 S^2}\left[\ln^2(T/\omega_k) - \tfrac{10}{3}\ln(T/\omega_k) - 0.3\right] . \tag{2.29}$$

This result is correct for $k < k^*$, where

$$ak^* = (T/\omega_{ex})^{1/2} \quad \text{if } T < T^* , \quad ak^* = (6\pi^2)^{1/3} \quad \text{if } T > T^* ,$$
$$T^* = (6\pi^2)^{2/3}\omega_{ex} \simeq 15\omega_{ex} . \tag{2.30}$$

In order to obtain eq. (2.29) it is necessary to calculate the integral (2.12) substituting the long-wavelength limit expression

$$T_{12,34} = (\omega_{ex}/2S)a^2(\boldsymbol{k}_1\cdot\boldsymbol{k}_2 + \boldsymbol{k}_3\cdot\boldsymbol{k}_4) \tag{2.31}$$

for the four-magnon amplitude. The region $\omega_k \lesssim T$ where the equilibrium distribution (2.14) can be considered in the classical limit

$$n_k^0 = T/\omega_k \tag{2.32}$$

is essential for the integration.

The exchange relaxation damping (2.29) decreases when $\boldsymbol{k} \to 0$ and at low temperature. In this case the magnetic dipole relaxation should be taken into account. The magnetic dipole relaxation frequency consists of two terms,

$$\gamma_d(\boldsymbol{k}) = \gamma_s(\boldsymbol{k}) + \gamma_c(\boldsymbol{k}) . \tag{2.33}$$

They are due to processes of splitting and confluence of magnons, correspondingly. The terms $\gamma_s(\boldsymbol{k})$ and $\gamma_c(\boldsymbol{k})$ depend on the amplitude of three-magnon interaction (2.22) and are fairly complicated. Nevertheless, all important properties of the magnetic dipole relaxation can be found in a simple approximation, when the amplitude of three-magnon interaction is considered constant,

$$V_{123} = V = \omega_M/\sqrt{2S}\,, \tag{2.34}$$

and the transformation (2.26) is neglected. The amplitude V is the mean square value of the exact three-magnon amplitude averaged over the directions of all wave vectors. The splitting processes are prohibited for small k by the energy and momentum conservation conditions. In our approximation, the splitting processes can occur if $\omega_k \leq 3\omega_0$,

$$\gamma_s(\boldsymbol{k}) = \frac{V^2 T}{\pi(ak)\omega_{ex}^2} \ln\left(\frac{\omega_k + \sqrt{(\omega_k - \omega_0)(\omega_k - 3\omega_0)}}{\omega_k - \sqrt{(\omega_k - \omega_0)(\omega_k - 3\omega_0)}}\right), \tag{2.35}$$

in this case [48]. The magnon confluence processes are allowed for almost all k, except very small ones. The conservation conditions can be satisfied if $(ak) \leq \omega_k/(2\pi\omega_{ex})$. The damping caused by the confluence processes is [49]

$$\gamma_c(\boldsymbol{k}) = \frac{V^2 T}{2\pi ak\omega_{ex}^2} \ln[(4\omega_k^2 - 3\omega_0^2)/(4\omega_k - 3\omega_0)\omega_0]\,. \tag{2.36}$$

The argument of the logarithm in (2.36) is close to unity if $(ak)^2 \ll \omega_0/\omega_{ex}$. In this case the damping (2.35) is

$$\gamma_c(\boldsymbol{k}) = (4/\pi)(V^2 T/\omega_0\omega_{ex})(ak)\,. \tag{2.37}$$

The relaxation frequencies $\gamma_{ex}(\boldsymbol{k})$, $\gamma_c(\boldsymbol{k})$, $\gamma_s(\boldsymbol{k})$, and their sum,

$$\gamma_k = \gamma_{ex}(\boldsymbol{k}) + \gamma_s(\boldsymbol{k}) + \gamma_c(\boldsymbol{k})\,, \tag{2.38}$$

are shown in fig. 6. In the region of small wave vectors the magnon damping is due to the confluence processes. At $(ak)^2 \leq 2\omega_0/\omega_{ex}$ there is some additional relaxation owing to the magnon spitting processes. For

$$k > \bar{k} = \left(12\pi^2 \frac{\omega_M^2 S}{T\omega_{ex}} \frac{\ln(\omega_{\bar{k}}/\omega_0)}{\ln^2(T/\omega_{\bar{k}}) - \frac{10}{3}\ln(I/\omega_{\bar{k}}) - 0.3}\right)^{1/5} \frac{1}{a}\,, \tag{2.39}$$

the magnon relaxation is due mainly to the ferromagnon exchange interaction.

2.2. Experimental results

2.2.1. Magnon relaxation frequency

Numerous experimental studies of the spin wave and ferromagnetic resonance relaxation in YIG were carried out in the sixties and seventies. We mention only few of them devoted to the magnon

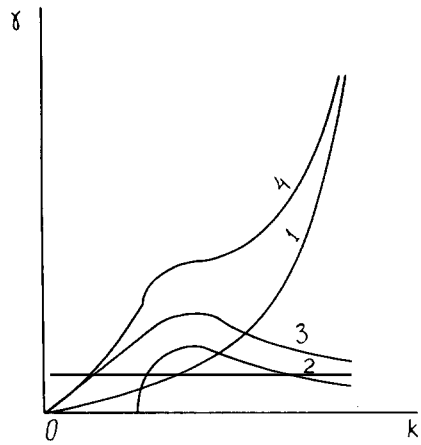

Fig. 6. Relaxation frequencies in ferromagnet; (1) exchange relaxation frequency, $\gamma_{ex}(\boldsymbol{k})$, (2) relaxation caused by the magnon confluence processes, $\gamma_c(\boldsymbol{k})$. (3) relaxation owing to the magnon splitting processes, $\gamma_s(\boldsymbol{k})$, (4) complete damping, $\gamma_k = \gamma_{ex}(\boldsymbol{k}) + \gamma_c(\boldsymbol{k}) + \gamma_s(\boldsymbol{k})$.

relaxation in pure monocrystals of YIG in the microwave frequency range and aimed at the investigation of physical mechanisms of the relaxation.

Probably, the first detailed research in this area was carried out by LeCraw and Spencer [12] and Kasuya and LeCraw [11]. They measured the threshold of magnon parametric excitation by parallel pumping in a wide temperature range (0–750 K). The threshold value of the pumping field is proportional to the relaxation frequency of excited magnons [50, 51, 43]. The parallel pumping creates pairs of magnons with opposite wave vectors and frequencies equal to one half of the pumping frequency ω_p,

$$\omega_k = \omega_p/2 \,. \tag{2.40}$$

The wave vectors of the parametrically excited magnons are perpendicular to the external magnetic field $\boldsymbol{H}_0$ in a wide range of the magnetic field. The parallel pumping frequency was $\omega_p = 2\pi \times 1.14 \times 10^{10}\ \mathrm{s}^{-1}$; the variation of the magnetic field $\boldsymbol{H}_0$ provided the variation of the wave number of the magnons from 5×10^4 to $2 \times 10^5\ \mathrm{cm}^{-1}$. It was found that in this range the magnon relaxation frequency γ_k is linear in the wave number k (fig. 7),

$$\gamma_k(T) = \Gamma_0(T) + \Gamma_k(T) \,, \tag{2.41}$$

where $\Gamma_0(T)$ is independent of k and $\Gamma_k(T)$ is proportional to k,

$$\Gamma_k(T) = Bk \,. \tag{2.42}$$

The reason for the separation of the k-dependent and the k-independent parts in the relaxation frequency is that in a pure ferromagnet the magnon damping resulting from magnon–magnon interaction tends to zero at $\boldsymbol{k} \to 0$, except for very small relaxation due to four-magnon magnetic dipole scattering. The results of the measurements of $\Gamma_0(T)$ in two series of experiments for $\omega_p/2\pi = 1.14 \times 10^{10}$ Hz [9] are shown in fig. 8. The low-temperature behaviour of $\Gamma_0(T)$ ($T < 100$ K for $\omega_p/2\pi = 1.14$ Hz and $T < 180$ K for $\omega_p/2\pi = 35.5$ GHz) is due to impurities. The high-temperature dependence of the relaxation frequency $\Gamma_0(T)$ is presented in fig. 9.

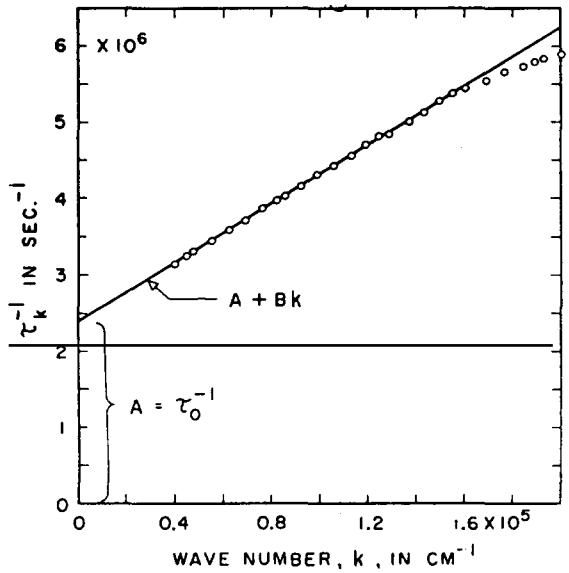

Fig. 7. Plot of γ_k versus k [12].

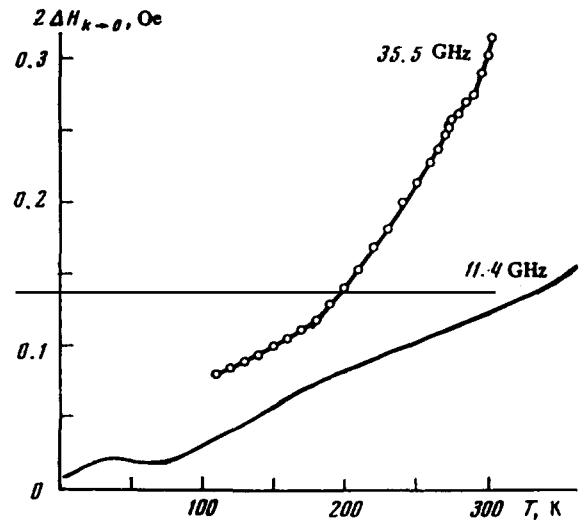

Fig. 8. Temperature dependence of the relaxation frequency $\Gamma_0(T) = g\mu\Delta H_{k\to 0}$ for two pumping frequencies $\omega_p/2\pi =$ 11.4 GHz [12] and $\omega_p/2\pi = 35.5$ GHz [9].

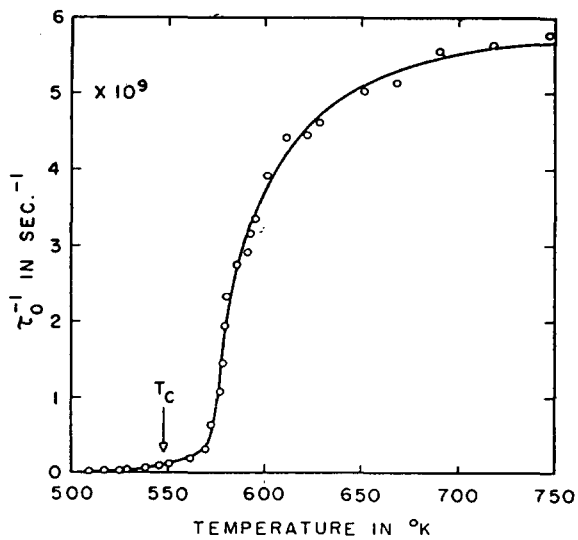

Fig. 9. Temperature dependence of Γ_0 at $\omega_k/2\pi = 5.7$ GHz in pure YIG in the Curie temperature region [12].

As for the k-dependent part of the relaxation frequency, $\Gamma_k(T)$, the most detailed research of it was carried out by Gurevich and Anisimov [9, 52]. They measured the parametric excitation threshold at higher frequency $\omega_p/2\pi = 3.55 \times 10^{10}$ s^{-1}, which provided an opportunity to vary the wave number in a wide range from 5×10^4 to 10^6 cm^{-1}.

It was found that the k-dependent part of the relaxation frequency $\Gamma_k(T)$ can be represented as a sum of two terms, linear and quadratic in T, $\Gamma_k^{(3)}$ and $\Gamma_k^{(4)}$, correspondingly (fig. 10),

$$\Gamma_k(T) = \Gamma_k^{(3)} + \Gamma_k^{(4)} . \tag{2.43}$$

It can be seen from the expressions for the relaxation frequencies (2.10) and (2.12) that the damping due to three-magnon processes is linear in T and the damping due to four-magnon processes is quadratic in T. Therefore the terms $\Gamma_k^{(3)}$ were determined as the three- and four-magnon relaxation frequencies. In fact, the expression for the exchange relaxation frequency in a ferromagnet (2.29) is not exactly quadratic in temperature. Nevertheless, a detailed analysis of both the temperature and the wavenumber dependences of the exchange damping allowed one to separate these contributions to the magnon relaxation [52].

The temperature dependence of the three-magnon relaxation frequency due to the magnetic dipole interaction is also somewhat more complicated than the linear one because of the temperature dependence of the magnetization,

$$\Gamma_k^{(3)} \sim TM(T)/M(0) . \tag{2.44}$$

An analysis of the relaxation frequencies $\Gamma_k^{(3)}$ and $\Gamma_k^{(4)}$ [52] showed that improved temperature dependences (2.29) and (2.44) for the relaxation frequencies $\Gamma_k^{(4)}$ and $\Gamma_k^{(3)}$ provide good agreement between the experimental data for the k-dependent part of the damping and the theoretical formulas (2.29), (2.35) and (2.36) for a ferromagnet. It should be noted that in ref. [52] the experimental temperature dependence of the magnon stiffness ω_{ex} in YIG was taken into account.

There is another way of magnon excitation which provides an opportunity of measuring the magnon relaxation time: the magnon kinetic instability [53]. The instability is caused by a highly excited packet of magnons created by an external microwave field. These magnons of the first generation decrease the relaxation frequency of magnons with small wave numbers because of the magnon–magnon interaction. At a certain critical number of magnons of the first generation, the relaxation frequency of the long-wavelength magnons becomes negative. This leads to a growth of the magnon packet of the second generation. The instability of the magnons of the second

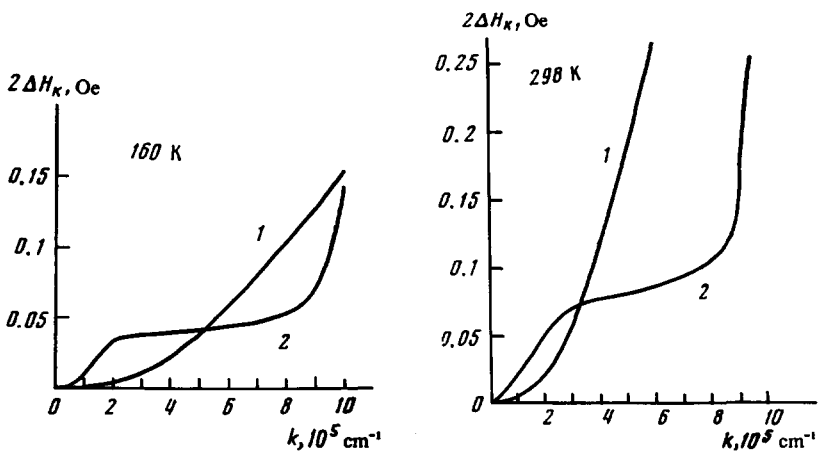

Fig. 10. Contribution of the three- and four-magnon processes to the spin wave relaxation at two temperatures. (1) $2\Delta H_k = 2\Gamma_k^{(4)}/g\mu$, (2) $\Delta H_k = 2\Gamma_k^{(3)}/g\mu$ [9].

generation is called kinetic instability. The most unstable magnons are those with the smallest damping in the absence of a microwave field. The electromagnetic radiation of the second generation magnons has been observed. It was found that the packet of the second generation magnons is narrow and it is located at the bottom of the ferromagnon spectrum, i.e. the wave vectors of these magnons are parallel to the magnetization, in contrast to the case of parallel pumping. After switching off the microwave field causing the instability, the decay time of the secondary magnon radiation was measured. It was found that the relaxation frequency of the second generation magnons is $\Gamma_0 \approx 5 \times 10^5\ s^{-1}$, their frequency is $\omega_k \approx 2\pi \times 2 \times 10^9\ s^{-1}$, and their wave number is $k_0 \approx 3 \times 10^3\ cm^{-1}$. This relaxation frequency is three times smaller than that determined from the linear extrapolation (2.4.2) for the data in the wave number range $k \geq 5 \times 10^4\ cm^{-1}$. This means that the linear extrapolation for the k-dependence of the magnon damping is not correct for small wave numbers.

2.2.2. *Temperature dependence of the magnon stiffness*

The temperature dependence of the magnon stiffness ω_{ex} is also due to the magnon–magnon interactions. The ferromagnon stiffness in YIG was measured by LeCraw and Walker [30]. They found that, in contrast to the case of a simple cubic ferromagnet, the magnon stiffness in YIG increases with the temperature in the low-temperature range $0 < T < 200$ K (see fig. 11). At $T > 250$ K the magnon stiffness decreases. The theory of the low-temperature magnon stiffness dependence in YIG is considered further in section 2.3.2.

2.2.3. *Summary of experimental results*

There are three experimental results which cannot be explained in the framework of the simple cubic ferromagnet model: (i) The k-independent magnon relaxation, which is roughly proportional to the temperature [12, 9], (ii) the discrepancy between the relaxation frequency of magnons with

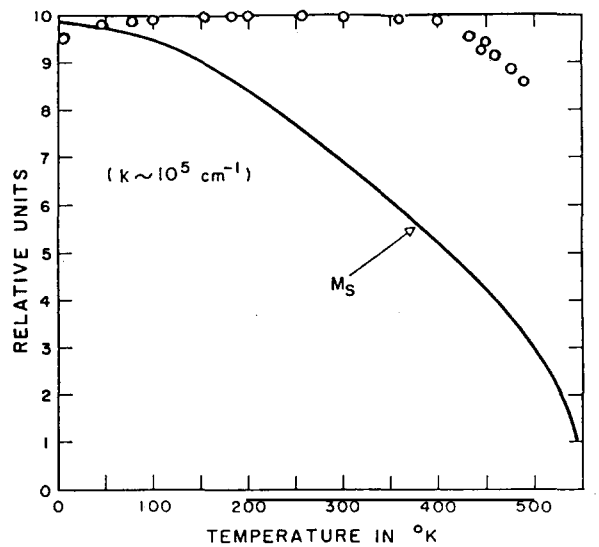

Fig. 11. Temperature dependence of the exchange constant D in YIG. The pumping frequency is 11.38 GHz and the dc magnetic field is along the [111] crystal axis. At $T = 30$ K, D is 0.96×10^{-2} erg cm^2 [30].

very small wave numbers measured directly [53] and that obtained from the linear extrapolation (2.42) [12, 9], and (iii) the temperature dependence of the magnon stiffness [30].

As far as the k-dependent part of the relaxation frequency is concerned, an agreement between the experiments and the theory was found. As for relatively small wave numbers of magnons ($5 \times 10^4 < k < 5 \times 10^4\,\mathrm{cm}^{-1}$), the agreement may be even improved using some interpolation parameters in the formula for the three-magnon damping (2.35) [54]. However, this agreement is based upon the assumption that the temperature dependence of the magnon stiffness substituted into the formulas for the relaxation frequency is found not from the theory but from the experimental data. This means that the theory for the k-dependent part of the magnon damping is inconsistent, and the good agreement between the simple theoretical model and experimental results is due to cancellation of the influences of various factors which appear in a consistent theory.

2.3. Exchange interaction of magnons

This section is devoted to the effect of the magnon–magnon exchange interaction on the ferromagnon stiffness and relaxation in YIG.

2.3.1. Hamiltonian of exchange interaction

In order to study these effects one has to express the exchange Hamiltonian (1.1) in terms of the magnon variables and expand the Hamiltonian up to the fourth order in the magnon amplitudes. The first step on this way is to express the exchange interaction Hamiltonian in terms of the local creation and annihilation operators $a_i^\dagger, a_i$ according to the Holstein–Primakoff transformation (1.6). The next step is to perform the Fourier transformation (1.14). As a result, the Hamiltonian takes the form:

$$H_{\mathrm{ex}} = H_{\mathrm{ex}}^{(2)} + H_{\mathrm{ex}}^{(4)} . \tag{2.45}$$

The quadratic Hamiltonian $H_{\mathrm{ex}}^{(2)}$ has been discussed in detail in chapter 1. It consists of three terms, each of them describing the spin interaction in pairs of sites (a)–(a), (d)–(d), and (a)–(d),

$$H^{(2)} = \sum_{\boldsymbol{k}} H_{\boldsymbol{k}}^{(2)} ,$$

$$H_{\boldsymbol{k}}^{(2)} = \sum_{i,j=1}^{8} A_{ij}(\boldsymbol{k}) a_{i\boldsymbol{k}}^\dagger a_{j\boldsymbol{k}} + \sum_{i,j=9}^{20} D_{ij}(\boldsymbol{k}) a_{i\boldsymbol{k}}^\dagger a_{j\boldsymbol{k}} + \sum_{i=1}^{8}\sum_{j=9}^{20} [B_{ij}(\boldsymbol{k}) a_{i\boldsymbol{k}}^\dagger a_{j-\boldsymbol{k}}^\dagger + \mathrm{h.c.}] . \tag{2.46}$$

Detailed expressions for the matrices A, B, and D have been given in eq. (1.16) in the previous chapter. The fourth-order term in the Hamiltonian (2.45), $H_{\mathrm{ex}}^{(4)}$, can be also expressed in terms of the matrices A, B, and D,

$$H_{\mathrm{ex}}^{(4)} = H_{\mathrm{ad}}^{(4)} + H_{\mathrm{dd}}^{(4)} + H_{\mathrm{aa}}^{(4)} , \tag{2.47}$$

$$H_{\mathrm{ad}}^{(4)} = -(4NS_0)^{-1} \sum_{1,2,3,4} \sum_{i=1}^{9}\sum_{j=9}^{20} \{B_{ij}(\boldsymbol{k}_{24}) a_{i1}^\dagger a_{j2}^\dagger a_{i3} a_{j4} \Delta(\boldsymbol{k}_1 + \boldsymbol{k}_2 - \boldsymbol{k}_3 - \boldsymbol{k}_4)$$

$$+ [B_{ij}^*(\boldsymbol{k}_4)(a_{i1}^\dagger a_{i2} a_{i3} a_{i4} + a_{j1} a_{j2}^\dagger a_{j3}^\dagger a_{i4}^\dagger) + \mathrm{h.c.}] \Delta(\boldsymbol{k}_1 - \boldsymbol{k}_2 - \boldsymbol{k}_3 - \boldsymbol{k}_4)\} , \tag{2.48}$$

$$H_{dd}^{(4)} = (8NS_0)^{-1} \sum_{1,2,3,4} \Delta(\boldsymbol{k}_1 + \boldsymbol{k}_2 - \boldsymbol{k}_3 - \boldsymbol{k}_4)$$

$$\times \sum_{i,j=9}^{20} \{D_{ij}(\boldsymbol{k}_{13}) a_{i1}^\dagger a_{j2}^\dagger a_{i3} a_{j4} + D_{ij}(\boldsymbol{k}_{14}) a_{i1}^\dagger a_{j2}^\dagger a_{j3} a_{i4}$$

$$+ D_{ij}(\boldsymbol{k}_{23}) a_{i1}^\dagger a_{j2}^\dagger a_{j3} a_{j4} + D_{ij}(\boldsymbol{k}_{24}) a_{i1}^\dagger a_{j2}^\dagger a_{i3} a_{j4}$$

$$- D_{ij}(\boldsymbol{k}_1) a_{j1}^\dagger a_{i2}^\dagger a_{i3} a_{i4} - D_{ij}(\boldsymbol{k}_2) a_{j1}^\dagger a_{i2}^\dagger a_{i3} a_{i4} - D_{ij}(\boldsymbol{k}_3) a_{j1}^\dagger a_{j2}^\dagger a_{i3} a_{j4}$$

$$- D_{ij}(\boldsymbol{k}_4) a_{j1}^\dagger a_{j2}^\dagger a_{j3} a_{i4} - [\text{terms with } (j \leftrightarrow i) \text{ and } (3 \leftrightarrow 4)]\} ,$$

$$\boldsymbol{k}_{\alpha\beta} \equiv \boldsymbol{k}_\alpha - \boldsymbol{k}_\beta , \quad a_{i\alpha} = a_i(\boldsymbol{k}_\alpha) , \quad \alpha, \beta = 1,2,3,4 . \tag{2.49}$$

The term H_{aa} can be obtained from eq. (2.49) by substitution of the matrix D_{ij} by A_{ij} and summation over i and j from 1 to 8. The last step consists in the linear transformation (1.26) from operators $a_{ik}^\dagger, a_{ik}$ to the magnon variables $b_{jk}^\dagger, b_{jk}$. The quadratic Hamiltonian $H_{ex}^{(2)}$ is diagonal in the magnon variables,

$$H_{ex}^{(2)} = \sum_{j,k} \omega_j(\boldsymbol{k}) b_{jk}^\dagger b_{jk} . \tag{2.50}$$

In chapter 1 we have proposed an efficient means of approximate diagonalization of the quadratic Hamiltonian by converting to a quasinormal basis in which the diagonal elements of the Hamiltonian matrix are close to the eigenfrequencies of the magnons while the off-diagonal terms are small (1.45). In this approximation, the eigenvector and the frequency of the ferromagnetic mode are

$$b_{1k} = \frac{u_k}{\sqrt{12}} \sum_{i=9}^{20} a_{ik} + \frac{v_k}{\sqrt{8}} \sum_{i=1}^{8} a_{i-k}^\dagger , \quad \omega_{1k} = \tfrac{1}{2}(\sqrt{C_k^2 - 4|B_k|^2} - A_k + D_k) , \tag{2.51}$$

where

$$\frac{1}{8}\sum_{i,j} A_{ij}(\boldsymbol{k}) \equiv A_k , \quad \frac{1}{12}\sum_{i,j} D_{ij}(\boldsymbol{k}) \equiv D_k , \quad \frac{1}{\sqrt{8\cdot 12}}\sum_{i,j} B_{ij}(\boldsymbol{k}) \equiv B_k ,$$

$$C_k \equiv A_k + D_k , \quad \begin{pmatrix} u_k \\ v_k \end{pmatrix} = \frac{\sqrt{C_k + 2|B_k|} \pm \sqrt{C_k - 2|B_k|}}{2(C_k^2 - 4|B_k|^2)^{1/4}} . \tag{2.52}$$

In the long-wavelength limit this leads to the well known formula (1):

$$\omega_{1k} = \omega_{ex}(ak)^2 , \quad \omega_{ex} = \tfrac{5}{16}(8J_{aa} + 3J_{dd} - 5J_{ad}) .$$

The last transformation results in the form of the desired four-magnon interaction term in the Hamiltonian

$$H^{(4)} = \frac{1}{2} \sum_{12,34} \sum_{i \le j, l \le m} T_{12,43}^{ijlm} b_{i1}^\dagger b_{j2}^\dagger b_{l3} b_{m4} \Delta(\boldsymbol{k}_1 + \boldsymbol{k}_2 - \boldsymbol{k}_3 - \boldsymbol{k}_4) . \tag{2.53}$$

We shall henceforth be concerned with the interactions of ferromagnons with one another and with low-lying optical magnons. In the quasinormal approximation it follows from (2.52) that

$$
\begin{aligned}
&T_{12,34}^{11,11} = T_{12,34} + \tfrac{1}{4}(\tilde{T}_{12,34} + \tilde{T}_{21,34} + \tilde{T}_{12,43} + \tilde{T}_{21,43}) ,\\
&T_{12,34} = (C_{12,34}/16NS_0)(\omega_1 + \omega_2 + \omega_3 + \omega_4 - \omega_{13} - \omega_{14} - \omega_{23} - \omega_{24}) ,\\
&C_{12,34} = \tfrac{1}{6}(2u_1u_2u_3u_4 - 3v_1v_2v_3v_4) ,\\
&\tilde{T}_{12,34} = -(B_{13}/24NS_0)[2\sqrt{6}\,u_1v_2u_3v_4 - 2u_1u_2u_3u_4(v_{13}/u_{13}) - 3v_1v_2v_3v_4(u_{13}/v_{13})] .
\end{aligned}
\tag{2.54}
$$

Here S_0 is the spin of a Fe ion, $\omega_1 \equiv \omega_1(\boldsymbol{k})$, $u_1 \equiv u(\boldsymbol{k}_1)$, $\omega_{13} \equiv \omega_1(\boldsymbol{k}_{13}) \equiv \omega_1(\boldsymbol{k}_1 - \boldsymbol{k}_3)$, $B_{13} \equiv B(\boldsymbol{k}_1 - \boldsymbol{k}_3)$, etc. In the limit of small $\boldsymbol{k}$ the expression for $T_{12,34}^{11,11}$ goes over into the familiar expression for the interaction of magnons in a ferromagnet in the continuum approximation. In the long-wavelength limit $T_{12,34} \propto k^2$, while $\tilde{T}_{12,34} \propto k^4$ and can be neglected. At the zone boundary $\tilde{T}_{12,34}$ is approximately one half $T_{12,34}$, and for purposes of estimation one can assume $T_{12,34}^{11,11} = T_{12,34}$. The form of the expression for $T_{12,34}$ is reminiscent of the familiar formula for ferromagnets with spin $\bar{S} = 4S_0$ and dispersion law ω_k [34]. It should, however, be kept in mind that $C_{12,34}$ falls off from 1 (at $\boldsymbol{k}_i \to 0$) to 0.5 (when all the k_i lie on the zone boundary) and that the form of ω_k for ferromagnons in YIG is considerably different from that of ω_k in ferromagnets.

2.3.2. Temperature dependence of the ferromagnon frequency

In the spin-wave approximation the temperature correction to the ferromagnon frequency is given by eq. (2.18), which can be written as

$$
\begin{aligned}
&\Delta\omega_k = \sum_j \Delta\omega_k^{(j)} , \quad \Delta\omega_k^{(1)} = 2\sum_{k'} T_{kk'}^{11} n_{k'}^{(1)} ,\\
&\Delta\omega_k^{(j)} = \frac{1}{2}\sum_{k'} T_{kk'}^{ij} n_{k'}^{(j)} , \quad j \neq 1 , \quad T_{kk'}^{ij} \equiv T_{kk',kk'}^{ij,ij} ,
\end{aligned}
\tag{2.55}
$$

where $n_k^{(j)}$ are the equilibrium occupation numbers for the magnons of branch j. For $T \lesssim 300$ K in YIG only the ferromagnons ($j = 1$) are excited, and for determining $\Delta\omega_k(T)$ it is sufficient to take into account only $T_{kk'}$. The expression for $\Delta\omega_k(T)$ even in this case will be awkward, and we shall therefore discuss only the long-wavelength limit ($k < k_0$, $\omega_{k0} = 40$ K) and allow for the fact that ω_k for ferromagnons in YIG is practically independent of the direction of $\boldsymbol{k}$. Then,

$$
\Delta\omega_k = 2\sum_{k'} T_{kk'}^{11} n_{k'} = \frac{a^3}{2\pi^2}\int_0^{k_B} \langle T_{kk'}^{11} \rangle n_{k'} k'^2 \, \mathrm{d}k' . \tag{2.56}
$$

Here $\langle T_{kk'}^{11} \rangle$ is the expression (2.54) for $T_{kk'}^{11}$ averaged over the angles of the wave vector $\boldsymbol{k}'$ and k_B is the average wave vector on the boundary of the Brillouin zone.

At low temperature ($T < 40$ K) the k' integration in (2.56) is taken over the long-wavelength region ($k' < k_0, \omega_{k0} = 40$ K), in which the dispersion relation simplifies to the quadratic form in eq. (1). Here the expression for $\langle T_{kk'}^{11} \rangle$ also simplifies substantially,

$$
\langle T_{kk'}^{11} \rangle \approx 0.32 |J_{aa}| (a^4 k^2 k' 2/N\bar{S}) . \tag{2.57}
$$

It is seen that even in the long-wavelength limit the matrix element $\langle T_{kk'}^{11} \rangle$ differs not only in magnitude but also in sign from the corresponding expression for a simple cubic ferromagnet with a nearest-neighbor interaction

$$\langle T_{kk'} \rangle = -0.04 J(a^4 k^2 k'^2 / N\bar{S}) . \tag{2.58}$$

In the continuum limit for ferromagnets, in which case $\omega_k \propto k^2$, one has $\langle T_{kk'}^{11} \rangle = 0$. This quantity therefore depends on the specific type of crystal structure and functional form of $J_{nn'}$. The possibility of a positive $\langle T_{kk'}^{11} \rangle$ in two-sublattice ferromagnets was pointed out in ref. [55]. It should also be noted that in evaluating $\langle T_{kk'}^{11} \rangle$ in YIG one cannot neglect in eq. (2.54) the terms $\tilde{T}$, which contribute substantially to the terms of order $k^2 k'^2$ in the expansion.

Substituting the expression for $\langle T_{kk'}^{11} \rangle$ into the integral (2.56), we obtain the temperature correction to the frequency: $\Delta\omega_k(T) = \Delta\omega_{ex}(T)(ak)^2$. The function $\Delta\omega_{ex}(T)$ is plotted in fig. 12. The dashed curve shows this function as evaluated in the low-temperature limit with the aid of eqs. (2.56) and (1),

$$\Delta\omega_{ex}/\omega_{ex} = 0.44(T/10|J_{ad}|)^{5/2} \approx 1.0(T/T_c)^{5/2} . \tag{2.59}$$

Strictly speaking, this expression is valid only at temperatures in the range $T < 10$ K, at which only long-wavelength magnons with the quadratic spectrum are excited. It is seen from fig. 12, however, that the expression (2.59) can be used with 10% accuracy up to $T = 150$ K; this situation is explained by the following circumstances: Firstly, in the higher-energy region $ak' > 1$, where the magnon dispersion law ω_k, becomes linear, there is a slowing of the growth of the matrix element $\langle T_{kk'}^{11} \rangle$. Secondly, in this region one has $\omega_{k'} < \omega_{ex}(ak')^2$, and so the occupation number n_k is greater than that on the quadratic spectrum for the same k'. As a result, the product $\langle T_{kk'}^{11} \rangle$ describing the temperature correction to the frequency turns out to be close to its long-wavelength limit at values $ak' < 3$. The temperature dependence of $\omega_{ex}(T)$ obtained here agrees with experimental data, both in sign and in magnitude of the effect, for temperatures up to 150–200 K.

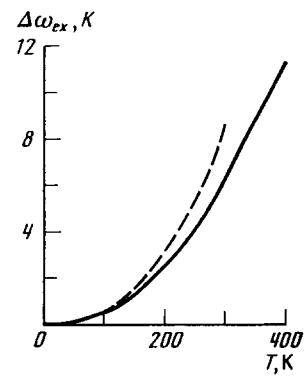

Fig. 12. Temperature dependence of the exchange frequency $\Delta\omega_{ex} = \omega_{ex}(T) - \omega_{ex}(0)$ in YIG. The dashed curve is the low-temperature expansion for $\Delta\omega_{ex}$ in a ferromagnet with a spin corresponding to the spin of the unit cell of YIG [56].

2.3.3. Exchange relaxation of ferromagnons

The relaxation rate of magnons is given by the well known expression

$$\gamma_k^i = 2\pi \sum_{1,2,3,b} \sum_{j,l,m} |T^{ijlm}_{k1,2,3}[n_1^j (n_2^1 + n_3^m + 1) - n_2^l n_3^m] \delta(\omega_k^i + \omega_1^j - \omega_2^l - \omega_3^m)$$

$$\times \Delta(\boldsymbol{k} + \boldsymbol{k}_1 - \boldsymbol{k}_2 - \boldsymbol{k}_3 + \boldsymbol{b}) , \tag{2.60}$$

where $\boldsymbol{b}$ are the reciprocal lattice vectors, $\boldsymbol{k}_1, \boldsymbol{k}_2$, and $\boldsymbol{k}_3$ run over the first Brillouin zone, $\Delta(\boldsymbol{k}) = 0$ for $\boldsymbol{k} \neq 0$ and $\Delta(0) = 1$, and i, j, l, and m number the magnon branches.

The relaxation of the low-frequency ferromagnons $\omega_k \lesssim 1$ K, corresponding to $ak \lesssim 0.1$, can currently be studied in experiment, and for this reason it is of greatest interest to evaluate the damping of these magnons. At moderate temperatures $T < 200$ K one can neglect the scattering by optical magnons, which have an activation energy $\gtrsim 260$ K, i.e., one can set $i = j = l = m = 1$ in eq. (2.60). In the long-wavelength limit one can neglect the contribution $\tilde{T}_{k1,2,3}$ (which is quadratic in ak) in expression (2.54) for the matrix element $T^{1111}_{k1,2,3}$. It can also be seen that when the conservation laws are taken into account, $C_{k1,2,3}$ varies by less than 15% over the entire Brillouin zone. As a result, we obtain for $T^{1111}_{k1,2,3}$ the approximate expression

$$T^{1111}_{k1,2,3} = -(1/8NS_0)(\boldsymbol{v}_2 + \boldsymbol{v}_3)\cdot\boldsymbol{k} , \tag{2.61}$$

where $\boldsymbol{v}_k = \partial\omega_k/\partial\boldsymbol{k}$ is the group velocity. This expression is valid for arbitrary $\boldsymbol{k}_1, \boldsymbol{k}_2$, and $\boldsymbol{k}_3$.

At temperatures which are not too high, the contribution of umklapp processes and the finiteness of the Brillouin zone are not important, and the dispersion law ω_k is spherically symmetric. This permits us to perform the integration over angles in eq. (2.60) and to reduce the five-dimensional integral to a double integral. Changing to the dimensionless variable $\varepsilon_k = \omega_k/10|J_{ad}|$, we obtain

$$\gamma_k = \frac{32}{3\pi^3} \frac{(ak)^2 \omega_k}{A^2 S^2} F(T/10|J_{ad}|, \varepsilon_k) , \tag{2.62}$$

$$F(\tau, \varepsilon) = \frac{1}{\tau} \int_{\varepsilon_2+\varepsilon_3>\varepsilon} \int^{\varepsilon_2+\varepsilon_3<\varepsilon_m} \left[\frac{(2\varepsilon_2+1)^2 - 1}{(2\varepsilon_2+1)^2 - 1} + \frac{(2\varepsilon_3+1)^2 - 1}{(2\varepsilon_3+1)^2} + \frac{8\varepsilon_2\varepsilon_3}{(2\varepsilon_2+1)(2\varepsilon_3+1)} \right]$$

$$\times \frac{(2\varepsilon_2 + 2\varepsilon_3 + 1)(2\varepsilon_2 + 1)(2\varepsilon_3 + 1)}{(e^{\varepsilon_2/\tau} - 1)(e^{\varepsilon_3/\tau} - 1)(1 - e^{-(\varepsilon_2+\varepsilon_3)/\tau})} d\varepsilon_2 \, d\varepsilon_3 , \quad \varepsilon_m = 0.88 . \tag{2.63}$$

Here we have used an approximation for ε_k which follows from (2.51) with our choice of exchange integrals,

$$\varepsilon_k = [(\sqrt{1 + Aq^2}) - 1]/2 , \quad \boldsymbol{q} = (a\boldsymbol{k})/8 ,$$

$$A = 40(1 - J_{dd}/2J_{ad} - 2J_{aa}/J_{ad}) \approx 25.7 \text{ K} .$$

This approximation is valid to within 20% over the entire Brillouin zone. At temperatures below 40 K, where magnons are excited in the quadratic part of the spectrum, the damping γ_k coincides

with the damping of magnons in a ferromagnet [34, 47] with a dispersion law $\omega_{ex}(ak)^2$ and a unit-cell spin $\bar{S}$. In this case

$$F = 16(T/10|J_{ad}|)^2[\ln^2(T/\omega_k) - \tfrac{10}{3}\ln(T/\omega_k) - 0.3] . \tag{2.64}$$

However, by analyzing eq. (2.63), one is readily convinced that the angle-averaged square of the matrix element – the expression in brackets – differs little from its long-wavelength asymptotic behavior at energies all the way up to 200 K, i.e., $\varepsilon_k \approx 0.5$. Therefore, eq. (2.64) can be used for the damping of ferromagnons in YIG at temperatures up to 200 K (see fig. 13). For the temperature range $200 < T < 350$ K one can obtain from (2.63) another approximate expression which corresponds to integration only over the linear part of the dispersion law,

$$F \approx 32(T/10|J_{ad}|)^4 . \tag{2.65}$$

2.3.4. The contribution of umklapp processes to the exchange relaxation of long-wavelength ferromagnons

The energy of the magnons which take part in these processes is approximately $\omega_B/2 \approx 150$ K (ω_B is the ferromagnon frequency at the boundary of the Brillouin zone). Therefore, starting at around this temperature, umklapp processes can be important. Integration over the magnon momenta and summation over the twelve reciprocal lattice vectors of the [110] type with allowance for the conservation laws yields

$$\gamma_k^u = 2.4 \times 10^{-4}\,\omega_k(ak)^2 \frac{10|J_{ad}|/T}{(e^{\omega_B/2T} - 1)^2(1 - e^{-\omega_B/T})} , \tag{2.66}$$

where ω_B is the ferromagnon frequency at the Brillouin zone boundary in the [110] direction. At $T = 300$ K the umklapp contribution (2.66) amounts to $\gamma_k^u = 8.5 \times 10^{-5}\,\omega_k(ak)^2$, which is considerably smaller than the damping (2.65) in normal processes: $\gamma_k^n = 6.2 \times 10^{-4}\,\omega_k(ak)^2$. At temperatures above 300 K one has $\gamma^u \propto T^2$, while $\gamma^n \propto T^4$, and so the relation $\gamma_k^u \ll \gamma_k^n$ remains valid. The smallness of γ_k^u is due to the smallness of the phase volume in which umklapp processes are allowed.

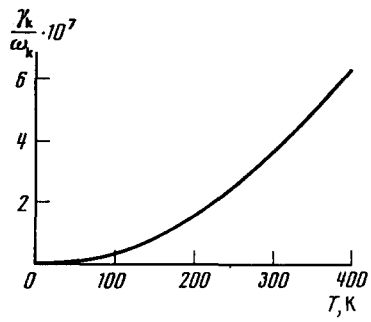

Fig. 13. Temperature dependence of the exchange relaxation rate of ferromagnons in YIG for $k = 10^5$ cm^{-1} [56].

2.4. Magnetic dipole interaction and relaxation of ferromagnons

2.4.1. The amplitude of the three-magnon magnetic dipole interaction

If the phase velocities of excitation in a magnet are small compared to that of light, the magnetic interaction can be taken into account through an effective Hamiltonian which has the form

$$H_{\mathrm{m}} = 2\pi \sum_{k} (|\boldsymbol{m}_k \cdot \boldsymbol{n}|^2 - \tfrac{1}{3}|m_k|^2) = \sum_{k} m_k^{\alpha} m_{-k}^{\beta} (k_\alpha k_\beta / k^2 - \tfrac{1}{3}\delta_{\alpha\beta}) \,. \tag{2.67}$$

Here $\boldsymbol{m}_k$ is the Fourier component of the ac magnetic moment density $\boldsymbol{m}(\boldsymbol{r})$, $\boldsymbol{n} = \boldsymbol{k}/k$, and the summation runs over the whole $\boldsymbol{k}$-space. In order to reduce the summation to the first Brillouin zone Ω, eq. (2.67) can be rewritten as

$$H_{\mathrm{m}} = 2\pi \sum_{k \in \Omega} \sum_{b} m_{k+b}^{\alpha} m_{k+b}^{\beta} [(k+b)_\alpha (k+b)_\beta / (\boldsymbol{k}+\boldsymbol{b})^2 - \tfrac{1}{3}\delta_{\alpha\beta}] \,, \tag{2.68}$$

where the vectors $\boldsymbol{b}$ run over the reciprocal lattice. In YIG, the Fourier components of the magnetization are not invariant with respect to the reciprocal lattice vector shift,

$$\boldsymbol{m}_{k+b} \neq \boldsymbol{m}_k \,.$$

However, if Λ is a symmetry transformation of the crystal, then

$$\boldsymbol{m}_{k+\Lambda b} = \boldsymbol{m}_{k+b'} \,.$$

The YIG symmetry group $G = O_h^{10}$ is sufficiently rich to provide the equality $\langle k_\alpha k_\beta / k^2 \rangle = \frac{1}{3}\delta_{\alpha\beta}$. The magnetic dipole interaction is significant in the long-wavelength limit only ($k \ll b$). The Hamiltonian of the magnetic dipole–dipole interaction in this case can be written

$$H_{\mathrm{m}} = 2\pi \frac{(g\mu_{\mathrm{B}})^2}{v_0} \sum_{k} \left| \boldsymbol{n} \cdot \sum_{i=1}^{26} \boldsymbol{s}_{i,k} \right|^2 \,, \tag{2.69}$$

where $\boldsymbol{n} = \boldsymbol{k}/k$, $\boldsymbol{s}_i$ is the deviation of the ith spin from equilibrium, g is a factor ≈ 2, v_0 is the volume of the primitive cell, and the Fourier transformation is defined in eq. (1.14). The term

$$\sum_{k \in \Omega} |\boldsymbol{m}_k|^2 \propto \sum_{n} \left(\sum_{j=1}^{20} \boldsymbol{s}_{j,n} \right)^2$$

has been omitted because it is taken into account by a redefinition of the Zeeman interaction (see below) and by a negligible shift of the exchange integrals.

Using the Holstein–Primakoff (1.6) transformation and expanding H_{m} up to the third order in the creation and annihilation operators $a_i^{\dagger}$, a_i,

$$H_{\mathrm{m}} \approx H_{\mathrm{m}}^{(2)} + H_{\mathrm{m}}^{(3)} \,, \tag{2.70}$$

one can obtain the terms $H^{(2)}$ and $H^{(3)}$. The quadratic Hamiltonian $H_{\mathrm{m}}^{(2)}$ is

$$H_{\mathrm{m}}^{(2)} = \frac{\omega_{\mathrm{m}}}{2}\sum_{k}\left\{\sin^2\theta_k\,\frac{1}{4}\left(\sum_{9}^{20} a_{ik}^{\dagger} + \sum_{1}^{8} a_{i-k}\right)\left(\sum_{9}^{20} a_{ik} + \sum_{1}^{8} a_{i-k}^{\dagger}\right)\right.$$
$$\left. + \frac{1}{2}\left[\sin^2\theta_k\,\mathrm{e}^{\mathrm{i}\varphi_k}\frac{1}{4}\left(\sum_{9}^{20} a_{ik} + \sum_{1}^{8} a_{i-k}^{\dagger}\right)\left(\sum_{9}^{20} a_{i-k} + \sum_{1}^{8} a_{ik}^{\dagger}\right) + \mathrm{h.c.}\right]\right\}, \tag{2.71}$$

$$\omega_{\mathrm{m}} = 16\pi S_0 (g\mu)^2 / v_0 . \tag{2.72}$$

Here θ_k and φ_k are the polar axial angles of the wave vector $\boldsymbol{k}$ in the coordinate system with the z axis directed along the equilibrium magnetization. The magnetic dipole interaction is essential for small k only. The oscillating part of the magnetization is

$$m_k^{\dagger} = \sqrt{2S_0}\left(\sum_{i=9}^{20} a_{ik} + \sum_{i=1}^{8} a_{i-k}^{\dagger}\right). \tag{2.73}$$

For small k ($ak \ll 1$) it is proportional to the ferromagnon amplitude b_{1k},

$$b_{1k} = \frac{1}{2}\left(\sum_{i=9}^{20} a_{ik} + \sum_{i=1}^{8} a_{i-k}^{\dagger}\right). \tag{2.74}$$

Consequently, the quadratic term in the Hamiltonian of the magnetic dipole interaction coincides with that for a ferromagnet in the long-wavelength limit [33],

$$H_{\mathrm{m}}^{(2)} = \frac{\omega_{\mathrm{m}}}{2}\sum_{k}\left[\sin 2\theta_k\, b_{1k}^{\dagger} b_{1k} + \tfrac{1}{2}(\sin^2\theta_k\,\mathrm{e}^{-2\mathrm{i}\varphi_k} b_{1k} b_{1-k} + \mathrm{h.c.})\right]. \tag{2.75}$$

The cubic term in (2.70), $H_{\mathrm{m}}^{(3)}$, takes the form:

$$H_{\mathrm{m}}^{(3)} = \frac{1}{2}\sum_{k_1 k_2 k}\left\{\left[\frac{V_k}{2}\left(\sum_{9}^{20} a_{ik}^{\dagger} + \sum_{1}^{3} a_{i-k}\right)\left(\sum_{9}^{20} a_{ik_1}^{\dagger} a_{ik_2} - \sum_{1}^{8} a_{i-k_2}^{\dagger} a_{i-k_1}\right)\right.\right.$$
$$\left.\left. + \frac{V_{k_1}}{2}\left(\sum_{9}^{20} a_{ik_1} + \sum_{1}^{8} a_{i-k_1}\right)\left(\sum_{9}^{20} a_{ik}^{\dagger} a_{ik_2} - \sum_{5}^{8} a_{i-k_2}^{\dagger} a_{i-k}\right)\right]\Delta(\boldsymbol{k} + \boldsymbol{k}_1 - \boldsymbol{k}_2) + \mathrm{h.c.}\right\},$$

$$V_k = -(\omega_{\mathrm{m}}/\sqrt{2S_0})\sin 2\theta_k\,\mathrm{e}^{\mathrm{i}\varphi_k} . \tag{2.76}$$

If in eq. (2.76) all the wave vectors $\boldsymbol{k}, \boldsymbol{k}_1$, and $\boldsymbol{k}_2$ are small, the Hamiltonian $H_{\mathrm{m}}^{(3)}$ can be transformed, taking advantage of the scalar product invariance against (u–v) transformations

$$\sum_{i=9}^{20} a_{ik}^{\dagger} a_{ik} - \sum_{i=1}^{8} a_{i-k}^{\dagger} a_{i-k} = \sum_{i=1}^{12} b_{ik}^{\dagger} b_{ik} - \sum_{i=13}^{30} b_{ik}^{\dagger} b_{ik} , \tag{2.77}$$

and equality (2.74), into the form:

$$H_{\mathrm{m}}^{(3)} = \frac{1}{2}\sum_{k_1 k_2 k}\Bigg\{\Bigg[V_k b_{1k}^{\dagger}\Bigg(\sum_{i=1}^{12} b_{ik_1}^{\dagger} b_{ik_2} - \sum_{i=13}^{20} b_{ik_1}^{\dagger} b_{ik_2}\Bigg) + V_{k_1} b_{1k_1}^{\dagger}\Bigg(\sum_{i=3}^{12} b_{ik}^{\dagger} b_{ik_2} - \sum_{i=13}^{20} b_{ik}^{\dagger} b_{ik_2}\Bigg)\Bigg]\Delta(\boldsymbol{k}+\boldsymbol{k}_1-\boldsymbol{k}_2) + \mathrm{h.c.}\Bigg\}. \tag{2.78}$$

In particular, the term (2.78) results in the well known long-wave length limit [57, 48] for the ferromagnon interaction amplitude

$$V_{kk_1,k_2} = V_k + V_{k_1},$$

$$H_{\mathrm{m,fm}}^{(3)} = \frac{1}{2}\sum_{kk_1k_2}\left[V_{kk_1,k_2} b_k^{\dagger} b_{k_1}^{\dagger} b_{k_2}\Delta(\boldsymbol{k}_1+\boldsymbol{k}-\boldsymbol{k}_2) + \mathrm{h.c.}\right]. \tag{2.79}$$

The term $H_{\mathrm{m,fm}}^{(3)}$ is suitable, within accuracy 10–15%, even if only one of the wave vectors is small and the other two are arbitrary. Indeed if only ferromagnons are excited the amplitudes a_{ik} are

$$a_{ik} = (u_k/\sqrt{12})b_k \quad i = 9, \ldots, 20, \quad u_0 = \sqrt{3},$$

$$a_{i-k}^{\dagger} = -(v_k/\sqrt{8})b_k \quad i = 1, \ldots, 8, \quad v_0 = \sqrt{2} \tag{2.80}$$

in the quasinormal approximation. Substituting (2.80) into (2.79), one obtains

$$H_{\mathrm{m,fm}}^{(3)} = \frac{1}{2}\sum_{kk_1k_2}\{[V_k(\sqrt{3}u_k - \sqrt{2}v_k)(u_{k_1}u_{k_2} - v_{k_1}v_{k_2}) + V_{k_1}(\sqrt{3}u_k - \sqrt{2}v_k)(u_k u_{k_2} - v_k v_{k_2})] \times b_k^{\dagger} b_{k_1}^{\dagger} b_{k_2}\Delta(\boldsymbol{k}+\boldsymbol{k}_1-\boldsymbol{k}_2) + \mathrm{h.c.}\}. \tag{2.81}$$

If $k \to 0$ ($ak \ll 1$) and $\boldsymbol{k}_2$ and $\boldsymbol{k}_3$ are arbitrary, one can transform eq. (2.81) neglecting terms of higher orders in k,

$$\sqrt{3}u_k - \sqrt{2}v_k = 1, \quad u_{k_1}u_{k_2} - v_{k_1}v_{k_2} \approx u_{k_1}^2 - v_{k_1}^2 = 1,$$

$$(\sqrt{3}u_{k_1} - \sqrt{2}v_{k_2})(u_k u_{k_2} - v_k v_{k_2}) = (\sqrt{3}u_{k_1} - \sqrt{2}v_{k_1})^2 = [1-(u_0-u_{k_1})^2 - (v_{k_1})^2]^2 = f(\boldsymbol{k}_1). \tag{2.82}$$

The expansion of the function $f(\boldsymbol{k}_1)$ in powers of $\boldsymbol{k}_1$ begins with the term of the fourth order, therefore the function $f(\boldsymbol{k}_1)$ is close to constant: $f(0) = 1$, $f(k_1 a = 2.5) = 1.05$ (in the middle of the Brillouin zone), and $f(ka = 4.9) = 1.3$ (at the edge of the spherical Brillouin zone).

The Zeeman Hamiltonian is

$$H_Z = -g\mu_B H \sum_{i,n} S_{in} = g\mu_B H \sum_k \left(\sum_{i=1}^{20} a_{ik}^\dagger a_{ik} - \sum_{i=1}^{8} a_{ik}^\dagger a_{ik} \right)$$

$$= \omega_H \sum_k \left(\sum_{i=1}^{12} b_{ik}^\dagger b_{ik} - \sum_{i=13}^{20} b_{ik}^\dagger b_{ik} \right) , \tag{2.83}$$

where $\omega_H = g\mu H$, H is the internal magnetic field.

2.4.2. Magnetic dipole relaxation

The magnetic-dipole damping of ferromagnons, as we know, is due to decay and coalescence processes,

$$\omega_k = \omega_{k_1} + \omega_{k_2} , \quad \boldsymbol{k} = \boldsymbol{k}_1 + \boldsymbol{k}_2 , \tag{2.84}$$

$$\omega_k + \omega_{k_1} = \omega_{k_2} , \quad \boldsymbol{k} + \boldsymbol{k}_1 = \boldsymbol{k}_2 . \tag{2.85}$$

For magnons with small $\boldsymbol{k}$ only the coalescence processes (2.85) are allowed by the conservation laws. The damping contribution from these processes is given by the well known formula

$$\gamma_{mk} = \pi \sum_{k_1,k_2} |V_{k1,2}|^2 (n_1 - n_2)\delta(\omega_k + \omega_1 - \omega_2)\Delta(\boldsymbol{k} + \boldsymbol{k}_1 - \boldsymbol{k}_2) , \tag{2.86}$$

where the matrix element $V_{k1,2}$ from eq. (2.79) has been substituted. In evaluating the integral in (2.86) one can assume that the ferromagnon dispersion relation consists of a quadratic and a linear part

$$\omega_k = \omega_0 - \omega_{ex}(ak)^2 , \quad k \le k_0 , \quad \omega_k = -\Delta + \omega_\prime(ak) , \quad k \ge k_0 , \tag{2.87}$$

where ω_0 is the gap in the ferromagnon spectrum (usually $\omega_0 \le 1$ K). The values of k_0 and Δ are determined from the continuity conditions for ω_k and for the group velocity $\boldsymbol{v}_k = \partial\omega_k/\partial\boldsymbol{k}$,

$$k_0 a = \omega_\prime/2\omega_{ex} , \quad \Delta = \omega_\prime^2/4\omega_{ex} - \omega_0 . \tag{2.88}$$

One finds that for $\omega_\prime = 2\omega_{ex}$ the values of ω_k evaluated with eqs. (2.87) differ from the ferromagnon dispersion relations (2.52) by no more than 10%. We shall therefore use

$$k_0 a = 1 , \quad \Delta = \omega = 40 \text{ K} , \quad \omega_\prime = 80 \text{ K} . \tag{2.89}$$

For $T < 40$ K the main contribution of γ_{mk} comes from the integration over the quadratic part of the spectrum and, consequently, the expression for γ_{mk} in YIG is the same as the familiar expression for ferromagnets (see, e.g., eq. (2.34)). For $T > 40$ K the integration over the quadratic part of the spectrum can be done using the Rayleigh–Jeans approximation $n_k = T/\omega_k$. The corresponding contribution to the magnon damping is then

$$\gamma_{m3}(\boldsymbol{k}) = \tfrac{1}{3}(k/k_\prime)(\omega_M^2 T/16\pi\bar{S}\omega_\prime^2)(1 - k_\prime^2/k^2)\{(1 + \tfrac{17}{2}\sin^2\theta_k - \tfrac{35}{4}\sin^4\theta_k)$$

$$+ (k_\prime^2/k^2)[\cos^2\theta_k(1 + \tfrac{11}{2}\sin^2\theta_k)$$

$$- 2(k_\prime^2/k^2)(\cos^2\theta_k(1 - 4\sin^2\theta_k) + \tfrac{3}{8}\sin^4\theta_k)]\} , \quad k \ge k_\prime . \tag{2.90}$$

On the linear part of the spectrum one must take the Planck distribution for n_k. The corresponding contribution to the damping is

$$\gamma_{m/}(\boldsymbol{k}) = (k_/ /k)(\omega_m^2 T/16\pi\bar{S}\omega_/^2)\,1.5(\omega_B/\omega_/)\,F(T)$$
$$\times\{\sin^2 2\theta_k - (1 - k_/^2/k^2)[\tfrac{1}{8}(7\sin^2 2\theta_k - \sin^4\theta_k)$$
$$-(k_/^2/k^2)(1 - \tfrac{5}{4}\sin^2 2\theta_k - \tfrac{5}{8}\sin^4\theta_k)]\}\,, \quad k \geq k_/\,. \tag{2.91}$$

The total three-magnon damping in coalescence processes is equal to the sum of (2.90) and (2.91). In these formulas $k_/ a = \omega_0/\omega_/$, $\omega_k \approx \omega_0$, and $F(T)$ is a dimensionless function of temperature given by the integral

$$F(T) = \frac{1}{1.5\omega_B T^2}\int_{\Delta}^{\omega_B} \frac{(\omega + \Delta)^2 e^{\omega/T}}{(e^{\omega/T} - 1)^2}\,d\omega\,, \quad F(T) \to 1 \quad \text{as} \quad T \to \infty\,. \tag{2.92}$$

The values of this function for $\omega_B = 350$ K and $\Delta = 40$ K are given in table 2. It can be seen from (2.90) that γ_{ms} is a linear function of temperature. It follows from (2.91), that the deviation of $\gamma_{m/}$ from a linear temperature dependence is determined by the factor $F(T)$, which is chosen such that $F \to 1$ when the temperature exceeds the maximum ferromagnon energy $\omega_B \approx 350$ K. The factor $F(T)$ is a slowly varying function of T: in particular, as T varies by a factor of three over the actual range from 100 to 300 K, F varies by only 30%. This means that the temperature dependence of $\gamma_{m/}$ for $T > 100$ K can also be assumed to be approximately linear.

Such an assumption is more accurate than it would seem at first glance. In fact, for $T > 100$ K it is generally necessary to take the temperature dependence of the magnetic dipole interaction matrix element into account. This question has not been studied in detail, but it is most natural to assert that the function $V_{1,23}(T)$ is obtained by replacing $\bar{S}$ by $\bar{S}(T)$, since the magnetic dipole interaction matrix element of long-wavelength spin waves should depend on the average magnetic moment $g\mu_B\bar{S}(T)$. This is taken into account in formula (2.91) for $\gamma_{m/}$ by replacing $F(T)$ by $\tilde{F}(T) = F(T)\bar{S}(T)/\bar{S}(0)$. As is shown in table 2, this function is even more slowly varying than $F(T)$ in the temperature range 100–300 K.

Let us now consider γ_{ms} and $\gamma_{m/}$ as functions of the magnitude and direction of the wave vector. We notice first of all that for $k < k_/ = (\omega_0/\omega_/)a^{-1}$ the coalescence process of forbidden by the conservation laws (2.85) because the ferromagnon group velocity is bounded by the value

Table 2
Temperature dependences of $F(T)$ (eq. (2.92)) and $\tilde{F}(T) = F(T)\bar{S}(T)/\bar{S}(0)$.

T (K)	$F(T)$	$\tilde{F}(T)$	T (K)	$F(T)$	$\tilde{F}(T)$
50	0.38	0.38	300	0.90	0.66
100	0.66	0.64	350	0.92	0.59
150	0.79	0.74	400	0.92	0.50
200	0.85	0.74	450	0.93	0.49
250	0.88	0.71			

$v_{max} = a\omega_{/}$. Accordingly, $\gamma_{ms} = \gamma_{m/} = 0$ if $k < k_{/}$. For $\omega_0 = 2\pi \times 17$ GHz ($\hbar\omega_0 \approx 1$ K) we have $k_{/} \approx 10^5$ cm^{-1}. For $k > k_{/}$ the damping coefficients γ_{ms} and $\gamma_{m/}$ are given by eqs. (2.90) and (2.91). At $k = k_{/}$, $\gamma_{m/}$ has the finite value

$$\Delta\gamma_m(\boldsymbol{k}) \equiv \gamma_{m/}(\boldsymbol{k}_{/}) = \frac{\omega_m^2 T}{16\pi\bar{S}\omega_{/}^2}\frac{\omega_B}{\omega_{/}} F(T)\sin^2 2\theta_k \,. \tag{2.93}$$

The value of $\Delta\gamma_m(\boldsymbol{k}_{/})$ is maximum at $\theta_k = \pi/4$, and at $T = 300$ K and $\omega_B = 350$ K it is equal to 7.2×10^6 s^{-1}. The occurrence of this jump can be easily understood by analyzing the conservation laws (2.85) with the spectrum (2.82). The coalescence processes (2.85) which are forbidden for $k < k_{/}$, become allowed at $k = k_{/}$ simultaneously with all the magnons belonging to the linear part of the spectrum and having wave vectors $\boldsymbol{k}_1 \| \boldsymbol{k}$. Since the distance k_B from the center to the boundary of the Brillouin zone depends on the direction of the wave vector, the size of the jump $\Delta\gamma_m(\boldsymbol{k}_{/})$ will depend on the direction of $\boldsymbol{k}_{/}$ with respect to the crystallographic axes. If we neglect the weak dependence of $F(T)$ on $\omega_B(\boldsymbol{k}_B)$, then $\Delta\gamma_m(k_{/})$ will be proportional to the zone-boundary magnon frequency ω_B in the direction of $\boldsymbol{k}$ (for a fixed angle θ_k with respect to the direction of the magnetization $\boldsymbol{M}$). The crystallographic anisotropy of the jump is rather large: $\Delta\gamma_m(\langle 100\rangle)/\Delta\gamma_m(\langle 110\rangle) \approx 1.5$.

It must be said that this simple geometric picture for the occurrence and anisotropy of the jump $\Delta\gamma_m$ results from the idealization (2.87) of the ferromagnet dispersion relation. In actuality the group velocity v_k depends, though slightly, on $\boldsymbol{k}$ at $k > k_0$: $\Delta v_k/v_k \sim 0.1$. This leads to a smearing of the jump $\Delta\gamma_m(\boldsymbol{k}_{/})$ over the interval $\Delta k/k_{/} \sim 0.1$ and to some decrease in the crystallographic anisotropy.

As we see from eqs. (2.90) and (2.91) for $k \gg k_{/}$ the damping $\gamma_{m/}$ decreases as k^{-1}, while γ_{ms} increases linearly with k. Asymptotically for $k \gg k_{/}$, eq. (2.90) describes the familiar function $\gamma_m(k, \theta_k)$ (see eq. (2.34)). The damping γ_m is a universal function of the dimensionless wave vector $\boldsymbol{x} = \boldsymbol{k}/k_{/}$, with the magnon frequency entering only in the expression for $k_{/}$: $ak_{/} = \omega_0/\omega_{/}$. In the region $k \approx k_{/}$ the function $\gamma_m(x)$ is shown in fig. 14 for $\theta_k = \pi/2$ and $\theta_k = \pi/4$.

We note that for $k < k_{/}$ there is a nonzero contribution to the ferromagnon relaxation from four-magnon scattering processes due to the magnetic dipole interaction,

$$\gamma_{4m} \approx (1/2 \cdot 8\pi)\omega_m^2 T^2/4\bar{S}^2\omega_{ex}^3 \,. \tag{2.94}$$

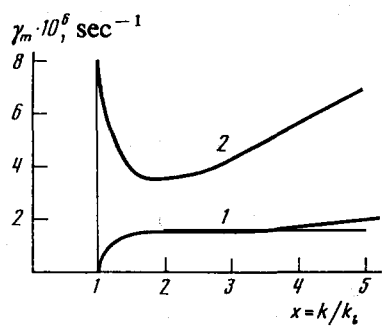

Fig. 14. Wave-vector dependence of the magnetic dipole relaxation rate of ferromagnons in YIG for the two directions: (1) $\theta_k = \pi/2$ and (2) $\theta_k = \pi/4$; $x = k/k_{/}$ ($k_{/} = \omega_0/\omega_{/}a$) [56].

Here we have taken into account both the direct contribution to the four-magnon scattering amplitude from the magnetic dipole interaction and the nonvanishing (at $\boldsymbol{k} \to 0$) exchange scattering which arises on account of the contribution of the magnetic dipole interaction to the magnon dispersion relation. At room temperature we have $\gamma_{4m} \approx 9 \times 10^2\ \mathrm{s}^{-1}$.

2.5. *Ferromagnon relaxation at $k \to 0$*

The ferromagnon damping $\gamma_{k\to 0}$ is due to the local uniaxial anisotropy of the Fe ions, which gives rise to a coalescence of the ferromagnons with magnons of the optical branches of the spectrum,

$$\omega_0 + \omega_{jk} = \omega_{j'k}\ , \quad j, j' \geq 2\ . \tag{2.95}$$

The symmetry of the nearest-neighbour environment of an ion is lower than cubic, and the anisotropy energy of an ion contains a term quadratic in S,

$$H_a^{(a)} = DS_\xi^2 + \tfrac{1}{6} A'^2 (S_x^4 + S_y^4 + S_z^4)\ . \tag{2.96}$$

Here ξ is the three-fold trigonal axis, the coefficient D for YIG is [58] of the order of 0.3 K, while $A'^2 \approx 0.03$ K. The term DS_ξ^2 is usually not taken into account, since its contribution to the interaction after summation over equivalent a positions goes to zero for ferromagnons with $\boldsymbol{k} \to 0$, which are homogeneous oscillations of the magnetic moment. For ferromagnons with $\boldsymbol{k} \neq 0$ the contribution proportional to D is suppressed by a factor $(ak)^2$ and, as a rule, is small compared to the contribution in A'^2. For the interaction involving optical magnons, however, there is no small long-wavelength factor $(ak)^2$, and the interaction DS_ξ^2 gives the main contribution to the amplitude of the processes of interest (2.95).

In the case when the equilibrium magnetization M_0 is directed along the [001] axes, the cubic term in the Hamiltonian $H_{n,a}$ expansion in powers of the Bose operators (1.6) $a_i^\dagger, a_i$ is due to the spins in the (a) sites only. The Hamiltonian of the a-ion local uniaxial anisotropy responsible for these processes has symmetry group O_h^{10} and is given by

$$\begin{aligned} H_a^{(a)} &= \sum_n H_{n,a}\ , \\ H_{n,a} &= \tfrac{1}{3} D[(S_{1x} + S_{1y} + S_{1z})^2 + (S_{2z} + S_{2y} - S_{2x})^2 + (S_{3z} + S_{3x} - S_{3y})^2 \\ &\quad + (S_{4z} - S_{4x} - S_{4y})^2 + (S_{5x} + S_{5y} + S_{5z})^2 + (S_{6z} + S_{6y} - S_{6x})^2 \\ &\quad + (S_{7z} - S_{7y} + S_{7x})^2 + (S_{8x} + S_{8y} - S_{8z})^2]\ . \end{aligned} \tag{2.97}$$

Here x, y and z are the crystallographic axes (the edges of the cubic unit cell), and S_i with $i = 1, \ldots, 8$, number the a ions of the nth primitive cell. The cubic term in the Hamiltonian takes the form:

$$\begin{aligned} H_{n,a} &= D\sqrt{S_0}[(a_1^\dagger a_1^\dagger a_1 - a_2^\dagger a_2 a_2 + a_3^\dagger a_3 a_3 - a_4^\dagger a_4^\dagger a_4 + a_5^\dagger a_5^\dagger a_5 \\ &\quad - a_6^\dagger a_6 a_6 + a_7^\dagger a_7 a_7 - a_8^\dagger a_8^\dagger a_8) \mathrm{e}^{-\mathrm{i}\pi/4} + \mathrm{h.c.}]\ . \end{aligned} \tag{2.98}$$

In order to obtain the relaxation frequency $\gamma_1(0)$ it is necessary to express the Hamiltonian $H_a^{(1)}$ in terms of the magnon amplitudes b_{ik}. The latter are linear combinations of the Bose operators $a_{ik}^\dagger$, a_{ik}.

The uniaxial anisotropy of the a ions only yields the cubic term in the Hamiltonian. Therefore after changing in (2.97) to the variables $b^\dagger, b$ which diagonalize the quadratic Hamiltonian, we obtain the matrix elements for the interaction of ferromagnons with the optical modes of types a and (a, d) only in the third order in the magnon amplitudes. The lowest-lying of these is the (a, d) triad of modes ω_{d9j}, $j = 1, 2, 3$, which is degenerate at $\boldsymbol{k} = 0$: $\omega_{d9j}(0) = \Omega \approx 290$ K. The excitation energy of the remaining modes of types a and (a, d) is substantially higher, and we shall not consider them. Because of the degeneracy, the eigenvectors b_{d9j} are rather complicated non-analytic functions of the wave vector at $\boldsymbol{k} \to 0$, they depend on the direction: $b_{d9j}(\boldsymbol{k}) = b_{d9j}(\boldsymbol{n})$, where $\boldsymbol{n} = \boldsymbol{k}/k$. The corresponding formulas are found in section 1.7. Omitting the awkward manipulations, we shall immediately give the expressions for the matrix elements of the Hamiltonian describing the interaction of $\boldsymbol{k} = 0$ ferromagnons with optical magnons of the lower (a, d) triad,

$$H_{\mathrm{FM},a-d}^{(3)} = \sum_{\substack{\boldsymbol{k}, j_1, j_2 = 1,2,3 \\ j_1 \neq j_2}} \left[V\begin{pmatrix} d9j_1 & 1, & d9j_2 \\ \boldsymbol{k} & 0, & \boldsymbol{k} \end{pmatrix} b_{d9j_1}^\dagger(\boldsymbol{k}) b_{10}^\dagger b_{d9j_2}(\boldsymbol{k}) + \mathrm{h.c.} \right], \tag{2.99}$$

$$V\begin{pmatrix} d9j_1 & 1, & d9j_2 \\ \boldsymbol{k} & 0, & \boldsymbol{k} \end{pmatrix} = Dv^2 \sqrt{S_0/2}\, W_{j_1, j_2}(\boldsymbol{n}), \quad \boldsymbol{n} = \boldsymbol{k}/k,$$

$$\left.\begin{matrix} |W_{12}(\boldsymbol{n})|^2 \\ |W_{13}(\boldsymbol{n})|^2 \end{matrix}\right\} = \frac{1}{2}\left(1 + 4n_z^4 - 3n_z^2 \pm \frac{3(4n_z^2 - 1)[n_z^2(1 - n_z^2)^2 - n_z^2 n_y^2(1 + n_z^2)]}{[f_4^2(n) - f_6(n)]^{1/2}}\right),$$

$$|W_{23}(\boldsymbol{n})|^2 = 9\,[n_y^6(n_x^2 - n_z^2)^2 + n_x^6(n_z^2 - n_y^2)^2]/[f_4^2(\boldsymbol{n}) - f_6(\boldsymbol{n})], \tag{2.100}$$

$$f_4(\boldsymbol{n}) = 3(n_x^2 n_y^2 + n_x^2 n_z^2 + n_y^2 n_z^2), \quad f_6(\boldsymbol{n}) = 27 n_x^2 n_y^2 n_z^2.$$

Here v is a coefficient of the u, v transformation for this (a, d) triad from the irreducible to the quasinormal basis. With the values (1.28) for the exchange integrals we have $v \approx 0.47$ when $\boldsymbol{M} \parallel [001]$.

To evaluate the damping,

$$\gamma_1(0) = 4\pi \sum_{\boldsymbol{k} j_1 j_2} \left| V\begin{pmatrix} d9j & 1, & d9j_2 \\ \boldsymbol{k} & 0, & \boldsymbol{k} \end{pmatrix} \right|^2 (n_{\boldsymbol{k}}^{d9j_1} - n_{\boldsymbol{k}}^{d9j_2}) \delta(\omega_0 + \omega_{d9j_1}(\boldsymbol{k}) - \omega_{d9j_2}(\boldsymbol{k})), \tag{2.101}$$

it is necessary to know the dispersion relation $\omega_{d9j}(\boldsymbol{k})$ at least for small $\boldsymbol{k}$ with $ak \lesssim 1$. An analysis with the aid of perturbation theory in $\boldsymbol{k}$ (see section 1.7) yields the following expressions (valid for $ak \lesssim 1$) for the frequencies of the (a, d) triad:

$$\Delta\omega_{32}(\boldsymbol{q}) = \omega_{d9,3}(\boldsymbol{q}) - \omega_{d9,2}(\boldsymbol{q}) = -2Zq^2[f_4^2(\boldsymbol{n}) - f_6(\boldsymbol{n})]^{1/2} + Rq^4[f_4^2(\boldsymbol{n}) - f_6(\boldsymbol{n})]^{1/4}, \tag{2.102}$$

$$\Delta\omega_{31}(\boldsymbol{q}) = \Delta\omega_{21}(\boldsymbol{q}) = Bq^2, \quad \boldsymbol{q} = a\boldsymbol{k}/8,$$

where

$$Z \approx 6\,\mathrm{K}\,, \quad R \approx 1200\,\mathrm{K}\,, \quad B \approx 370\,\mathrm{K}\,. \tag{2.103}$$

The coefficient of the q^2 term in $\Delta\omega_{32}$ turns out to be anomalously small, and this term can be neglected in comparison with the q^4 term,

$$\Delta\omega_{32}(\boldsymbol{q}) = Rq^4[f_4^2(\boldsymbol{n}) - f_6(\boldsymbol{n})]^{1/4}\,. \tag{2.104}$$

The damping (2.101) is given by the sum of three terms: $\gamma_1(0) = \gamma_{32}(0) + \gamma_{31}(0)$, corresponding to the coalescence processes

$$\omega_0 = \Delta\omega_{32}(\boldsymbol{q})\,, \quad \omega_0 = \Delta\omega_{31}(\boldsymbol{q})\,, \quad \omega_0 = \Delta\omega_{21}(\boldsymbol{q})\,. \tag{2.105}$$

For the frequencies of the a, d triad we obtain from (2.103) and (2.102)

$$\begin{aligned}
\gamma_{32}(0) &\approx v^4 \frac{D^2 \mathrm{e}^{\Omega/T}}{T(\mathrm{e}^{\Omega/T}-1)^2}\left(\frac{\omega_0}{R}\right)^{3/4}\frac{4\bar{S}}{\pi^2}C\,, \\
\gamma_{31}(0) + \gamma_{21}(0) &\approx v^4 \frac{D^2 \mathrm{e}^{\Omega/T}}{T(\mathrm{e}^{\Omega/T}-1)^2}\left(\frac{\omega_0}{B}\right)^{3/2}\frac{128\bar{S}}{5\pi}\,.
\end{aligned} \tag{2.106}$$

Here Ω is the gap of the a, d triad, and the constant C is given by

$$C = \int \mathrm{d}\boldsymbol{n}\, \frac{|W_{23}(\boldsymbol{n})|^2}{[f_4^2(\boldsymbol{n}) - f_6(\boldsymbol{n})]^{3/16}} \approx 6.8\,. \tag{2.107}$$

If we take for Ω the value of the gap of the a, d triad at zero temperature ($\Omega \approx 290$ K), then the damping $\gamma_1(0)$, evaluated by formulas (2.106) turns out to be $0.36 \times 10^6\ \mathrm{s}^{-1}$. This is several times smaller than the experimentally observed (at room temperature) value of $\gamma_1(0)$. However, at $T = 300$ K it is necessary to take into account the temperature dependence of the gap of the (a, d) triad. Certain experimental facts (see ref. [4]) indicate that the gaps of the optical modes in YIG behave under changes in temperature like the average magnetization of the sample. With allowance for this circumstance the gap of the (a, d) triad at $T = 300$ K becomes $\Omega \approx 200$ K, and accordingly, the damping (2.107) is

$$\gamma_1(0) \approx 0.9 \times 10^6\ \mathrm{s}^{-1}\,, \tag{2.108}$$

in fair agreement with the experimental data (see chapter 3). The damping $\gamma_1(0)$ as a function of T with allowance for the temperature dependence of the gap Ω is shown in fig. 15.

We note that processes involving coalescence with optical magnons at the corners of the Brillouin zone give a nonzero contribution to the damping of ferromagnons with $\boldsymbol{k} \to 0$. However, simple estimates show that the volume of $\boldsymbol{k}$-space in which these processes are allowed is small, and the contribution from these processes is substantially smaller than the contributions which we have calculated.

It should be noted that magnon–magnon and magnon–phonon processes due to the local uniaxial anisotropy were considered by Kasuya and LeCraw [11] and Sparks [10] in order to

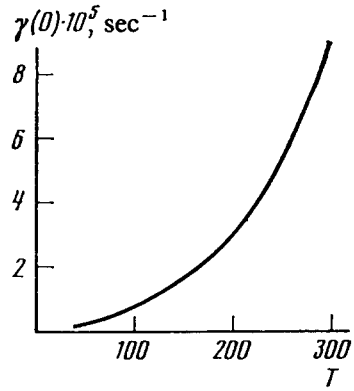

Fig. 15. Temperature dependence of the relaxation rate $\gamma(0)$ at $k \to 0$ due to the interaction with optical magnons.

explain the relaxation of magnons with $k \to 0$. They found that magnon-phonon processes owing to the uniaxial anisotropy could explain the experimental data [11, 12]. However, a more detailed analysis of these calculations [10] based on known eigenvectors of the magnon modes in YIG (1.45) shows that the amplitude of the ferromagnon–phonon interaction was overestimated at least four times. This means that the relaxation frequency due to the magnon–phonon interaction caused by the uniaxial anisotropy was overestimated at least sixteen times. Therefore these so-called Kasuya–LeCraw processes are not responsible for the relaxation of magnons with small wave numbers.

2.6. *Comparison of theoretical and experimental results*

Each of the elementary ferromagnon relaxation processes considered here – the exchange scattering, the magnetic dipole interaction, and relaxation involving optical magnons – is dominant in a certain parameter region. Figure 16 shows the regions of temperature T and wave vector k in which the various elementary processes give the leading contribution. For long-wavelength magnons with $k < k_f$ the magnetic dipole interaction is forbidden and the amplitude of the exchange interaction is very small, so that in the region $k < k_f$ ($k_f = \omega_0/a\omega_f$) the leading contribution to the relaxation is that due to scattering by optical magnons; this scattering was considered in section 2.5 (see (2.106)). At low temperatures $T \lesssim 150$ K the damping $\gamma(0)$ falls off exponentially. In this temperature region the leading intrinsic relaxation process is four-magnon magnetic-dipole scattering (2.92) but, as a rule, under real conditions the ferromagnon damping at $T \lesssim 120$ K and $k < k_f$ is due to defects [10, 45]. The contributions from the exchange and three-magnon magnetic-dipolar damping, as can be seen from eqs. (2.62) and (2.88) are comparable for $T \propto k^{-2}$ in the low-temperature region. At higher temperatures this dependence becomes smoother and asymptotically approaches $T \propto k^{-2/3}$ (see (2.62)).

There were many experimental researches concerned with interaction and relaxation of ferromagnons in YIG. The most detailed accounts were discussed in section 2.2. As for the temperature dependence of the magnon stiffness in YIG, which is probably the most direct manifestation of the magnon–magnon interaction, it was found that it differs from that in a simple cubic ferromagnet significantly [30] (see section 2.2.2). The temperature dependence of the magnon stiffness calculated in section 2.3.2 is in good agreement with the experimental data both for the sign and the value of the temperature dependent term in the temperature range $0 < T < 180$ K. At higher

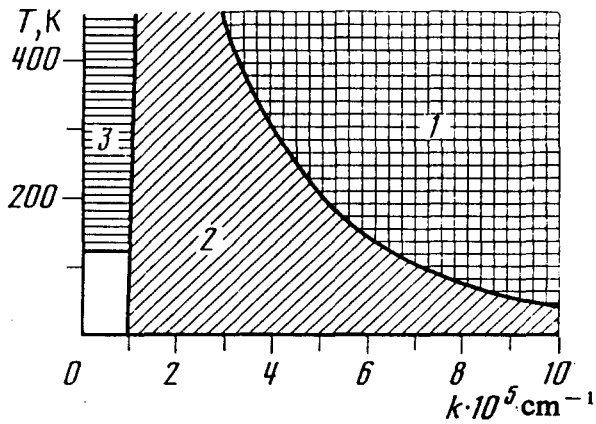

Fig. 16. Diagram of the relative contributions of various relaxation processes in YIG: 1) the region in which exchange relaxation is dominant (see chapter 1), (2) the region of magnetic dipolar relaxation (see chapter 2), (3) the region of relaxation involving optical magnons (chapter 3), (4) the region in which the leading contribution is from relaxation involving defects ($\omega_0 = 1$ K) [56].

temperature the interaction with optical magnons and the temperature dependence of the magnon spectra are essential, therefore the formula (2.59) is not correct at higher temperature, as it was explained in section 2.3.2.

As far as the ferromagnon relaxation is concerned, the problem of correspondence between theoretical (section 2.3) and experimental (section 2.2) results is more complicated. As to the k-dependent part of the ferromagnon relaxation frequency, its interpretation is relatively simple. There is a very good agreement between the theory (section 2.3.3) and the experimental data [9, 52] (section 2.2) in the region on the (T–k) plane (fig. 16) where the exchange relaxation dominates. The exchange relaxation frequency in YIG is close to that in a simple cubic ferromagnet because of the compensation between fairly complicated k-dependences of the four-magnon amplitude and the ferromagnon spectrum in a wide energy range discussed in section 2.3.3. The relaxation frequency owing to the three-magnon splitting processes in the microwave frequency range in YIG coincides with that in a ferromagnet with the same magnetization and magnon stiffness [59, 44] because only low-energy magnons are involved in these processes. The low energy magnons can be described in the continuous medium approximation which is based on the macroscopic parameters: the magnetization and the magnon stiffness [44]. The relaxation frequency due to the magnon splitting processes is in good agreement with experimental data [9]. The relaxation due to the three-magnon coalescence processes is close to that in a ferromagnet for relatively large wave numbers $k \ll ke = \omega_0/\omega_{ex}a$. In particular, the relaxation frequency γ_k^c is linear in k for

$$(\omega_0/\omega_{/})(ak_{/}) \ll ak_{/} \lesssim \sqrt{\omega_0/\omega_{ex}} \tag{2.109}$$

and it decreases with k for $ak > \sqrt{\omega_0\omega_{ex}}$ according to eq. (2.36). The linear dependence of the magnon damping on k was observed in experiment [11]. This dependence is due to interaction with ferromagnons with energies smaller than 40 K. The spectrum of these magnons is quadratic in k, therefore the coefficient before k in the relaxation frequency can be found from the formula (2.37) for a ferromagnet. This coefficient coincides with that measured in experiment [9]. The k-independent part of the damping measured in the wave number range (2.109) consists of two parts:

(i) the relaxation frequency due to the magnetic dipole three-magnon coalescence processes γ_m (2.89) on the plateau (fig. 14) and (ii) the relaxation owing to the interaction with optical magnons $\gamma(0)$ (2.106). The former damping is $1.5 \times 10^6\ s^{-1}$ at $k = 2k_\prime$ and room temperature. It does not depend on the magnon frequency. The latter relaxation frequency depends on the magnon frequency, it is $0.9 \times 10^6\ s^{-1}$ at room temperature and $\omega_0 = 1$ K. The total k-dependent relaxation rate is $2.4 \times 10^6\ s^{-1}$ at $T = 300$ K and agrees well with experimental data for $\omega_0 = 1$ K [9] both in magnitude ($2.7 \times 10^6\ s^{-1}$) and in temperature dependence in the 150–300 K region. At a lower magnon frequency the magnetic dipole in interaction dominates. In particular, for $\omega_0 \simeq 0.3$ K [11, 12] the damping due to interaction with optical magnons is 2.5 times smaller and therefore the relaxation frequency Γ_0 measured in these experiments is due to the magnetic dipole interaction mainly. The temperature dependence of Γ_0 is almost linear in the temperature region 80–350 K and it is close to the theoretical evaluation $1.5 \times 10^6\ s^{-1}$ for the k-independent part of the magnetic dipole relaxation frequency. When $k/k_\prime$ is changed from 1.5 to 1, the magnetic dipolar relaxation is turned off, and the damping decreases sharply to $\gamma(0)$.

It must be said that in the experiments on parametric excitation of magnons by the method of parallel pumping, our predicted "dip" in the damping for $k \leq k_\prime$ was not observed clearly. However, such a dip can be seen in fig. 10 for the relaxation frequency at $T = 160$ K. The difficulty in the dip observation appears because magnons with $k < k_\prime$ and $\theta_k = \pi/2$ were not excited even though the reasonance conditions $\omega_p/2 = \omega(k, \pi/2)$ were satisfied. Instead, magnons with $k > k_\prime$ and $\theta_k < \pi/2$ were excited. We believe that this is explained by the presence of elastic scattering of magnons (two-magnon processes) by defects and the boundaries of the sample. Nevertheless, this dip has been observed in experiments on the relaxation of magnons excited under conditions of kinetic instability [53] discussed in section 2.3.

In this case magnons were excited to the bottom of the spectrum, with $k < k_\prime$ and $\theta_k = 0$. The elastic scattering could not remove the magnons from this region and was therefore unimportant. The experimentally determined relaxation rate was $5 \times 10^5\ s^{-1}$ at a magnon frequency $\omega_k = 2\pi \times 2 \times 10^6\ s^{-1}$. This value is smaller by a factor of three than the magnetic dipolar damping on the plateau, but it is larger than the rate $\gamma(0) = 1.7 \times 10^5\ s^{-1}$ for scattering by optical magnons. The discrepancy between the theoretical value of $\gamma(0)$ and the experimentally measured damping may be due, on the one hand, to experimental error in determining $\gamma(0)$ as a result of the strong fluctuations in the emission from the magnons and, on the other hand, to the dependence of the damping $\gamma(0)$ on the direction of the field (we evaluated $\gamma(0)$ for $\boldsymbol{H} \parallel [100]$, but $\boldsymbol{H}$ was parallel to the [111] axis in the experiment, and to insufficiently accurate knowledge of the local uniaxial anisotropy constant, and also to relaxation processes involving impurities.

3. Conclusion

The history of studies of YIG properties has begun with the leadership of experimental researchers in the late fifties and early sixties. In the mid and late sixties the theory explained many fundamental properties of this ferrite. However, during the seventies new experimental research was carried out and some new questions arose. Today's state of our knowledge about YIG can be characterized as deuce in the permanent competition between experimenters and theorists. The game seems to be close to its finish: we know very much about this interesting and complex magnet. We list some important gains obtained in this game.

Experiment:	*Theory*:
– crystal and magnetic structure of YIG,	– spectra of the homogeneous magnon modes,
– magnon spectra,	– quasinormal approximation for the magnon spectra,
– temperature dependence of the magnetization and specific heat,	– thermodynamic properties in the magnon approximation,
– relaxation in the microwave frequency range.	– mechanisms of magnon interaction,
	– theory of the ferromagnon relaxation.

There are some open problems left, nevertheless the basic facts have been well established now. We know the values of the exchange integrals, the magnon spectra, in particular, the ferromagnon spectrum, which is quadratic for small k only and it is linear in almost the whole Brillouin zone, the relaxation frequencies due to the exchange and magnetic dipole interactions, and the temperature dependence of the magnon stiffness.

Acknowledgements

The research was supported by the Academy of Sciences of the former USSR, the Natural Science and Engineering Research Council of Canada, Meyerhoff Foundation of the Weizmann Institute of Science, and the Winnipeg Institute for Theoretical Physics. We are grateful to A.N. Anisimov, A.G. Gurevich and G.A. Melkov for helpful discussions of the experimental results on magnon relaxation in YIG and to A.I. Chernykh for his help in numerical calculations.

References

[1] R.L. Douglass, Phys. Rev. 120 (1960) 1612.
[2] A.B. Harris, Phys. Rev. 155 (1967) 499.
[3] S. Geller and M.A. Gilleo, J. Phys. Chem. Solids 3 (1957) 30.
[4] J.S. Plant, J. Phys. C 10 (1977) 4805.
[5] I.V. Kolokolov, V.S. L'vov and V.B. Cherepanov, Sov. Phys. JETP 57 (1983) 605–613.
[6] Yu.A. Izyumov, V.E. Naish and R.P. Ozerov, Neitronografia Magnetikov [Neutron-Diffraction Studies in Magnets] (Nauka, Moscow, 1981).
[7] E.E. Anderson, Phys. Rev. A 134 (1964) 1581.
[8] K.P. Belov, Ferrity v Sil'nykh Magnitnykh Polyakh [Ferrites in Strong Magnetic Fields] (Nauka, Moscow, 1972).
[9] A.G. Gurevich and A.N. Anisimov, Sov. Phys. JETP, 41 (1975) 336.
[10] M. Sparks, Ferromagnetic Relaxation Theory (McGraw-Hill, New York, 1964).
[11] T. Kasuya and R.C. LeCraw, Phys. Rev. Lett. 6 (1961) 223.
[12] R.C. LeCraw and E.G. Spencer, J. Phys. Soc. Japan Suppl. 17(B1) (1962) 401.
[13] F. Bertaut and F. Forrat, Compt. Rend. 242 (1956) 382.
[14] S. Geller and M.A. Gilleo, Acta Crystallogr. 10 (1957) 239.
[15] M.A. Gilleo, Ferromagnetic insulators: garnets, in: Ferromagnetic Materials, Vol. 2, ed. E.P. Wohlfarth (North-Holland, Amsterdam, 1980).
[16] R. Pauthenet, Ann. Phys. (Paris) 3 (1958) 424.
[17] S. Ogawa and S. Morimoto, J. Phys. Soc. Japan 17 (1962) 654.
[18] E.L. Boyd, V.L. Moruzzi and J.S. Smart, J. Appl. Phys. 34 (1963) 3049.
[19] R. Aléonard, J. Phys. Chem. Solids 15 (1960) 167.
[20] T.D. Edmonds and R.G. Petersen, Phys. Rev. Lett. 2 (1959) 499.
[21] J.E. Kunzler, L.R. Walker and J.K. Galt, Phys. Rev. 119 (1960) 1609.
[22] S.S. Shinozaki, Phys. Rev. 122 (1961) 388.
[23] A.B. Harris and H. Meyer, Phys. Rev. 127 (1962) 101.

[24] I. Solomon, Compt. Rend. 251 (1960) 2675.
[25] C. Robert, Compt. Rend. 251 (1960) 2684.
[26] G.K. Wertheim, Phys. Rev. Lett. 4 (1960) 403.
[27] L.D. Khoi and M. Buyle-Bodin, Compt. Rend. 253 (1961) 2514.
[28] G.F. Dionne, J. Appl. Phys. 41 (1970) 4874.
[29] E.H. Turner, Phys. Rev. Lett. 5 (1960) 100.
[30] R.C. LeCraw and L.R. Walker, J. Appl. Phys. Suppl. 32 (1961) 167S.
[31] P.J. Woijtowicz, J. Appl. Phys. 33 (1962) 1257.
[32] A.B. Harris, Phys. Rev. 132 (1963) 2398.
[33] T. Holstein and H. Primakoff, Phys. Rev. 58 (1940) 1098.
[34] F. Dyson, Phys. Rev. 102 (1956) 1217.
[35] S.V. Maleev, Sov. Phys. JETP 6(33) (1957) 776.
[36] V.E. Zakharov, Sov. Phys. JETP 33 (1971) 927.
[37] P.W. Anderson, Phys. Rev. 86 (1952) 694.
[38] P.W. Anderson, Phys. Rev. 83 (1951) 1260.
[39] B. Dreyfus, J. Phys. Chem. Solids 23 (1962) 287.
[40] L.D. Landau and E.M. Lifshitz, Quantum Mechanics: Nonrelativistic Theory (Pergamon Press, Oxford, 1979)..
[41] I.V. Kolokolov, V.S. L'vov and V.B. Cherepanov, Preprint No. 183, Institute of Automation and Electrometry, Siberian Branch Acad. Sci. USSR, Novosibirsk (1982).
[42] R.L. Comstock and W.G. Nielsen, Phys. Rev. 136 (1964) 445.
[43] V.S. L'vov, Wave Turbulence under Parametric Excitation with Special Applications to Magnetics (Springer, Berlin, 1992).
[44] A.I. Akhiezer, V.G. Bar'yakhtar and S.V. Peletminskii, Spin Waves (Wiley, New York, 1968).
[45] A.G. Gurevich, Magnitnyi Resonans v Ferritakh i Antiferromagnetikakh [Magnetic Resonance in Ferrites and Antiferromagnets] (Nauka, Moscow, 1973).
[46] C.W. Haas and H.B. Callen, Ferromagnetic Relaxation, and Resonance Line Widths in Magnetism, Vol. 1, eds G.T. Rado and H. Suhl (Academic Press, New York, 1963).
[47] A.B. Harris, Phys. Rev. 172 (1968) 674.
[48] M. Sparks, R. Loudon and C. Kittel, Phys. Rev. 122 (1961) 791.
[49] M. Sparks, Phys. Rev. 160 (1967) 364.
[50] H. Suhl, J. Phys. Chem. Solids 1 (1957) 209.
[51] E. Schlömann, J.J. Green and U. Milano, J. Appl. Phys. 31 (1960) 386S.
[52] A.N. Anisimov and A.G. Gurevich, Sov. Phys. Solid State 18 (1976) 20.
[53] A.V. Lavrinenko, V.S. L'vov, G.A. Melkov and V.B. Cherepanov, Sov. Phys. JETP 54 (1981) 542.
[54] C.E. Patton, Phys. Status Solidi B 92 (1979) 211; 93 (1979) 63.
[55] V.N. Krivoruchko and D.A. Yablonskii, Sov. Phys. JETP 47 (1978) 1179.
[56] I.V. Kolokolov, V.S. L'vov and V.B. Cherepanov; Sov. Phys. JETP 59 (1984) 1131–1139.
[57] A.I. Akhiezer, J. Phys. (USSR) 10 (1946) 217.
[58] S. Krupicka, Fizika Ferritov [Physics of Ferrites] Vol. 2 (Nauka, Moscow, 1976).
[59] E. Schlömann, Phys. Rev. 121 (1961) 1312.